Pedogenic mud aggregates in Pennsylvanian strata near Joggins, Nova Scotia

By: Jordana Gardiner

Submitted in Partial Fulfillment of the Requirements
for the Degree of Bachelor of Science, Honours
Department of Earth Science
Dalhousie University, Halifax, Nova Scotia

April 29, 2005
Advisor: Dr. Martin Gibling

Dalhousie University

Department of Earth Sciences
Halifax, Nova Scotia
Canada B3H 3J5
(902) 494-2358
FAX (902) 494-6889

DATE: April 26, 2005

AUTHOR: Jordana Gardiner

TITLE: Pedogenic mud aggregates in Pennsylvanian strata near Joggins, Nova Scotia

Degree: B.Sc. ERTH Convocation: May 2005 Year: 2005

Abstract

Pedogenic mud aggregates are sand- and silt-sized particles composed largely of clay flakes, and are commonly formed in modern vertisol-type soils during seasonal wetting and drying. Where the soils are rich in smectite, clays expand and shrink seasonally, causing aggregation of the flakes under pressure, and the aggregates may be transported as fluvial bedload. A major problem associated with studying mud aggregates is their low preservation potential, as they tend to be destroyed by compaction during burial. The presence of calcretes in the Pennsylvanian Boss Point and Little River formations near Joggins, suggesting semi-arid and seasonal conditions, led to a successful search for aggregates using thin sections and the scanning electron microscope (SEM).

Samples from fluvial channel sandstones, crevasse-splay sandstones and floodplain mudstones all contain preserved aggregates. Although sand-sized aggregates are present, most aggregates are typically 10-15 μ in diameter in all three sediment types, suggesting a common origin. The abundance of aggregates in these samples is highly variable, ranging from 10-50%. Some of the best occurrences are concentrated in thin laminae of floodplain mudstones, where they occur with a few silt-sized grains of quartz and feldspar. Small aggregates are also prominent in large mud fragments within channel sandstones, probably eroded from river-bank soils. Chemical analysis of clays using the SEM-EDS and XRD techniques shows a predominance of illite with lesser chlorite and kaolinite. Smectite was not observed but may have altered to illite during deep-burial diagenesis.

The Boss Point is now one of few formations in the rock record that have yielded pedogenic aggregates. However, many aggregates are an order of magnitude smaller than those identified in most previous studies. They are also unusually well preserved within floodplain muds, where small aggregates were probably concentrated by overbank floods and transported across floodplains and into channels. Aggregate preservation probably reflects early carbonate and hematite cementation and shielding by silicate grain frameworks in coarser sediments, as well as fast burial in the rapidly subsiding Cumberland Basin.

Keywords: Joggins, pedogenic aggregates, floodplains, paleosols, Pennsylvanian, calcretes, vertisols

Table of Contents

Table of Figures

Table of Tables

Acknowledgements

I would like to thank Dr. Martin Gibling, my thesis supervisor. Your guidance, support, and enthusiasm throughout the course of this project is much appreciated. My thesis would not have been possible without your generous time and valued advice. Thanks to Gordon Brown, Patricia Stoffin, Frank Thomas, and Keith Taylor for their help with the technical aspects of this project, as well as Dr. Yawooz Kettanah and Tom Duffett for their help in the department. I would also like to thank Mike Rygel for his help with figures and information on the Little River Formation. Finally, thanks to family and friends for all the support and encouragement over the last year.

1.0 Introduction

1.1 Problem

Pedogenic mud aggregates are a relatively new discovery in sedimentary geology. Mud aggregates are sand- and silt-sized particles composed mainly of clay flakes and form as a result of pedogenic processes in the vertic soils of areas with arid to semi-arid climates. Pedogenic mud aggregates were discovered recently on a floodplain in Central Australia, where aggregates were, and still are, actively forming on floodplains and being transported by the river system (Rust and Nanson, 1989). Scientists who made this discovery were surprised to find both braided and anastomosing fluvial deposits almost entirely composed of mud. Previously the geological community believed only sandy or gravelly sediment to be capable of forming braided river networks. Individual sediment grains must be large and non-cohesive enough to be transported as bedload in order to form braid bars and other channel deposits. Whereas quartz and other sand-sized clastic grains meet this requirement, clay flakes are known to be light enough to travel as suspended sediment in water, and settle out of suspension only under calm flow conditions. Evidence in Central Australia suggests that aggregated clay behaves in a rather uncharacteristic manner compared to that of non-aggregated clay flakes.

This is an exciting topic to study because the existence of pedogenic mud aggregates provides an alternate method to suspension settling for the formation of mudstone deposits, expanding the range of environments where mudstone deposits can form. Discovery of this textural feature may have implications for many previously studied formations containing fluvial mudstone bodies. Because the aggregates are easily destroyed during burial, mudstone deposits originally formed by aggregated mud could

be incorrectly interpreted as suspension settling deposits. The aggregate texture, where preserved, can be difficult to identify, and may be relatively small; therefore, the texture can easily be overlooked even when it is present.

The goal of this thesis is to determine, firstly, whether pedogenic mud aggregates are present in the Pennsylvanian Boss Point and Little River formations, near Joggins, Nova Scotia, through experimentation with different techniques related to composition analysis, as well as imaging. Secondly, this study will focus on determining the texture and occurrence of the aggregates in key stratal intervals; and finally to link aggregate preservation to processes having occurred within these formations.

1.2 Previous Work

To date, very few studies have focused on aggregates; therefore, knowledge about the distribution and occurrence of pedogenic mud aggregates in the geologic record is limited. Table 1.1 contains a brief summary of previous studies of pedogenic mud aggregates in both modern and ancient environments. Only five formations prior to this project have yielded pedogenic mud aggregates in the rock record. Of these, four formations yielded mud aggregates preserved in channel sandstones and siltstones (Rust and Nanson, 1989; Gierlowski-Kordesch and Gibling, 2002). Only one study, by Müller et al. (2004), found mud aggregates preserved in floodplain mudstones. The above mentioned studies focus on the formation, transportation, composition, and preservation of aggregates, as well as descriptions and interpretations of the sedimentary deposits where preserved aggregates reside.

Table 1.1 - Previous studies focusing on pedogenic mud aggregates

Study	Facies/ Environment	Formation/Age	Aggregate Attributes			Insitu/ Reworked	Preservation Mechanism
			Size, Shape	Occurrence	Composition		
Nanson et al., 1986; Rust and Nanson, 1989; Maroulis and Nanson, 1996; Gibling et al. 1998	Coexisting braided and anastomosing channels transporting primarily clay rich mud.	Cooper Creek, NE Lake Eyre Basin, central Australia. Modern.	Fine sand-size, 0.13mm, when reworked. <1 to 2 mm insitu.	Aggregates develop primary bedform structures, plane beds, ripples, antidunes. Aggregates deposit in shallow braid channels and bars.	Clay contents typically >50%, commonly contain smectite with minor kaolinite. Floodplain salt concentrations very low (<200 ppm)	Insitu/ Reworked	Aggregate texture completely lost at depth of 2 m on the floodplain and frequently vague to undetectable below a few decimeters.
Müller et al., 2004	1) Channel Sandstone, 2) Proximal overbank (levee and crevasse splay sandstones), and 3) Distal overbank and floodplain mudrock	Lunde Formation, Triassic Hegre Group. North Sea.	Range 0.3-4 mm (MF2) and 0.1-0.3 mm (MF3), Spherical to slightly elongate, sub angular to rounded.	From thin discontinuous laminae to thick homogeneous accumulation. Up to 70-90% aggregates in some intervals.	Variable, with illite/smectite up to 70%, other intervals show illite 65% and smectite 15-20%	Layers of reworked and insitu aggregates recognized	Rapid burial of floodplain mudrock helps preserve aggregates, reducing degree of pedogenic modification and overprinting. Early carbonate cementation may have aided preservation. Burial depth 2500-3000 m.
Gierlowski-Kordesch and Gibling, 2002	Channel bodies with sheet complexes of sandstone and mudstone	New Haven Arkose, Hartford Basin, Connecticut. U. Triassic - L. Jruassic.	Silt to sand-sized particles. Rounded to sub-angular.	Channel sandstone with bimodal grain size containing aggregates. Mud-dominated laminae in muddy siltstone.	Upper mudstone, mostly illite and smectite. Lower mudstone, contains illite, smectite, chlorite, and mixed illite/smectite	Reworked	Aggregate preservation is related to larger grains in the bimodal sand protecting them from compaction. Early calcite cement may have helped.

Table 1.1 - Con't

Study	Facies/ Environment	Formation/Age	Aggregate Attributes			Insitu/ Reworked	Preservation Mechanism
			Size, Shape	Occurrence	Composition		
Rust and Nanson, 1989	Floodplain mudstone with minor sandstone channel deposits and flood deposit sandstones.	East Berlin Formation, Newark Supergroup, Hartford Basin. Mesozoic	Sand-sized aggregates	Aggregates in horizontally stratified and cross-stratified quartz sandstone. Rare in mudstone units.	?	Reworked	Aggregates preserved in mud only where individual aggregates surrounded by quartz grains. Mud deposits interpreted as bedload units, lack of texture attributed to compaction.
	Alternating floodplain mudstone and very fine sandstone interpreted as deposits of sheet floods and ephemeral meandering streams.	Maringouin Formation, Fundy Basin, Nova Scotia and New Brunswick. Mid-Carboniferous	Sand-sized aggregates up to 10 times larger than associated quartz grains.	Aggregates present in rippled and horizontally stratified sandstone. Associated with fossil vertisols.	?	Reworked	Aggregates appear to be armoured by a single grain layer of quartz silt. Aggregate texture not present in mudstones, likely due to loss of texture during compaction.
	Stratified and massive sandstone (channel fill deposits), and minor mudrock assemblage (overbank deposit) including, mudstone and rippled silt to fine sandstone.	Hawkesbury Sandstone, New South Wales, Australia. Mid-Triassic.	Medium sand-sized aggregates	Aggregates abundant in massive sandstone, and less common in cross-stratified sandstone. No evidence of aggregates in mudrock units.	Mixture of kaolinite/dickite, illite, and mixed layer species. 20-40% mud in sandstone.	Reworked	Squeezing between quartz grains has changed the shape of aggregates but some retain rounded shape; most appear to have been equidimensional.
Ékes, C. 1993	Poor to moderatly sorted conglomerates with siltstone interbeds. Alluvial fan-braided river environment.	Ridgeway Conglomerate Formation, SW Wales. L. Devonian	?	Cross bedded siltstone with swelling clay, dessication cracks, pseudo-anticlines, and calcrete horizons	Illite, chlorite and mixed layer swelling clays (7-30%)	N/A	Mud aggregate texture obliterated by compaction. Mud layers in siltstones formed by bedload deposition based on 3D bedforms and large trough fills.

2.0 Pedogenic Aggregates and Geological Setting

2.1 Introduction to Pedogenic Aggregates

Pedogenic mud aggregates are, for the most part, sand-sized particles composed of silt and clay flakes (Gierlowski-Kordesch and Gibling, 2002). These aggregates form during wetting and drying cycles in soils containing clays that expand and shrink in response to seasonal changes in moisture. Three important issues to consider in the study of pedogenic mud aggregates involve clay composition, aggregate transport mechanism, and the preservation of this feature in the geologic record.

The presence of a soil horizon in the geologic record indicates slow or no deposition for extended periods, depending on the maturity level and type of paleosol (Plint and Browne, 1994). Vertisols or vertic soils are soils that contain at least 30% clay, usually rich in smectite. These soils develop in regions where soil moisture changes rapidly from wet to dry and are characterized by pronounced changes in volume (Bates and Jackson, 1987). Classifying a paleosol as a vertisol can not rely solely on the presence of expandable clays for, during diagenesis, expandable clay is commonly converted to other types of clay (Mack et al., 1993). Smectite, for example, is altered to illite during diagenesis. Mack et al. (1993) suggested that desiccation cracks, wedge-shaped peds, hummock and swale structures, slickensides, and clastic dikes are other morphological features common to vertisols.

2.1.1 Aggregate Formation and Clay Composition

Seasonally wet and dry environments capable of producing vertisols are found extensively today in the tropics. The shrink-swell phenomenon, caused by seasonality of climate, results in a process termed "self mulching" (Maroulis and Nanson, 1996; Gierlowski-Kordesch and Gibling, 2002). This process is an effective way to churn the upper zone of soil.

Self mulching causes wet clay to expand, and the resultant pressure increase forces soil material to shift upward and outward. With drying, soils crack and disperse, then re-aggregate into small clumps, known as peds, which can range in size from <1 mm to 10 mm (Fig. 2.1). Small granular peds form on the soil surface and more angular peds form at depth. Granular peds can also be found inside deep cracks in floodplain soils as a result of topsoil instability and illuvation processes (Gierlowski-Kordesch and Gibling, 2002).

Papers by Rust and Nanson (1989), Gierlowski-Kordesch and Gibling (2002), and Müller et al. (2004) all note the importance of smectite as one of the key clay minerals in the formation of peds in vertisols. The exact proportion of expanding clay needed in the soil to form aggregates is still undetermined. Müller et al. (2004) recorded a relatively low content of smectite in some mudrocks composed of aggregates. This may imply that only a limited amount of swelling clay is required for the formation of pedogenic mud aggregates, although smectite may have been lost during diagenesis. The class of clay minerals known as smectite, the most familiar of which is montmorillonite, is important in mud aggregate formation because the clays readily absorb water. The incorporation of water into the smectite structure causes the minerals to become expandable in one direction, and the clays can almost double their size in wet conditions (Prothero and Schwab, 2001). Differing ratios of illite and kaolinite are also noted as being present in some of the aggregates observed by Muller et al., (2004). Unlike smectite, these are not expandable clays, but as mentioned earlier smectite does alter to illite.

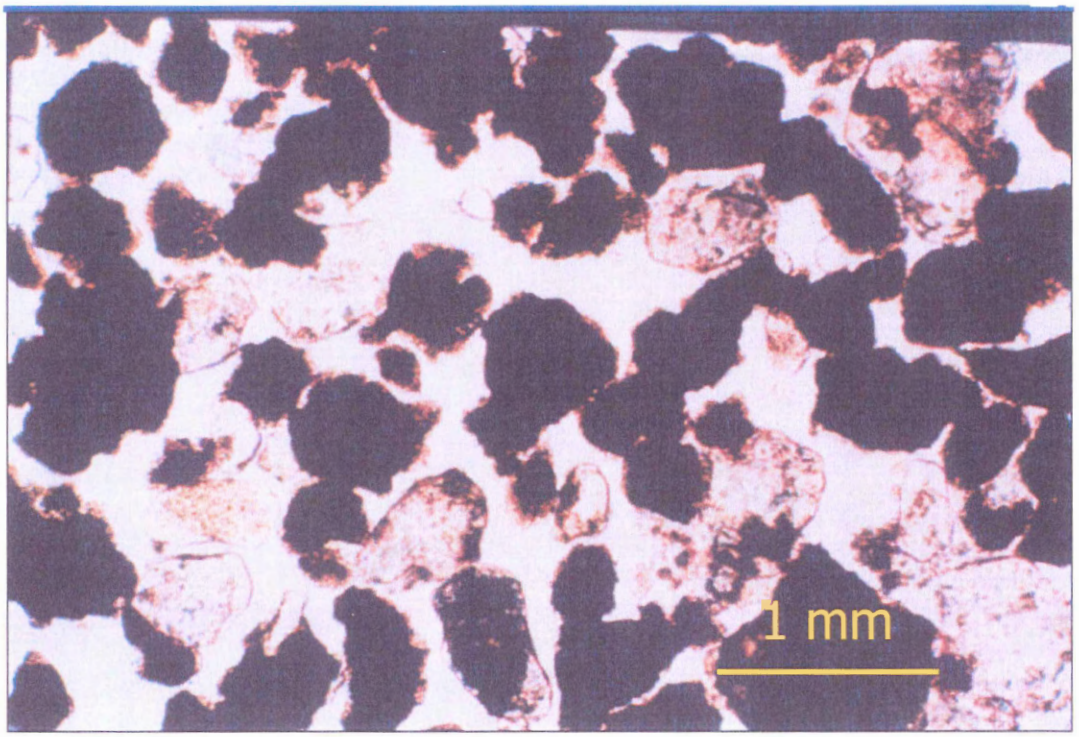

Figure 2.1 – Transmitted light microscope image of reworked pedogenic mud aggregates (dark grains) and quartz grains from the Cooper Creek floodplain in the Lake Eyre Basin. Courtesy of the late B.R. Rust.

2.1.2 Aggregate Transport Mechanism

Traditionally, most fluvial systems in the geologic record have been thought to transport mud in suspension. In calm flow conditions, suspension settling results in weakly laminated to structureless mud deposits. As clay drops out of suspension, mud will accumulate in channel deposits or as overbank deposits on flood plains (Rust and Nanson, 1989). The transport of pedogenic mud aggregates has recently been proposed as an alternate explanation for some mud and mudstone deposits. Higher energy river systems are now recognized to be capable of transporting aggregated mud as bedload in the form of sand-sized pedogenic aggregates.

Several studies of pedogenic mud aggregates have been carried out in the Lake Eyre Basin, Central Australia. This location is ideal for interpreting the morphology of the aggregates, because they are actively forming in the flood plains and are being transported by the river systems. Three major rivers drain the eastern and northern parts of the Lake Eyre Basin; they involve braided and anastomosing systems and transport mainly mud (Rust and Nanson, 1989). One of the rivers, Cooper Creek, contains what was initially believed to be mud-draped braided bars, meaning that the bar forms were believed to be composed entirely of sand with a thin coating of overlying mud due to later flooding events. Further investigation showed that surficial braids had no relation to underlying sand sheets; mud cover was much too thick for surficial features to reflect those of the underlying sand (Fig. 2.2) (Nanson et al., 1986). In order for these mud bars to have formed, the mud aggregates must have been transported as bedload, just as sand-sized quartz is transported and deposited under similar fluvial conditions. Maroulis and Nanson (1996) conducted a flume study designed to test sediment transport and bedform development under differing flow conditions, using mud aggregates taken from the floodplain of Cooper Creek. The results of this study showed that mud aggregates have sufficient stability to

A

B

Figure 2.2a and b - (A) Aggregated mud from channel deposits at Cooper Creek, central Australia, penny for scale. (B) Aerial photo of the Cooper Creek floodplain, braided fluvial system with large (pale) braid bars composed entirely of mud aggregates. Note anastomosing channel in foreground.

develop primary bedform structures typical of sand-sized quartz grains, including such features as plane beds, ripples, and antidunes (Fig. 2.3a, b). Aggregate stability during transport is attributed to calcium ions present in the soil and the large electrostatic attraction between clay sheets (Maroulis and Nanson, 1996).

Maroulis and Nanson's flume study has suggested that mud aggregates with a mean d_{50} (grain diameter) of 0.13 mm are readily transported and deposited as rolling bedload in a manner similar to fine siliciclastic sand. The observed bedforms and migration generally occurred at lower stream velocities than would be required for migration of the equivalent sized quartz sand. The high rates of transport and mobile nature of the aggregate is attributed to the aggregate having a lower density than equal sized quartz sand (Maroulis and Nanson, 1996).

It is uncommon for high sinuosity anastomosing and low sinuosity braided channel systems to coexist as they do in Central Australia (Fig. 2.2b) (Maroulis and Nanson, 1996). Anastomosing rivers are active during low to moderate flow and braided systems are active during high velocity flow over flood plains during major floods (Nanson et al., 1986). Anastomosing channels are expected to form in such clay-rich sediment. Braided channels typically require steeper gradients to form; however, the low density of the mud aggregates has resulted in braid-like channels forming at lower slopes than would normally be expected.

2.1.3 Aggregate Preservation

A major problem associated with studying pedogenic mud aggregates in the geologic record is the low potential for preservation. Sediments containing large proportions of mud easily lose their structure due to burial and compaction (Gierlowski-Kordesch and Gibling, 2002). Low likelihood for preservation leaves one to conclude that, upon burial, mudstone

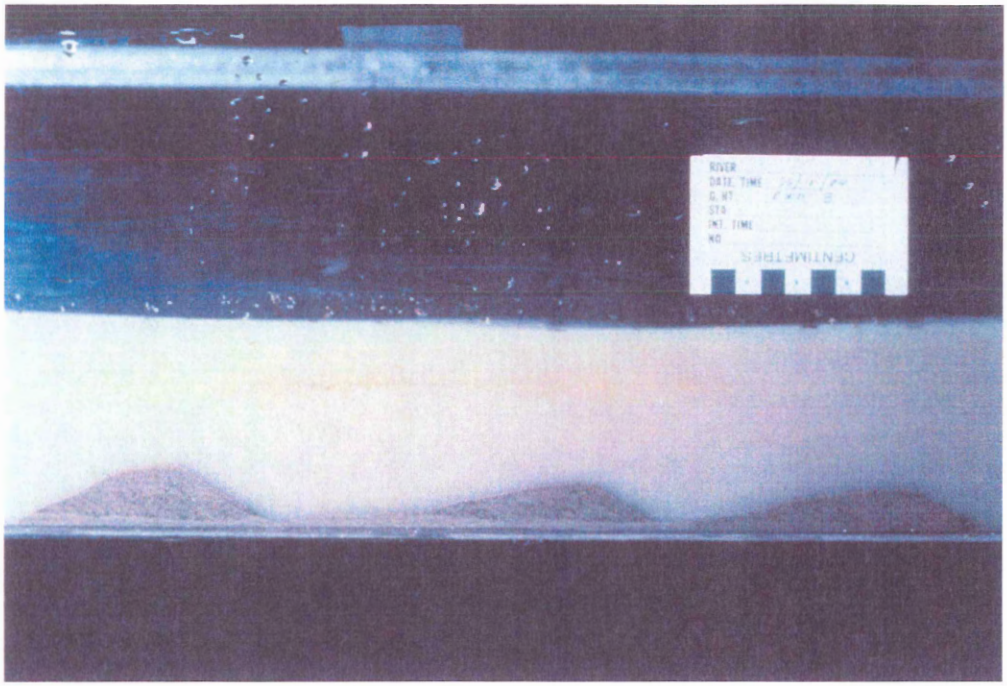

Figure 2.3a – Mud aggregates taken from the Cooper Creek floodplain, in a flume forming asymmetrical ripples.

Figure 2.3b – Dune composed largely of mud aggregates from Cooper Creek channels, showing development of primary bedform structure. Cut through bedform shows alternate dark laminae (aggregates) and pale laminae (quartz-rich).

composed of aggregate material will lose most or all of the structures initially present in the material. All obvious indication of bedload deposition is lost. Rust and Nanson (1989) noted that the aggregate texture becomes obscured with depth and is difficult to see at burial depths of 2 m in the floodplain soils of Cooper Creek. Preservation potential can increase during burial under certain conditions, if aggregates become isolated between framework minerals such as quartz in sand, and through the process of early cementation (Gierlowski-Kordesch and Gibling, 2002). Framework minerals and cementation reduce the degree of compaction the mud experiences during burial. Evidence for the presence of mud aggregates is also indicated where bedforms are preserved in mudstone. Bedforms are traction structures and cannot form through suspension settling (Rust and Nanson, 1989). In studies of the Triassic Lunde Formation, northern North Sea, Müller et al. (2004) found well preserved aggregate textures at burial depths of 2500-3000 m. Although such preservation could be attributed to high overpressure in an area, reducing the effective stress and limiting the degree of compaction, overpressure is considered to have been too low in this case to explain the preservation of mud aggregates (Müller et al., 2004). Müller et al. (2004) suggested that, like other delicate structures (burrows, root structures), aggregates have greater chance for preservation if they survive shallow burial. A poor to moderate degree of paleosol development is indicative of high sedimentation rates. High sedimentation rates are believed to reduce the likelihood for pedogenic overprinting and soil modification, therefore increasing the preservation potential of mud aggregate texture in the Lunde Formation (Müller et al. 2004). Cooper Creek, on the other hand, experiences slow sedimentation rates, reducing the probability that aggregates will survive shallow burial.

2.1.4 Alternate Explanations

Processes, other than pedogenesis, exist that may form textures similar to that of the mud aggregate texture. Features formed by these processes include, pellets found in aeolian dunes, eroded mud fragments, clay precipitated into cavities, clay-rich lithoclasts, and fecal pellets. Each feature forms in a different way and usually contains some characteristic that distinguishes it from pedogenic mud aggregates.

Aeolian clay pellets typically occur near saline pans, and their origin is related to mud desiccation in the presence of saline ground water, followed by aeolian reworking (Nanson et al., 1986). Maroulis and Nanson (1996) found salt to be unimportant for aggregate formation on the Cooper Creek floodplain, where total solute concentrations in waterholes and floodplains are on the order of 100 ppm or less. This salt concentration is insufficient to be a major factor in aggregate development. Aeolian clay pellets form in strongly seasonal environments associated with high wind speeds. The clay pellets form on occasionally flooded lake floors, where saline surface and ground waters flood the lake floor during the wet season. During evaporation, the salts loose water and the drying clay surface breaks up into irregular clay fragments of varying sizes (Dare-Edwards, 1982). The pellets are then transported by wind through saltation and surface creep, finer pellets move as suspended load. Eventually the pellets accumulate in the form of dunes and loess-sheets. According to Dare-Edwards (1982), during pedogenesis clay pellets collapse and fuse and salts are leached. Essentially, the pellets gradually lose their form with soil formation.

Clay-rich lithoclasts form in sandstones by means of diagenetic alteration of minerals like feldspars and volcanic glass. According to Rust and Nanson (1989), these unstable clay-rich clasts are rapidly eliminated from most deposits other than immature sandstones by compaction

during burial. If these lithoclasts are present, their size distribution should be similar to other grains and the lithoclasts should not be sorted into strata (Rust and Nanson, 1989).

No petrographic criteria currently exists to distinguish between eroded mud fragments and pedogenic aggregates (Gierlowski-Kordesch and Gibling, 2002). However, large abundance of aggregates in a sample and uniform size distribution of these aggregates supports a pedogenic rather than erosional origin.

Dissolution of carbonate or evaporite material will leave open cavities in rock, where clay can then deposit. These clay-filled pores are unlikely to be confused with aggregates because the textures should be distinctive of pore-filling cement, for example pores may exhibit a texture containing radial fibers (Rust and Nanson, 1989).

Whereas fecal pellets may appear similar to fine aggregates, they are unlikely to be confused with mud aggregates where the latter are abundant. There would have to be strong independent evidence of biogenic activity in an area for this option to be considered, and the pellets might be expected to occupy recognizable burrows locally.

2.2 Regional Geology

During the Carboniferous Period, sediments were actively accumulating in a complex of rapidly subsiding basins which have come to be known as the Maritimes Basin (Browne and Plint, 1994; Davies and Gibling, 2003). Today, the Maritimes Basin is located in Atlantic Canada, but during Carboniferous time, the basin lay in paleoequatorial latitudes (Davies and Gibling, 2003). The Cumberland Basin (Fig. 2.4) is the westernmost sub-basin of the larger Maritimes Basin where active subsidence, accompanied by high sedimentation rates, was associated with strike-slip faulting from late Devonian to Early Permian times (Gibling, 1987; Falcon-Lang, 2003). The basin is bounded by major strike-slip faults and experienced both rapid

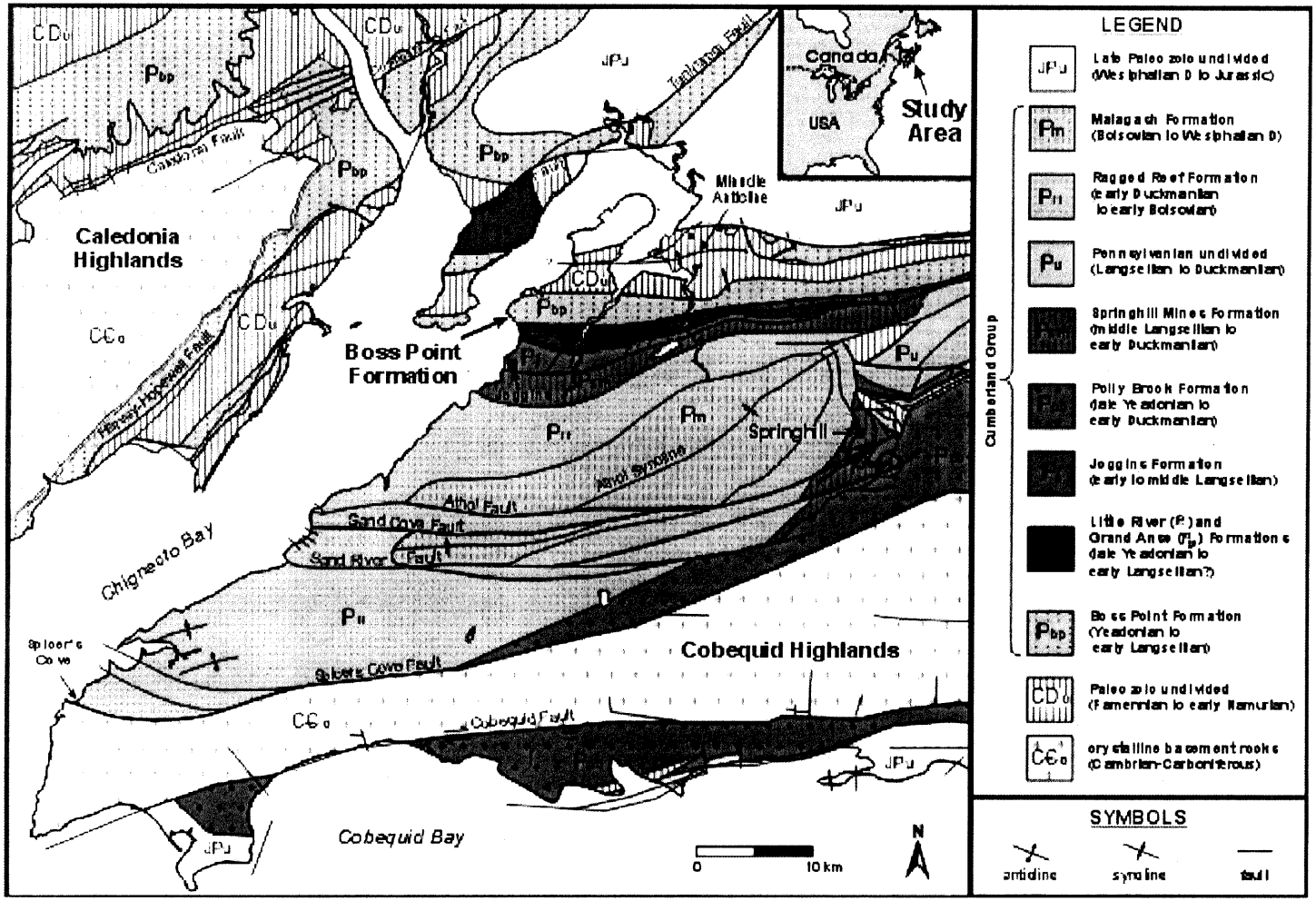

Figure 2.4 – Geological map of the western Cumberland sub-Basin. The main area of interest, Boss Point Formation, is indicated on the map. The Little River Formation is located directly below the Boss Point Formation and is denoted by P_b, Calder et al., submitted.

subsidence and transpressional uplift, particularly during the Mississippian and Pennsylvanian (Plint and Browne, 1994).

The Cumberland Basin contains a 7 km thick succession of Upper Devonian to Lower Permian strata (Fig. 2.5) (Browne and Plint, 1994). Apart from the occasional marine highstand phase, the strata are continental in nature. Thick carbonate-evaporite cycles of the Visean Windsor Group are overlain by lacustrine and alluvial beds of the Visean to early Namurian Mabou Group. Later basin sedimentation, Namurian to Westphalian, is dominated by alluvial deposits. The Cumberland basin is bounded to the south by the Cobequid Highlands and the Cobequid-Chedabucto Fault. To the north, the basin is bounded by a basement horst on the Harvey-Hopewell fault near the Caladonia Highlands.

2.3 Boss Point Formation

The Boss Point Formation was deposited in the Cumberland Basin during the Pennsylvanian (early Westphalian), when the basin was located at 8° South latitude (Browne and Plint, 1994). Today, this formation can be found in southeastern New Brunswick and northern Nova Scotia. This 861 m thick formation has been interpreted by Browne and Plint (1994) to represent two major depositional facies associations, namely sandy braidplain and muddy lacustrine, which contain 16 depositional megacycles. One megacycle is defined by one braidplain package erosively overlying one lacustrine package. The base of each megacycle is defined by a sharp contact with the underlying braidplain package, with well-preserved bedforms in the sandstone underlying the mudstone (Plint and Browne, 1994). The braidplain facies association contains up to 90 m thick sandstone-dominated packages containing minor conglomerate and mudstone (Browne and Plint, 1994; Plint and Browne, 1994), and have been interpreted as multistory fluvial channel bodies deposited in a braidplain setting.

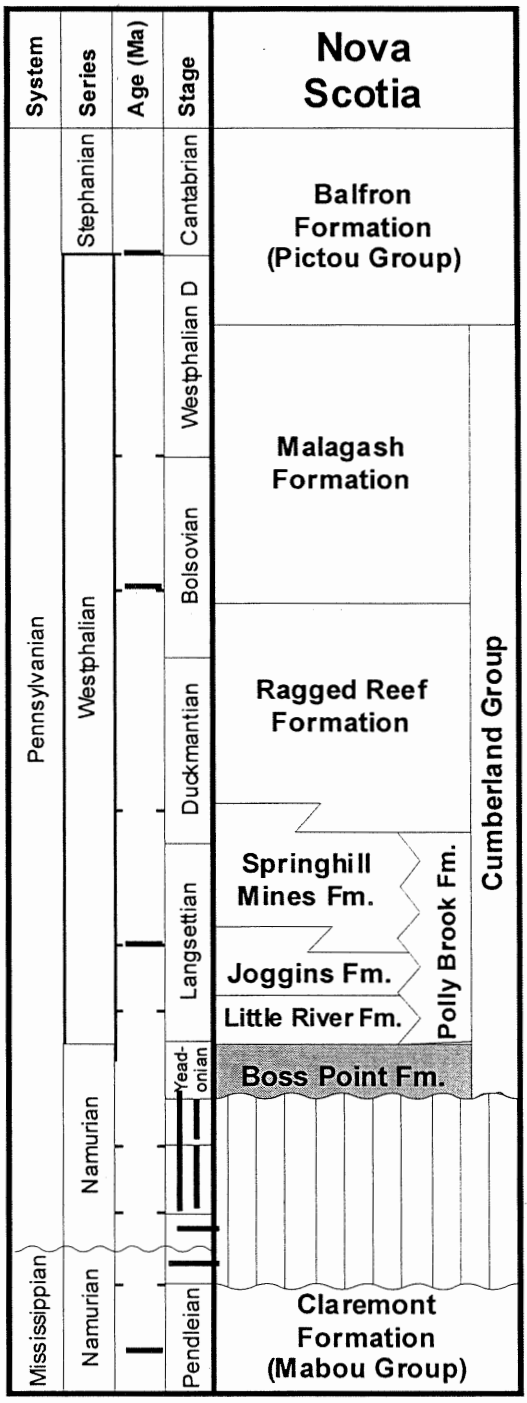

Figure 2.5 – Stratigraphic units of the Joggins costal section, from Calder et al. (submitted).

Occurrences of the lacustrine facies association are thinner, 50 m at most, and are mudstone-dominated strata with fine sandstone, thin coal, claystone, limestone, and abundant pedogenic horizons; they are interpreted to represent broad shallow lakes and lacustrine deltas (Browne and Plint, 1994; Plint and Browne 1994).

Conglomerate represents about four percent of the Boss Point Formation, and is concentrated around the Caledonia Highlands, near the margins of the Cumberland Basin. Browne and Plint (1994) argued that this distribution of conglomerate suggests that river gradients were steep near basin margins. Sandstone represents about 70% of the Boss Point Formation, and can be divided into 7 facies: trough-cross-bedded sandstone (dominant facies), pebbly sandstone, plane-laminated sandstone, ripple-cross-laminated sandstone, planar-tabular cross-bedded sandstone, sigmoidal cross sets, and hummocky cross stratification (Browne and Plint, 1994; Plint and Browne 1994). These sands are interpreted to be fluvial in origin, based on identified sedimentary structures, lack of marine plant and body fossils, abundant rooted pedogenic horizons, unimodal paleocurrent direction and evidence for changing water flow strength and depth (Browne and Plint, 1994). Browne and Plint (1994) noted that true channel widths are impossible to determine based on lack of continuous exposure; however they noted a channel scour at least 100 m wide, and depth of channel incision varied from 2.5 to 8 m. This seemingly high width:depth ratio is a strong indicator of a braided channel pattern, and the lack of abandoned channels, absence of levee deposits and low paleocurrent variance also supports a braided fluvial system (Browne and Plint, 1994).

A variety of paleosols have been identified by Plint and Browne (1994) in the Boss Point Formation, particularly in the lacustrine facies association. They include immature, aggrading paleosols through hydromorphic paleosols (gleys), carbonate soils and organic hydromorphic paleosols (peats/coals), as well as vertisols. The presence of vertisols and calcretes in the

lacustrine facies is evidence for variable climate with alternating wet and dry periods, resulting in a soil that periodically expands and contracts, destratifying the original soil (Plint and Browne, 1994). The "lacustrine" intervals high in the formation are composed largely of red floodplain deposits (not truly "lakes").

Plint and Browne (1994) suggested that the sharp transition from braidplain to lacustrine facies, as well as preserved bedform structures at the top of the braidplain packages, are good evidence for catastrophic subsidence. The Cumberland Basin is bounded by major faults, which are documented as being active during the Westphalian. Therefore, it is not unreasonable to interpret the base of each megacycle as an instantaneous non-erosive flooding event, associated with major earthquake activity (Plint and Browne, 1994). Megacycle thickness varies from 15 to 150 m, putting the emphasis on tectonic control, more episodic in nature, rather than solely on climatic control, which would be more cyclical. Plint and Browne (1994) proposed that Milankovitch cycles may have interacted with tectonic subsidence events by driving climatic oscillation between strong wet-dry variability and more humid conditions. Fluvial erosion at the top of the lacustrine facies association could be related to increased discharge during the transition from a humid climate with low degree of seasonality to a seasonally wet-dry climate (Plint and Browne, 1994).

2.4 *Little River Formation*

The Little River Formation is a recently proposed formation that redefines the lower portion of the Joggins Formation (Calder et al., submitted). The type section is located at Lower Cove near Joggins, Nova Scotia, just north and south of Little River. This 636 m thick section is interpreted as late Namurian to basal Westphalian in age and overlies the Boss Point Formation. The formation can be traced 30 km to the east along the Athol Syncline where it pinches out

between the underlying Polly Brook Formation and the overlying Joggins Formation (Fig. 2.5) (Calder et al., submitted).

The Little River Formation consists of 12 major channel bodies (>2 m thick). The channel bodies are an order of magnitude smaller than those of the Boss Point Formation and are generally composed of quartz- and calcite- cemented, very fine- to medium-grained feldspathic arenites (Calder et al., submitted). This formation is mudstone rich, more specifically the mudstone is red in colour and is composed of claystone and silty claystone. Preliminary interpretations suggest that the mudstones contain three types of paleosols: entisols, alfisols, and inceptisols (Calder et al., submitted). Development of calcic horizons is common in these soil profiles. Small channel bodies (<2 m) and thin sandstone sheets (<1m) are also common throughout the mudrock-dominated intervals.

The major sandstone channel bodies represent deposits of alluvial drainage channels that were characterized by moderate incision. The rivers experienced rapid, flashy flow, forming channel deposits that were shallow and broad in nature (Calder et al., submitted). Mudstones in the Little River Formation generally reflect oxidation and well-drained soil conditions. Drab haloed root traces, however, indicate that moisture conditions were sufficient to promote plant growth. Calcic-paleosol horizons, absence of coal beds, flashy paleoflow, and reddening of the mudstone in this formation are all indications of a seasonally dry climate during deposition (Calder et al., submitted).

3.0 Methods

3.1 Field Methods

Two days of field work were carried out during the summer of 2004 along the Joggins cliffs in Nova Scotia. The field study focused on the upper strata of the Pennsylvanian, Boss Point Formation and, to a lesser extent, a portion of the Little River Formation. These formations were chosen because a significant portion of the strata here are fluvial in nature with numerous braided channel deposits and floodplain mud intervals. Carbonate is prominent in these formations which is evident by the presence of carbonate nodules and calcrete paleosols in the strata. Carbonate is also indicative of semi-arid paleoclimate, analogous to present day Australia.

Figure 3.1 is an aerial photo of a portion of the Joggins cliffs indicating the three fieldwork locations where field observations were made and 24 samples collected for further analysis (Appendix B). Facies of particular interest to this study include fluvial channel sandstones, crevasse-splay sandstones, and floodplain mudstones. Field locations were chosen based on the likelihood that the strata contain some or all of these deposits. Because aggregates form on floodplains and are transported in fluvial channels, these facies represent the greatest probability of finding pedogenic mud aggregates.

Locality 1 was chosen because a broad channel body in the cliff face could be seen, along with a number of associated sandstone and mudstone beds (Fig. 3.2). Locality 2 was chosen based on initial recognition of calcrete-like soil development in several stratigraphic layers, in conjunction with small, siltstone and sandstone channel bodies in the predominantly mudstone strata of this area (Fig. 3.3). Locality 3 is a multi-story channel complex containing many mud and sand clasts (Fig. 3.4).

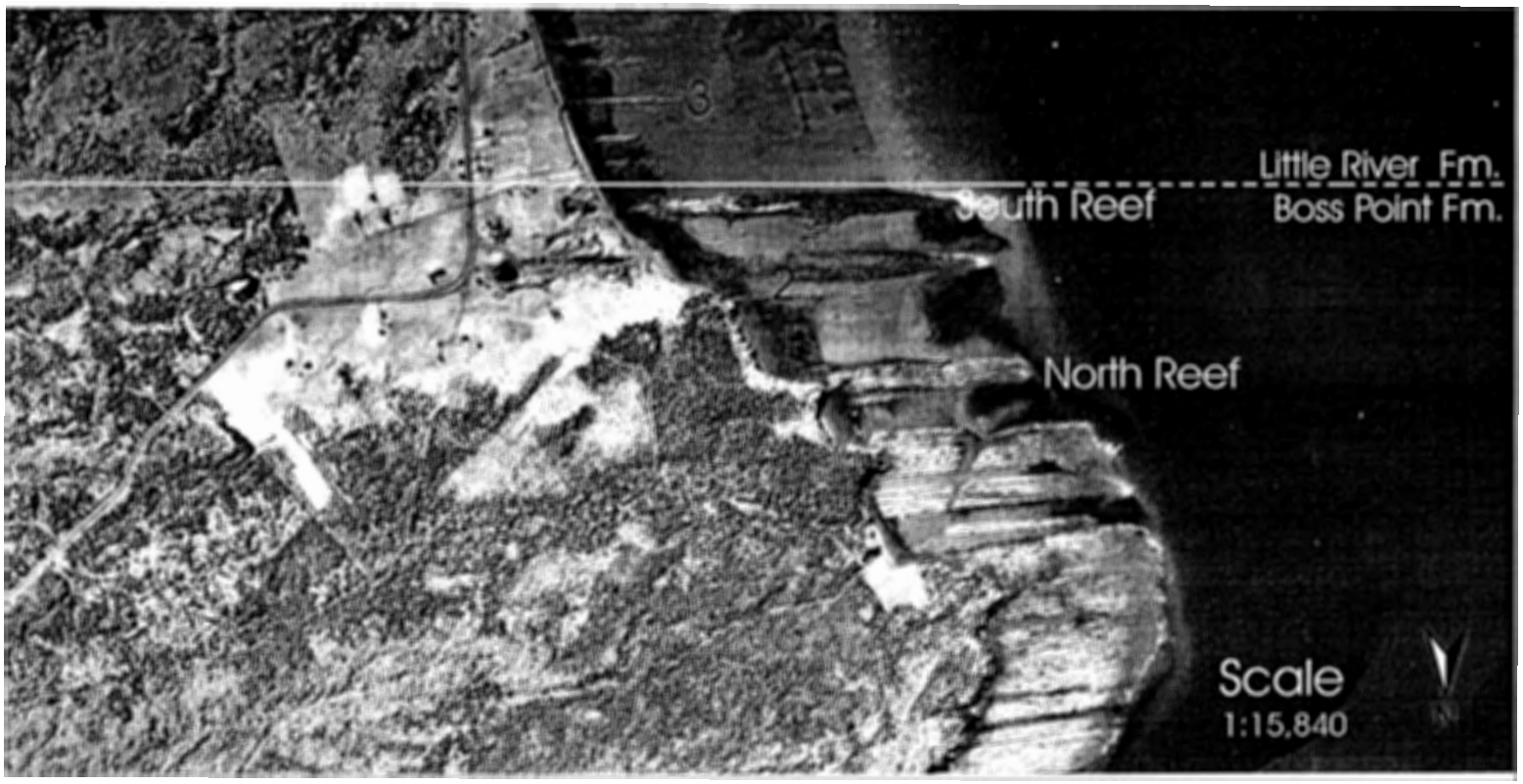

Figure 3.1 - Airphoto # A18580-121 from Joggins, Nova Scotia. This photo is taken along the Joggins cliffs at the contact between the Boss Point and Little River formations. Fieldwork locations are marked in black. Beds dip southward at about 31degrees. Light coloured areas on tidal platform and headlands are mainly sandstones, whereas modern tidal-flat muds overlie strata that are mudstone-dominated. Photo illustrates the upward transition of braided-fluvial sandstones of the Boss Point Formation to muddy floodplain deposits with small channel bodies of the Little River Formation.

Figure 3.2 – Field location 1 along the Joggins cliffs, Boss Point Formation. Photo shows broad channel body in the cliff face with associated floodplain mudstone and crevasse splay sandstone beds. Meter stick for scale.

Figure 3.3 – Field location 2. Image shows the site of the measured section along the Joggins cliffs, Boss Point Fm. Section consists of small siltstone and sandstone channel bodies in predominantly mudstone strata. Person for scale.

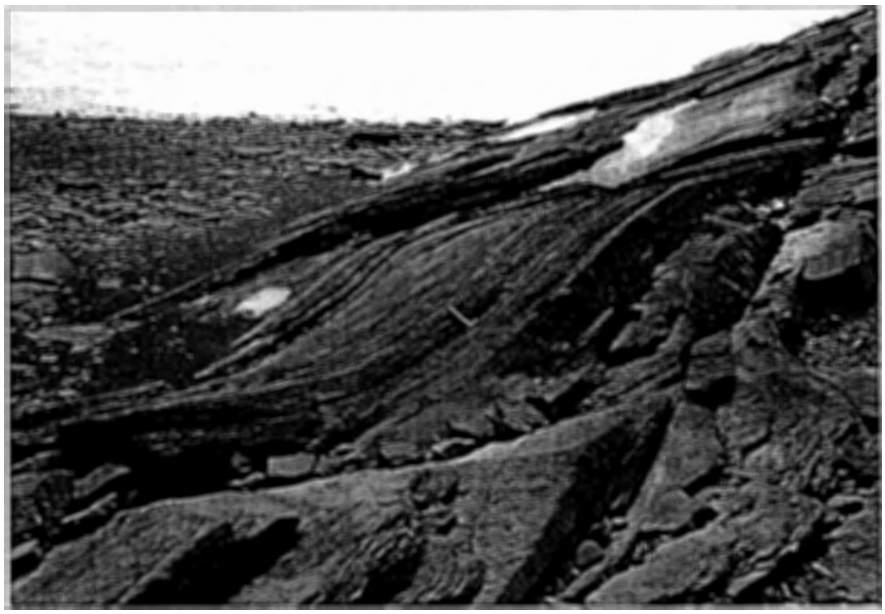

Figure 3.4 – Field location 3, Little River Formation. Large, sigmoidal bedform at 96 m of measured section found in figure 4.8, hammer for scale (image from Calder et al., submitted).

3.2 Petrography

All 24 hand samples gathered from the Boss Point and Little River formations during fieldwork were cut into thin sections for petrographic microscope analysis. Microscope work was conducted using a transmitted light microscope with magnifications of 6.3, 16, and 40x. All thin sections were initially studied, but in-depth microscope work was done only on those samples that clearly displayed the aggregate texture. The focus of the microscope work was placed on texture identification, percent and size distribution of aggregates, and the reasons for aggregate preservation.

3.3 X-Ray Diffractometer (XRD)

The XRD is an analytical tool used to determine the composition of crystalline substances, more specifically minerals. The instrument directs an X-ray beam at a sample that has been powdered and thinly distributed on a slide with acetone. The beam interacts with the sample at different angles and measures the diffraction of the beam as it encounters various mineral planes on the slide. Diffraction patterns produced by this technique are then compared to patterns stored in the computer's memory bank to identify compounds.

More detailed mineral identification was conducted using the method outlined by Cook et al. (1975). This method involves identifying peaks in the spectra that correspond with known mineral peaks. Each mineral has a diagnostic peak which can be used to produce a semi-quantative proportion of the minerals present in the sample. The diagnostic peak is measured from the top of the peak to the baseline on the spectrum. This peak height is then multiplied by a pre-determined intensity factor (Fig. 3.5). Once

Minerals Sought in Diffraction Data Analysis

Mineral	Window (°2θ, CuKα Radiation)	Range of D-Spacings (Å)	Intensity Factor
Calcite	29.25-29.60	3.04 - 3.01	1.65
Chlorite	18.50-19.10	4.79 - 4.64	4.95
Hematite	33.00-33.40	2.71 - 2.68	3.33
Kaolinite	12.20-12.60	7.25 - 7.02	2.25
Mica	8.70-9.10	10.20 - 9.72	6.00
Plagioclase	27.80-28.15	3.21 - 3.16	2.80
Quartz	26.45-26.95	3.37 - 3.31	1.00

Figure 3.5 – Minerals sought in diffraction analysis. Diagnostic peak for each mineral is given under window column. Intensity factors are determined in a 1:1 ratio with quartz; the intensity factor is multiplied by the diagnostic peak height to get the average mineral abundance present in an analysis. Modified from Cook et al., 1975.

this process has been completed for each identified mineral, the values obtained are converted to a percentage.

3.4 Environmental Scanning Electron Microscope (ESEM)

The environmental scanning electron microscope (ESEM) is located at the Bedford Institute of Oceanography in Dartmouth, Nova Scotia. The ESEM technique has a dual purpose in this study: 1) high magnification 3D imaging of the aggregates and their relationship to the surrounding sediment, and 2) chemical analysis of individual micron-scale grains and aggregates in the samples. Chemical analysis is carried out by the energy dispersive spectrometer (EDS), a device attached to the ESEM. Two samples were analyzed using ESEM and EDS, one siltstone and one mudstone. The siltstone, JG-2-7, was a difficult medium in which to find the aggregates. The lower aggregate abundance within Boss Point siltstones in general, and the very small scale at which the ESEM operates, made locating the aggregates a challenge. The quantity of aggregates present in the mudstone sample, JG-2-9, proved this to be the better of the two. The focus of this section will be placed on the mudstone sample, JG-2-9, from which 42 analyses were carried out.

Samples used in the ESEM were small rock fragments, approximately 5 by 10 mm in size with a fresh surface. Using a fresh, broken surface provides a much better 3D image of the rock surface. The fragments used in this study were not coated with carbon or gold, although coating the samples is common in ESEM studies. The EDS was set to 20 KV for this analysis. Interpretation of EDS spectra was carried out by comparing analyses from this study to those found within the SEM Petrology Atlas (Welton, 1984).

EDS spectra commonly showed a number of minor elements present among the dominant elements that composed the analyzed grain. These minor elements result from a combination of interference with chemical constituents from adjacent grains, mixed mineral assemblage of the analyzed grain, and cementing material. To reduce the amount to interference of nearby grains, careful grain selection was necessary, specifically through avoiding grains located in hollows.

3.5 Electron Microprobe

The electron microprobe at Dalhousie University is a fully automated JEOL 8200. It is equipped with 5 wavelength spectrometers, energy dispersive spectrometer (EDS), and a cathodoluminescence photomultiplier. The instrument provides chemical analysis of solid substances and provides imaging feedback in the form of secondary electron, backscattered electron, characteristic X-ray elemental maps, and cathodoluminescence.

For electron microprobe analysis in this study, elemental mapping was used. Elemental mapping scans a selected area for a specific element, or number of elements, and then provides an image showing the distribution and relative abundances of that element. Prior to scanning, the microprobe slides were cleaned in acetone and carbon coated. Using a petrographic microscope, areas containing mud aggregates were pre-selected. The selected areas were found and scanned on the microprobe. Titanium, potassium, magnesium, aluminum, iron, calcium, and silicon were selected for analysis. Calcium and silicon were scanned with the EDS, the five other elements were scanned with the wavelength spectrometers. Aluminum and potassium were selected because they are the major elements in illite. Titanium and iron were selected to isolate heavy

minerals; silicon to identify quartz; and calcium and magnesium to identify cementing material.

Scans were set with the following parameters:

Table 3.1 – Microprobe Parameters

Settings for figures with 50 μ scale bars	Settings for figures with 10 μ scale bars
Stage Scan Acc. V 15.0 Kv Probe C 5.023e-08Å Probe Diam. 1μ Dwell (ms) 20.00 Direction: Single Points 350*350 Interval (μ) X: 1.00 Y: 1.00	Stage Scan Acc. V 15.0 Kv Probe C 4.996e-08Å Probe Diam. 0 μ Dwell (ms) 12.00 Direction: Single Points 256*256 Interval (μ) X: 0.30 Y: 0.30

Due to the very small size of the aggregates (10-20 μ), it proved difficult to identify (image) them under the probe, even using photographs to guide the site selection. So, the mapping method was employed as a less direct but more comprehensive approach to analysis.

3.5.1 Combination Maps

One of the benefits of the electron microprobe is the ability to manipulate obtained data in a number of different ways. One method of data manipulation (when working with elemental maps) is creating combination maps from the original map scans. Two to three elements are selected and then combined to form a map that shows the distribution of these elements with respect to one another - where these elements co-exist and where they remain secluded. The distribution of illite and quartz is of primary concern to this study, so aluminum, potassium, and silicon were selected to create

combination maps for this section. Each original element is assigned a colour, in this case, potassium is red, aluminum is green, and silicon is blue. When these maps are combined, areas containing only one of the above mentioned elements will be displayed with its assigned colour. Areas containing a combination of 2 or 3 of these elements will be displayed as a unique colour assigned to that specific combination of minerals.

4.0 Stratigraphic Interpretation

4.1 Facies Description and Interpretation

Table 4.1 divides the strata from the three field locations (Fig. 3.1) of the Boss Point and Little River formations into six different facies, which are described in the following text.

4.1.1 Large Channel Bodies (facies A)

Large channel bodies are present at all three field locations. Locations 1 and 3 contain large channel bodies, whereas the section at location 2 is composed mainly of small channel bodies, but is bounded above and below by larger channel bodies. The grain-size of the sediment in the large channel sands ranges from fine to coarse, and the channel sequences range from approximately 2 - 5 m in thickness. The sandstone contains well-developed trough cross-stratification in locations 2 and 3, but has lost structure in location 1, where the bottom of the channel contains a large, oxidized slump block.

The channel body at location 1, exhibits no signs of lateral migration, and appears to have accreted vertically. At location 2, several large, shallow channel elements are present within the body, suggesting that these channels existed as part of a larger braided fluvial system. Location 3 includes a sandy conglomerate containing sub-angular mudstone fragments. This unit is part of a multi-story channel complex, as is the channel body at location 1.

Table 4.1 - Facies description with reference to stratigraphic log at site 2 (Fig. 4.7) and image of traced bedforms at site 1 (Fig. 4.6)

Facies	Bed ID	Location	Colour	Grain Size	Sedimentary Features / Fossils	Thickness	Interpretation
(A) Large Channel Bodies	20	Location 2	grey	medium sand	Sandstone, large bedforms, cross stratification	3m	Large channel sandstone, braided stream
	B, C, E, D	Location 1	red/brown, some mottling	very fine to fine sand	Channel sand, locally destratified, oxidized, no lateral migration. Climbing ripples, trough cross stratification (2-4 cm sets) in sandstone with interbedded mudstone	2.5m	Slump block in channel body, oxidized by soil forming processes. Erosionally based sand sheets and lenses.
		Location 3	white	medium-coarse sand	Conglomerate with sand matrix and sub-angular mud/silt fragments. Erosional base, cross stratification.	4m	Represents a multi- story channel complex.
(B) Small Channel Bodies	19c	Location 2	red	coarse silt	Siltstone, local channel fills	0.8m	Small floodplain channels.
	18	Location 2	red	coarse silt/ very fine sand	Bedforms, ripple marks (paleo flow 4˚), mudstone interbeds.	1m	Channel sandstone with interbedded floodplain mudstones. Channels cut into floodplain muds.
	14	Location 2	red and grey (mottled)	coarse silt	Slightly undulating top, poorly developed soil, root traces, small channel forms.	0.7m	Small floodplain channels.
	12	Location 2	red	coarse silt/ very fine sand	Low angle channel forms, adhesion structures, cross stratification, ripple marks, mudstone interbeds.	0.6m	Channel siltstone/sandstone with interbedded floodplain mudstone. Channels cut into floodplain muds.
	8	Location 2	red	coarse silt	Ripple marks (paleo flow 288˚, 315˚), small channel forms, adhesion structures, some interbedded mud. Tetrapod trackway.	0.3m	Small floodplain channels with interbedded floodplain mud . Channels cut into floodplain muds.
	6	Location 2	red	coarse silt/very fine sand	Siltstone thickening laterally to very fine sand channel body.	0.4m	Channel sandstone with crevasse splay siltstone.

Table 4.1 - Con't

Facies		Bed ID	Location	Colour	Grain Size	Sedimentary Features / Fossils	Thickness	Interpretation
(C) Calcrete		Base of strat section	Location 2	red	very fine to fine sand	Irregular undulating surface (20 cm relief), carbonate nodules, carbonate cement, root traces, adhesion structures, plant fossils, rain prints.	>2m	Carbonate soil developed on top of a large sandstone channel body
(D) Mudstone	Structurless mudstone	19b	Location 2	red, minor mottling	mud	structureless mudstone	2.4m	Floodplain mud
		7	Location 2	red	mud	structureless mudstone	0.55m	Floodplain mud (overlying channel sand unit).
		3	Location 2	red	mud	structureless mudstone (20% exposure)	1.0m	Floodplain mud
	Rubbly mudstone	19d	Location 2	red	mud	Rubbly, desication cracks filled with dark organic material and conchoidal weathering found in upper region.	0.45m	Floodplain mud (overlying channel sand unit), developing into a soil profile.
		15	Location 2	red with grey drab mottles	mud	Rubbly, few interbedded dark shales with plant fragments. Developing weak silty stratification in upper region.	3.6m	Floodplain mud that developed into a soil, upper stratification likely related to gentle overbank flood. Lower bed developed as abandoned channel fill deposit.
	Mottled mudstone	13	Location 2	red, mottled	mud	structureless mudstone, with abundant grey mottling.	0.35m	Floodplain mud (overlying channel sand unit).
		5	Location 2	red, mottled	mud	structurless mudstone, with abundant grey mottling.	0.55m	Floodplain mud (overlying channel sand unit).
	Laminated Mudstone	11	Location 2	red	mud	Mudstone interbedded with thin silt layers.	1.7m	Floodplain mud with interbedded crevasse splay deposits

Table 4.1 - Con't

Facies	Bed ID	Location	Colour	Grain Size	Sedimentary Features / Fossils	Thickness	Interpretation
(E) Siltstone and sandstone sheets	19a	Location 2	red	coarse silt	structureless siltstone	0.2m	
	19e	Location 2	red	coarse silt	structureless siltstone	0.6m	
	17	Location 2	red	mud	Muddy bed transitioning into a coarse siltstone	1.65m	Floodplain mud transitioning into a crevasse splay deposit.
	4	Location 2	red	coarse silt	structureless siltstone	0.1m	Crevasse splay silt (overlying floodplain mud).
	2	Location 2	red	coarse silt	cross stratification, poorly developed ripple cross-lamination, scour marks	0.1m	Crevasse splay deposit
	H	Location 1	dark grey to brown/red	very fine sand	Sandstone with very fine clay lenses	0.1-0.4m	Crevasse splay sandstone with interbedded floodplain muds.
(F) Abandoned channel fill	F, G	Location 1	Grey	mud	Structureless mudstone, with some sandy layers	0.4-2m	Abandoned channel fill
	1	Location 2	red with some grey (mottled)	coarse silt/ very fine sand	Carbonate cement, mudstone filling in small channels on top of sandstone, root traces, joint sets, conchoidal weathering, generally structureless.	2.2m	Abandoned channel fill, developing into a soil profile.

4.1.2 Small Channel Bodies (facies B)

The small channel body facies contains coarse silt to fine sand-sized sediment. The channel bodies comprise planar bedsets typically 0.3 - 1 m in thickness and up to a few meters in apparent width. Strata are red in colour, and often retain a grey mottled appearance. Sedimentary features common to this facies are scour fills, cross stratification, ripple cross-lamination (from which paleo-flow direction is obtained), and sand adhesion structures (Fig. 4.1a and b). Thin interbedded mudstone layers are also common throughout this facies. Occasional units contain root traces, as well as undulating surfaces (20 cm relief) which indicate either some degree of erosion or soil erosion, possibly pseudo-anticline formation. One bed contains a tetrapod trackway (Fig. 4.2).

This facies contains variable proportions of siltstone, sandstone, and mudstone, and is interpreted to represent small floodplain channels within floodplain mudstone intervals. In some intervals, the channel sands/silts have been modified into poor to moderately developed soil horizons, in which root traces and mottled appearance are evidence of pedogenic development.

4.1.3 Calcrete (facies C)

Location 2 contains evidence of calcrete soil development within the top of a single stratigraphic unit composed of a large sandstone channel body. Sedimentary features present in this deposit include conchoidal weathering, adhesion structures, rain-drop imprints, plant remains, and carbonate nodules (Fig. 4.3). The deposit also shows significant calcareous cementation.

Figure 4.1a – Truncated cross-sets preserved in siltstone, found at location 2 (facies B). Lens cap for scale is 6 cm in diameter.

Figure 4.1b – Sand adhesion structures found on upper surface of siltstone bed in field location 2 (facies B). Lens cap for scale is 6 cm in diameter.

Figure 4.2 – Tetrapod trackway in siltstone bed found in field location 2, bed also contains ripple cross-laminations (facies B). Lens cap for scale, 6 cm in diameter.

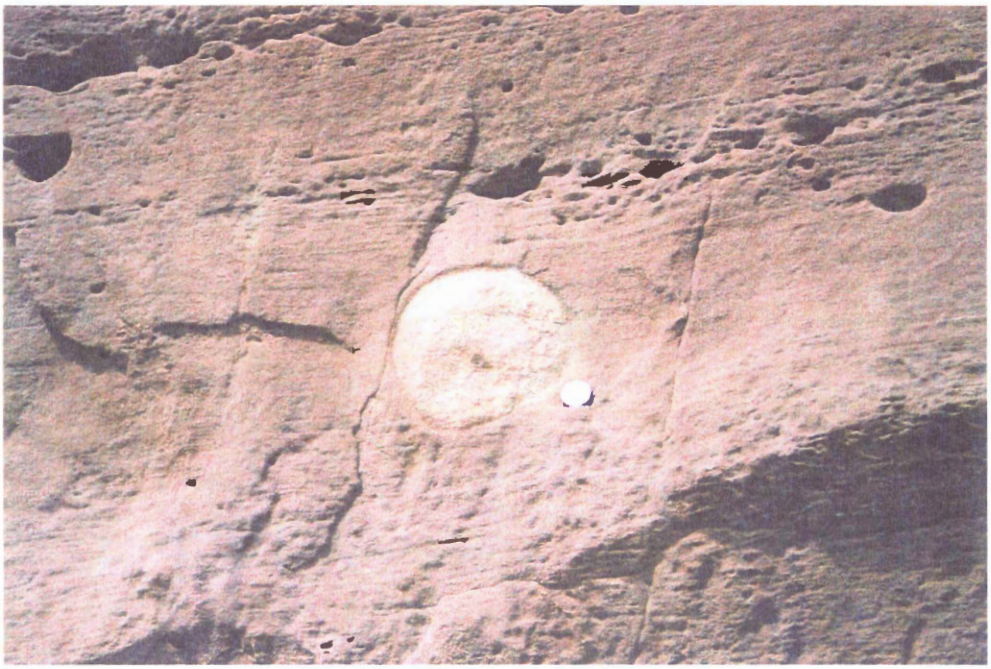

Figure 4.3 – Carbonate nodule in channel sandstone at field location 2 (facies C). Quarter for scale, 2.4 cm in diameter.

A calcisol is a paleosol in which a calcite-rich horizon is the prominent pedogenic feature. The term "calcrete" is a more specific term that refers to terrestrial deposits of calcium carbonate that have accumulated in or replaced a pre-existing soil, unconsolidated deposit, or weathered rock material, to produce an indurated calcic soil or pedogenic calcrete (Machette, 1985). Calcic soils, known to form in arid to semi-arid climates, are characterized by a layer of secondary carbonate that is enriched in comparison to the soil's parent material. According to Machette (1985), calcic horizons range from layers of carbonate-coated pebbles or carbonate-coated filaments and nodules, to thick, massive, and indurated carbonate-enriched layers. Carbonate coated grains and coalesced carbonate nodules, present in Boss Point strata, correspond to stages 1 to 3, respectively, of the six stage, morphology based classification scheme described by Mack et al. (1993).

The original sediment appears to have been modified into a moderately developed soil horizon. Horizons with significant secondary calcrete are known as the "K" horizon. These K horizons are usually a component of the B horizon and are more easily distinguished when accompanied with the A and C horizons, the common horizons found in soil profiles (Machette, 1985; Mack et al., 1993). The A horizon in Boss Point paleosols is not easily distinguishable and may not be present at all. In the Moor Cliff Formation of Wales, the upper soil horizons in the calcic vertisols are generally not present in the soil profiles, yet other pedogenic features exist in the strata allowing for a paleosol classification (Marriott and Wright, 2004). The calcic deposits of the Boss Point Formation can be interpreted as calcrete soils, where calcite cement and large carbonate nodules are evidence for stage 1 to 3 morphology. Mottled appearance, root traces, and

plant remains in the sediment are also strong evidence of pedogenic processes. Carbonate soils require a prolonged period of soil accumulation in order for the K horizon to develop. Thus, the top of the basal channel body at location 2 marks a period of landscape stabilization.

4.1.4 Mudstone (facies D)

The mudstone facies can be divided into a number of sub-facies based on sedimentary features present in the mud-dominated strata: structureless mudstone, rubbly mudstone, mottled mudstone, and laminated mudstone.

4.1.4.1 Structureless Mudstone

Strata are red and range from approximately 0.5 - 2.4 m in thickness. The mudstone contains very little structure and some beds are poorly exposed. This sub-facies is interpreted to represent floodplain mudstone based on its relationship with the surrounding strata, including underlying and overlying sequences of crevasse splay deposits and siltstones containing small channel bodies. The structureless nature of this mudstone suggests pedogenic modification, although poor exposure precluded a fuller analysis.

4.1.4.2 Rubbly mudstone

Rubbly mudstone comprises mainly red beds with some grey mottling. Mudstone beds range from 0.5 – 3.6 m in thickness and are rubbly in nature. There are two occurrences at site 2 where the rubbly texture is prominent, the mudstone above the large

channel body (base of bed 1) and above small channel body comprising coarse silt and very fine sand (bed 15a). Rubbly refers to the fragmental nature of the mudstone, it breaks up easily when removed from the outcrop. This rubbly nature may be the result of patchy cementation, making this facies more susceptible to weathering, or the deposit could have been originally formed of detrital mud fragments. A few interbedded dark shales with plant fragments are found in this facies and represent organic layers (Fig. 4.4). In figure 4.4, having been filled in with overlying dark shale material, deep desiccation cracks are visible in the lower red mudstone bed. Weak, silty stratification is present in the upper part of one of the two rubbly mudstone beds found at field locality 2.

This sub-facies is interpreted to be floodplain mudstone that matured into a soil horizon. The rubbly texture formed as a result of soil processes and desiccation. Occurrences directly above channel bodies may be part of abandoned channel fills. The stratification in the upper part of the facies is attributed to the gentle overbank flooding of nearby channels.

4.1.4.3 Mottled Mudstone

This sub-facies contains beds that are red with distinct drab mottling. Strata range from 0.3 - 0.6 m in thickness and are generally structureless. Mottling is also common in the pedified units of the Moor Cliff Formation of southwest Wales, where the mottled appearance is related to the oxidation/reduction potential of plant roots, burrowing activity, and past submersion of the sediment in water (Marriott and Wright, 2004). The mottled mudstone sub-facies is interpreted to be floodplain mudstone that experienced pedogenic modification during and after deposition, resulting in a mottled appearance.

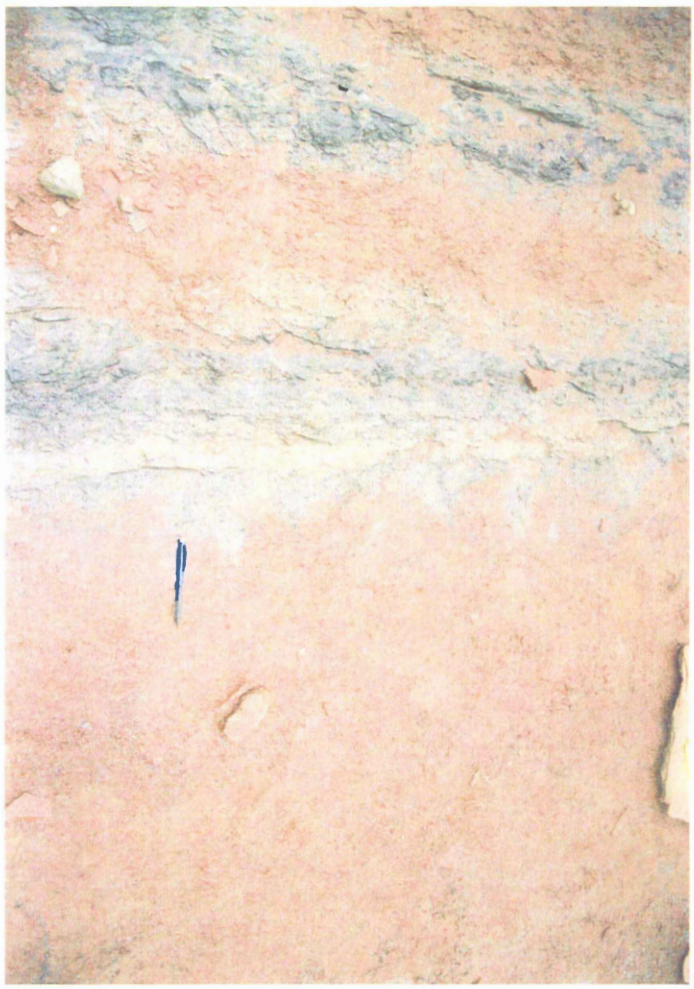

Figure 4.4 – Organic layering in mudstone, with a network of organic material permeating downward into a desiccation cracked surface (field location 2, facies D). Pen for scale, 14 cm long.

4.1.4.4 Laminated Mudstone

The laminated mudstone sub-facies is red and contains thin interbedded sand/silt layers (a few mm to a few cm thick). The thin sand/silt layers found within the floodplain mudstone are formed by overbank floods and crevasse splays that periodically spread over the floodplain.

4.1.4.5 Mudstone Interpretation

These strata were deposited in a flood-dominated environment, where mud deposition is attributed to seasonal flooding events. Many of the sub-facies previously discussed show some evidence of soil development. These paleosols appear to be gleyed protosols according to the classification scheme of Mack et al. (1993). Figure 4.5 shows a flow chart of the paleosol orders based on the most prominent sedimentary feature. A protosol is characterized by weak development of soil horizons unrelated to homogenization by pedoturbation (Mack et al., 1993). The soils studied here have poor horizon development but contain other characteristics typical of soils: root traces, plant fragments, and significant mottling. The grey mottled appearance that many of the mudstones display, some more than others, results in the modifier "gleyed" being added to the soil classification "protosol". Gleyed describes a horizon with a mottled appearance, suggesting that many of the muds experienced low redox conditions (Mack et al,. 1993). This condition commonly develops in areas with a high or fluctuating water table.

Because this environment is flood-dominated, soil development is likely the result of a cumulative sedimentation processes. With each flooding event, newly deposited

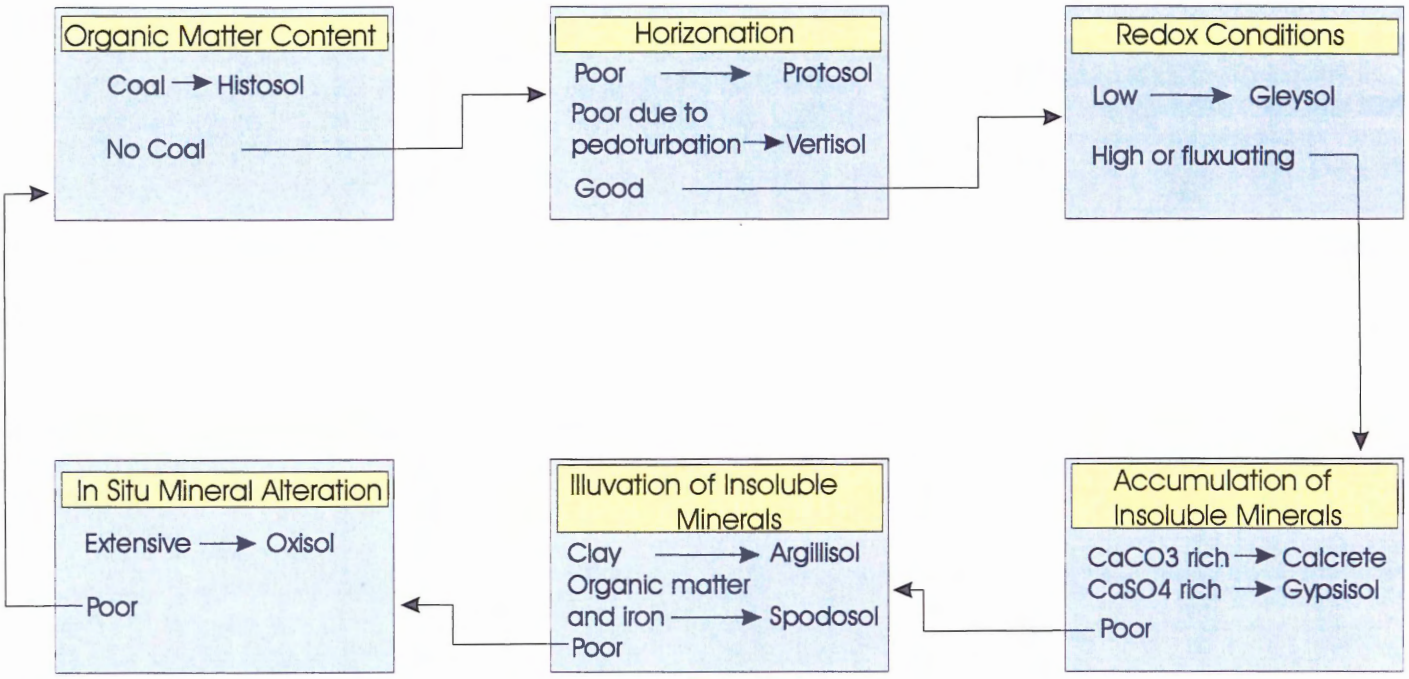

Figure 4.5 - Flow chart of paleosol orders based on the most prominent sedimentary feature or process in a rock unit. The prominent sedimentary feature is listed in the yellow box and subsequent descriptions are listed below. Modified from Mack et al. (1993).

sediments become worked into the continually maturing soil. Where increments of sediment are added to the surface in small amounts, the soil moves effectively upward abandoning lower levels where little further pedogenic activity will take place (Marriott and Wright, 2004). In this situation, carbonate activity and nodule development, as well as continued disruption by vegetation, may begin to occur in what would have originally been considered the upper soil horizon of earlier formed soils, and this can cause overprinting or destruction of the original horizons.

Evidence for vertisol development is present in some of the red mudstones found at site 2. Conchoidal weathering, deep desiccation cracks, joint sets, drab mottles, and structureless form can all be attributed to vertisol development. In the Mack et al. (1993) classification, illustrated in figure 4.5, the prominent sedimentary feature listed for vertisol development is described as poor horizonation due to pedogenesis. Mudstone deposits lacking structure at site 2 could be the result of complete disruption of the sediment during soil formation. Undulose surfaces detected in several beds may represent pseudo-anticlines or gilgai soil relief. Ekes (1993) likened the undulose surfaces found in the Ridgeway Conglomerate Formation of southwest Wales to gilgai found in clay rich alluvial soils. The above mentioned sedimentary features, in conjunction with Plint and Browne's (1994) description of slickensided surfaces, pseudo-anticlines, and desiccation cracks within the Boss Point Formation, provide good evidence for vertisol development.

4.1.5 Crevasse Splay Deposits (facies E)

The crevasse splay facies is generally red with some grey mottling, and beds at location 1 tend to be more grey in colour. These deposits range from coarse silt to fine

sand and comprise beds and bedsets 0.1 to 1.65 m in thickness. The strata are often structureless, but a few layers contain climbing ripples, cross-stratification, and planar stratification. These deposits are generally interbedded with floodplain mudstone and overlie channel sandstones.

This facies is interpreted to be the result of crevasse splay deposits. Crevasse splay deposits form when levee collapse occurs along channels carrying sand and silt as bedload and suspended load. The channel sediments are then rapidly deposited over the floodplain through the crevasse.

4.1.6 Abandoned Channel Fill Mudstone (facies F)

This facies consists of red, lens-shaped, structureless mudstone containing some interbedded sandy layers. A major abandoned channel fill mudstone (>10 m wide) is present at field location 1, overlying the main sandstone channel body. Several smaller scale fills (1-3 m wide) are present within the measured section at site 2. Due to limited exposure, it was not easy to determine which mudstone beds are within abandoned channels and which are floodplain mudstone sheets. Some of the facies D subtypes are present in facies F (e.g. rubbly mudstone beds). The active river system caused channel incision, but deposition of the mudstone did not occur until after channel abandonment. Channel abandonment is a natural part of channel switching, but abandonment could have been initiated by sudden uplift related to one of the several active faults surrounding the Cumberland Basin during the Pennsylvanian Period.

4.2 Field Location 1: Cliff Face

Figure 4.6 is a photo of the strata at field location 1, with the features in the cliff face traced out for interpretation purposes. (A) marks the channel incision into the underlying sediment, (C, D) and (E) are the main beds in a vertically accreted sandstone channel, (B) appears to be a slump block that collapsed into the bottom of the channel, (F) and (G) are abandoned channel fill mudstones, with minor sandstone layers, and (H) represents thin sandy crevasse splay deposit material.

Strata here represent a single flood-dominated channel found in a seasonal type environment. This narrow, incised channel body is similar in morphology to a single channel body formed by an anastomosing fluvial system. Rust et al. (1984) noted aggrading fill, limited lateral migration, multistory form, stepped bases, and internal erosion surfaces as features common to anastomosing channel deposits. This multistory fluvial channel, located in a muddy floodplain, does not appear to have experienced any lateral migration, but accreted vertically with time. Internal erosion surfaces are also present within the channel body as sand sheets and mud lenses.

4.3 Field Location 2: Measured Section

Figure 4.7 contains a stratigraphic column depicting a 25 m measured section within the top of the Boss Point Formation. Individual bed interpretations are found in Table 4.1, and are referenced with a facies number to the stratigraphic column. Facies present in this section are: large channel bodies, small channel bodies, crevasse splay deposits, floodplain mudstones, calcretes and abandoned channel fills.

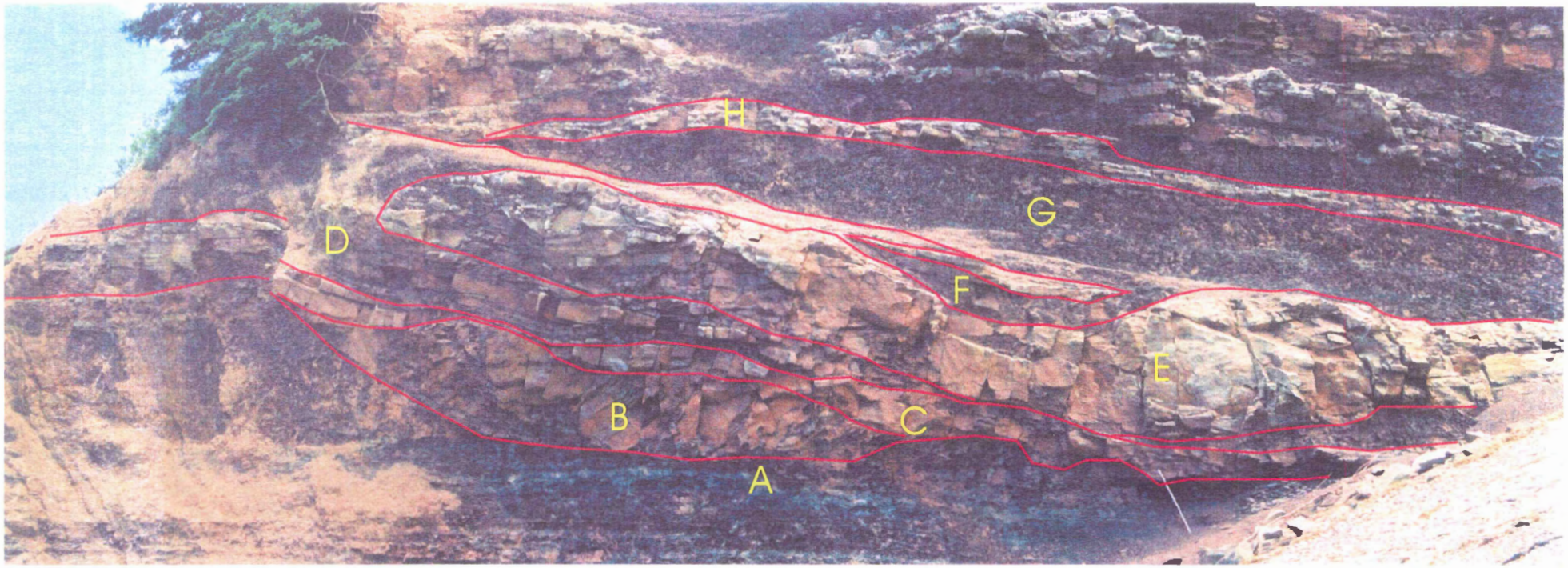

Figure 4.6 - Boss Point Formation, site 1 . Image shows the features in the cliff face traced out for interpretation purposes. (A) marks original channel incision into sandy crevasse splay deposits, (C, D) and (E) are beds in a vertically accreted sandstone channel body, (B) represents a slump block that collapsed into the lower channel, (F) and (G) abandoned channel fill mudstone with minor sandstone layers, and (H) thin sandy crevasse splay deposit. Strata is inclined at about 45 degrees (structural dip). Meter stick in lower left corner for scale.

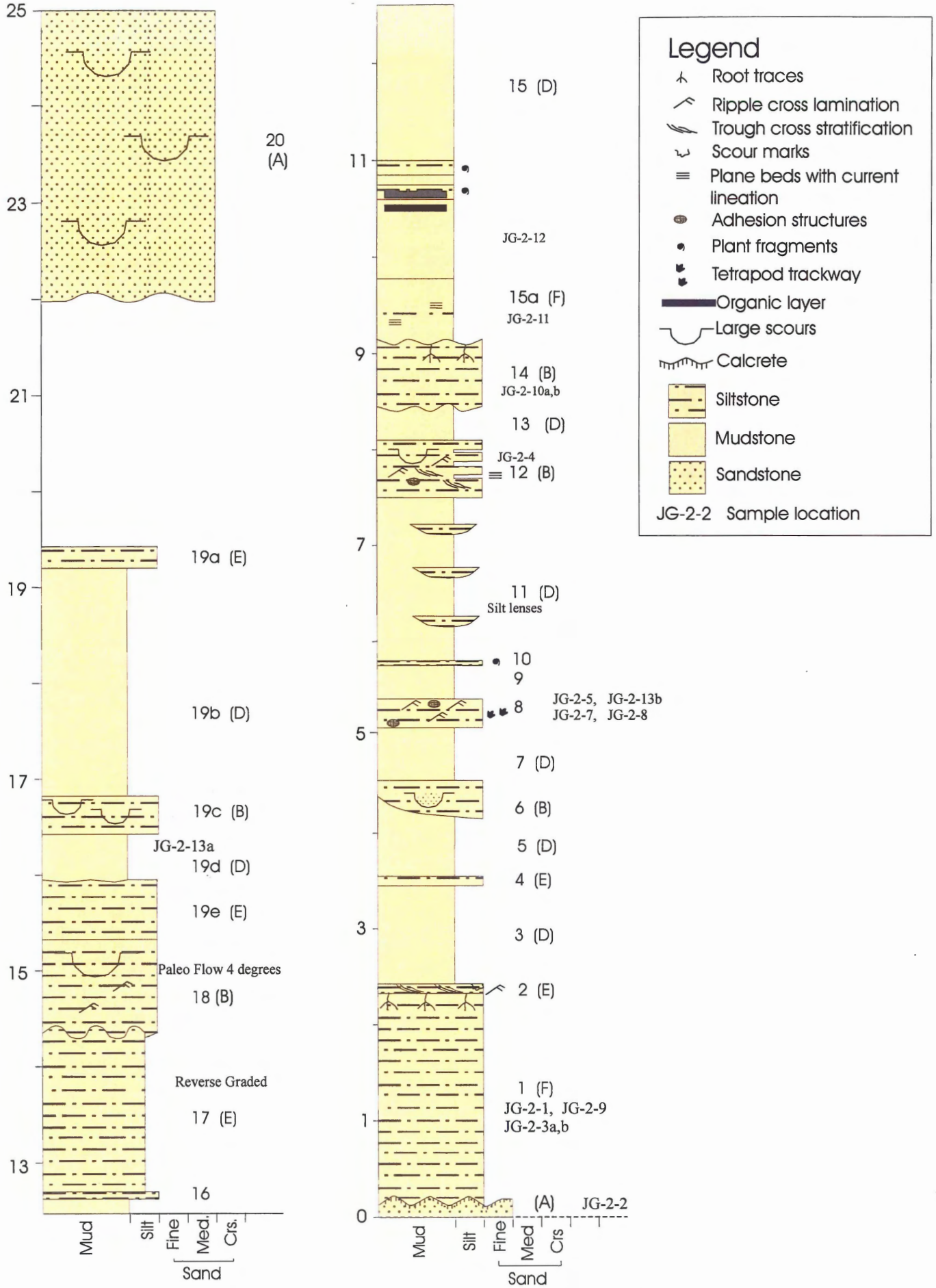

Figure 4.7 - Measured section from field locality 2, Boss Point Formation, Joggins Cliffs. Numbers and letters associated with beds correspond with bed Ids and facies codes (In brackets) from the facies table in Table 4.1.

The strata here are interpreted to have formed in a seasonal climate that experienced both wet and dry climatic conditions. The many small channel bodies and layers of floodplain mud are strong evidence of periods of significant precipitation. The soils that formed in this flood-dominated environment probably developed cumulatively. Thin muds added with each flood became worked into the developing soil after they were laid down. On the other hand, rain-drop imprints and calcrete soil development indicate dry conditions at times. Calcretes develop when precipitation brings water, enriched in minerals, down to the water table. As seasonal moisture changes and significant evaporation begins, calcium carbonate is precipitated out of solution and remains behind. Over several thousand years the soil develops into a calcrete or caliche. Most likely the small channel bodies were formed by small drainage systems that became active on the floodplain during the wet season. The channel bodies are shallow, and several are commonly present in one stratigraphic layer.

4.4 Location 3 – Little River Formation

Figure 4.8 shows a 5 m thick channel body (91-96 m on figure) studied at site 3. The channel body comprises several erosionlly bases lenses that contain conglomerate rich in feldspathic granules and pebble-sized mud clasts. Sandstones show trough- and planar-crossbeds, and mounded barform prominent at top (Fig. 3.4), capped by sheets of ripple cross-lamination. Interpreted by Calder et al. (submitted) as a sand-bed, probably a braided channel that experienced strongly seasonal flow.

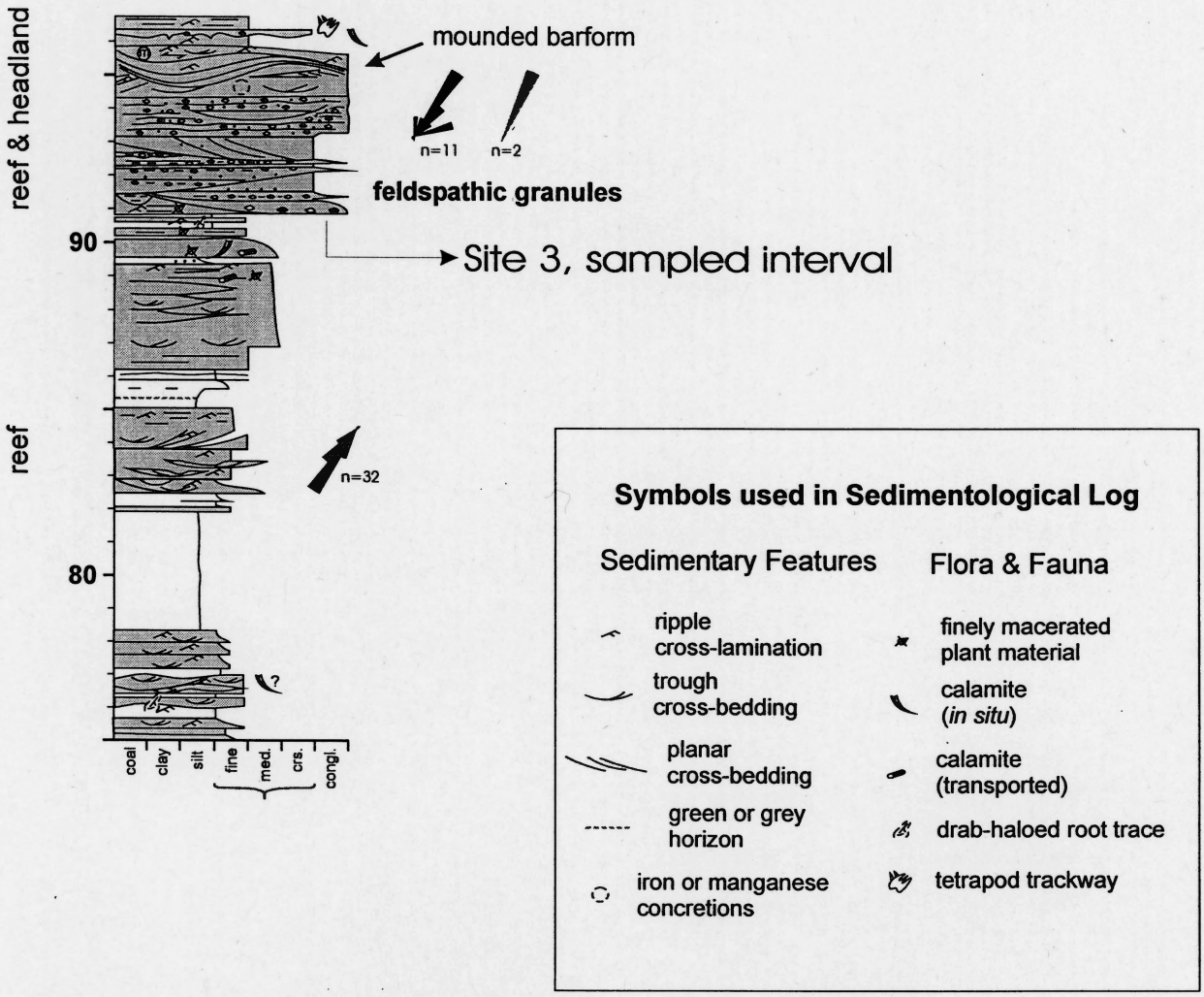

Figure 4.8 - Portion of measured Section from the Little River Formation (75- 97 m). Location Of field site 3 is indicated in the section. From Calder et al. (Submitted).

4.5 Overall Interpretation

The top of the Boss Point Formation was once an active fluvial environment containing braided and narrow, incised fluvial systems during deposition in the Pennsylvanian. Study areas along the Joggins cliffs contain a combination of large and small channel bodies, floodplain mudstones, crevasse splay deposits, calcretes, and abandoned channel fill deposits. The presence of these types of deposit tell a story of a dynamic, flood-dominated environment during deposition. This was a river environment where water levels rose, where banks collapsed, and sediment spread into surrounding floodplain land. Layers of floodplain mudstone and crevasse splay deposits illustrate this repeated process. This environment, at times, experienced decreased precipitation, resulting in increased evaporation and lowering of the water table, leading to dissolution and deposition of minerals into developing soils.

The proximal floodplain area allowed the channels to increase in size during frequent flooding events that occurred in the wet season. These frequent flooding events would have activated small, braided floodplain channels, and would have entrained, transported, and reworked mud aggregates from the floodplain surface (Marriott and Wright, 2004). According to Marriott and Wright (2004), calcrete soils require periods of landscape stabilization, as well as prolonged drying to develop. Paleosols located on top of channel bodies presumably record channel switching events leading to reduced sedimentation and calcrete development. Therefore, these paleosols were likely located on the distal floodplain and only reached by mid-frequency flooding events.

From observation of modern environments and literature on paleo-environments,

it is well documented that calcrete soils do not develop in wet climates and floodplain muds rarely form in dry climates. The strata in the Boss Point Formation, therefore, contains strong evidence of a seasonally wet-dry environment, exactly the type of environment necessary for pedogenic mud aggregates to form, based on modern analogues. The Boss Point Formation appears to have had a similar morphology to the modern Cooper Creek floodplain environment and to the paleo-environment of the Moor Cliffs Formation, both of which are known to contain pedogenic mud aggregates (Maroulis and Nanson, 1996; Marriott and Wright, 2004).

5.0 Mud Aggregate Occurrences

5.1 Petrographic Descriptions

5.1.1 - Introduction

Detailed thin section study of samples taken from the Boss Point and Little River formations has revealed interesting information on the preservation styles, sizes, and abundances of mud aggregates found in this area. The aggregates are found in one of three forms, as reworked aggregates in siltstones, as in-situ/reworked aggregates in mudstones, and within carbonate concretions. Aggregates occur in siltstone laminae, mud fragments, muddy matrix patches, mudstone, and in carbonate rhizo-concretions. Aggregates tend to be preserved in highest abundance in the laminated mudstones that formed during overbank floods. These flooding events resulted in minor reworking of the floodplain.

The aggregates appear near spherical and well rounded in thin section. They have an apparent diameter ranging from 5-20 μ and no internal texture is discernible at highest magnification (40x). Aggregate size is generally quite uniform within a given sample and within the different styles of preservation, carbonate concretions being the exception where the aggregates are slightly smaller. For the most part individual aggregates are discrete, but there is some blending of the aggregate into the surrounding material. Aggregates preserved in siltstone are on average smaller than the main minerals, quartz, plagioclase, etc., that make up the rock. Table 5.1 contains a summary of the aggregates and their occurrence in the Boss Point and Little River formations, which are discussed in further detail in the following sections. Clay mineral identifications are given in a few cases throughout this chapter, but are discussed fully in Chapter 6.

Table 5.1 - Comparison of Aggregate Occurrences

Feature	Aggregate Information		Carbonate cement/reworked fragments	Matrix	Aggregate Preservation
	Size	Proportion			
Aggregates preserved in siltstone laminae	5-15μ, 10μ avg.	10-40% of lamination	Little cement in laminae, 0-10%. Few carbonate fragments, 0-10%	Mud matrix is concentrated in individual mud rich layers and in well laminated sediments. Grain supported.	Preservation appears mostly due to strong mineral framework of the laminae and in some cases carbonate cement appears to play a minor role.
Aggregates in reworked mud fragments	5-20μ, 15μ avg.	aggregates compose 20-50% of mud fragments; fragments compose 10-15% of sediment.	Carbonate cement ranges 0-30% of fragment, but in general the value is toward the lower end.	Muddy matrix ranges from sporadic to even coverage, with 0-15% cement in matrix rich areas.	Preservation appears to reflect a combination of the strong mineral framework and carbonate cement in most cases.
Aggregates in muddy matrix patches	5-20μ, 10-15μ avg.	< 5-30% of slide	Cement ranges from 0-20% in matrix mud. Most slides have few carbonate blocks locally up to 20%.	Muddy matrix in slide ranges from sporadic to relatively constant distribution.	Preservation appears to reflect a combination of the strong mineral framework and carbonate cement appears to play a role in some cases. Textures best preserved with 10% carbonate.
Aggregates in reworked mudstone	5-20μ, 15μ avg.	5-60% in any given area of a slide	Cement ranges from <5-30%, approx. 10% cement in well preserved areas. Carbonate fragments range from 0-40%.	N/A	Preservation appears to be due to the amount of carbonate cement. If too much cement is present the texture is not well preserved. In some cases rigid carbonate fragments and quartz grains play a role.
Aggregates in carbonate rhizo-concretions and reworked fragments	5-10μ	10-30% within reworked carbonate fragments and concretions	Carbonate fragments range in size from 0.1-3 mm.	Very well cemented (15%) to minor cement present within matrix.	Aggregate texture in the carbonate is related to early carbonate concretionary growth preserving the original textures in the mud.

5.1.2 - Aggregates in Laminated Siltstone

Table-5.2 contains a brief description of several thin sections found to contain mud aggregates preserved within fine muddy laminae. For the most part, the laminae are found as individual mud-rich layers within a planar laminated siltstone or cross-laminated siltstone. Less commonly found are well laminated mudstone fragments. The laminae range in size from 0.1-2 mm and are defined by an increase in the proportion of mud relative to the mineral framework of an area within the slide (Fig. 5.1a). In some cases more organic fragments and heavy minerals are also present in the laminae. The apparent diameter of individual aggregates within the laminae have a range of 5-15 μ, approximately 10 μ in size is average (Fig. 5.1b). The proportion of mud aggregates within the lamina is variable, ranging from 10-40%. Variability in the proportion of aggregates within a sample is related to the amount of mud matrix within the lamina and the degree to which the texture has been preserved in the rock.

Preservation of the aggregate texture in these laminae appears to be related to the strong mineral framework of the siltstone. Even within the laminae themselves, enough quartz, feldspar, and in some cases small carbonate nodules are typically present to provide a good framework for the aggregates. Carbonate cement may play a role in preserving the delicate mud aggregate structure by filling in the spaces between the aggregates, although most thin sections show very little cementation in the laminae, on average $\leq$ 5% carbonate cement.

5.1.3 - Aggregates in Reworked Mud Fragments

Mud aggregates are commonly preserved in small mud fragments within detrital quartz siltstone, especially in field locality 2. Table-5.3 contains a brief description of thin sections found to contain aggregate-rich mud fragments. The mud fragments range in size from 0.1-0.5

Table - 5.2 Aggregates Preserved in Laminae

Thin Section	Feature	Aggregate Information		Carbonate in Laminae	Laminae Texture	Aggregate Preservation
		Size	Proportion	Cement/Reworked fragments		
JG-2-10b	Detrital aggregates present in very fine, mud rich silt laminations (2.0 - 0.4 mm thick).	0.005 - 0.01 mm	20 to 30 % of lamination	Very little to none	Muddy material surrounding detrital quartz. Grain supported.	Aggregate preservation appears to be due to a strong mineral framework including quartz, plag, carbonate.
JG-2-4	Detrital aggregates present in very fine, mud rich silt laminations (1.2-0.25 mm).	0.005 -0.015 mm	15 - 20 % of lamination	Very few carbonate fragments (4%) and little to no cement	Muddy material surrounding detrital quartz. Grain supported.	Aggregate preservation appears to be due to a strong mineral framework (quartz, plag, carbonate). Enough quartz within the laminae to provide framework for the aggregates.
JG-2-9	Well laminated mud fragments (0.1-0.2 mm).	0.005 - 0.01 mm	35-40% in more muddy layers 25-30% in less muddy layers	Carbonate present in minor amount (5%)	Some laminations are slightly more silty in nature. Minerals (qtz. ?) finer than the aggregates.	Aggregates are well preserved in the mud fragments, likely due to early cementation of the mud by carbonate.
JG-2-13b	Fine cross-laminated siltstone containing detrital aggregates. Laminations (1.4mm) are defined by concentration of heavy minerals or organic fragments.	0.005-0.015 mm	10% of slide, and about 30 % of individual laminae	None ?	Mud matrix is about 20% of slide and is concentrated in some laminae. Grain supported.	Aggregate preservation appears to be due to a strong mineral framework (quartz, plag, etc.) protecting the structure.
JG-2-14	Fine cross-laminated siltstone containing detrital aggregates. Laminations (1.5mm) are defined by concentration of heavy minerals or organic fragments, finer quartz, more mud.	0.005-0.015 mm	10% of lamination	Carbonate fragments compose about 10 - 15% of lamination, probably very minor cementation as well	Mud matrix is about 10-15% of slide and is concentrated in the lamina. Grain supported.	Aggregate preservation appears to be due to a strong mineral framework (quartz, plag, etc.) protecting the structure. Detrital carbonate fragments present may suggest some degree of carbonate cementation.

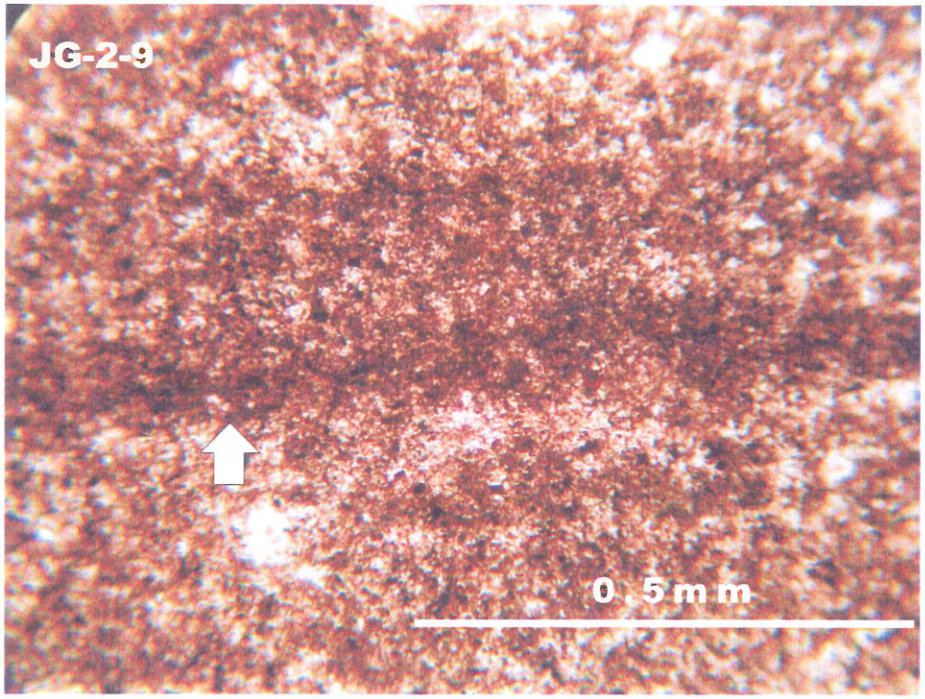

Figure 5.1a - Muddy laminae in a silty mudstone displaying aggregate accumulations, which appear as the dark dots in this figure, sample JG-2-9 at 20x magnification.

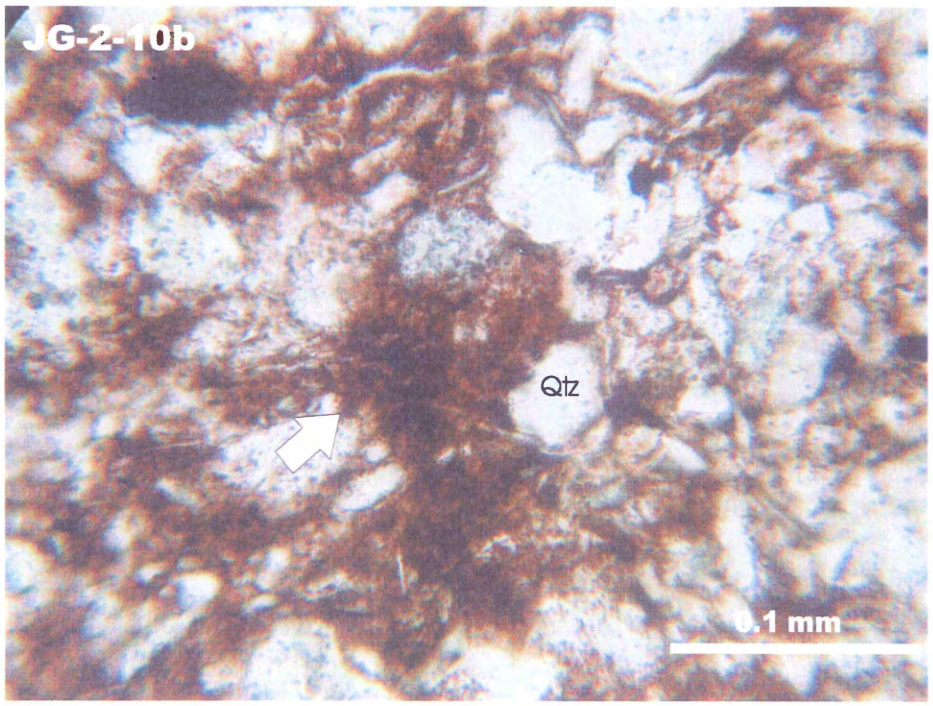

Figure 5.1b - High power view of muddy lamina in a siltstone. Individual aggregates are visible at 50x magnification, JG-2-10b.

Table - 5.3 Aggregates in Reworked Mud Fragments						
		Aggregate in Chunks		Carbonate in Mud		
Thin Section	Feature	Size	Proportion	Fragments	Matrix and Cement	Aggregate Preservation
JG-2-10b	Mud fragments (0.2-0.5mm in size) in detrital quartz siltstone. Approx. 10% of slide.	0.015 - 0.02 mm	40%	Some fragments have about 5% carbonate, others have no visible carbonate.	Little to no matrix in majority of slide, minor carbonate cement. Laminae have muddy matrix.	Aggregate preservation appears to be due to a strong mineral framework (quartz, plag, chert, carbonate fragments), framework approx. 0.2-0.05 mm in size.
JG-2-8	Mud fragments (0.1-0.3 mm) in detrital quartz siltstone. Approx. 15% of slide.	0.008-0.015 mm	20-40%	Carbonate in mud fragment ranges from 5-20%	Thin muddy matrix consistently coating minerals. 5-10% carbonate in matrix.	Aggregate preservation appears to be due to both mineral framework (quartz, plag ,chert, carbonate fragments), and carbonate cement.
JG-2-10a	Mud fragments (0.15-0.3mm) in detrital quartz siltstone. Approx. 10% of slide.	0.005-0.015 mm	50%	fragments have about 10% carbonate	Majority of slide has minor carbonate cement up to 10%. Mud ranges from 0 to 15%.	Aggregate preservation appears to be due to a strong mineral framework (quartz, plag ,chert, carbonate fragments) and the carbonate cement.
JG-3-1a	Mud fragments (0.1-0.2 mm) in medium to coarse sandstone. Approx 15% of slide.	0.005-0.01 mm	40%	Fragments have about 30% carbonate	Very well cemented, approx 15% of slide.	Preservation of mud aggregates in the fragments is directly related to the degree of carbonate cement present.

mm, and on average, are slightly larger than the silicate framework within their host siltstone body (Fig. 5.2a). These mud fragments tend to represent about 10-15% of the thin section and each contains 20-50% aggregates, with about 40% being the average proportion. The individual mud aggregates range in size from 5-20 μ but the average is approximately 15 μ(Fig. 5.2b).

The range of mud matrix present in the thin sections is almost 0% in some samples and up to 15% in others. Mud fragments in the siltstone are quite distinct from the matrix material. The degree of cementation in the host siltstone ranges from very well cemented to a minor degree of carbonate cementation. Carbonate cement is also present within the mud fragments themselves, variably 5-20%. Well cemented areas in the siltstone tend to correspond with well cemented mud fragments. Preservation of aggregates in mud fragments is strongly related to both the relatively high degree of carbonate cementation and the strong mineral framework provided mainly by quartz, but also feldspar, chert, and reworked carbonate fragments.

5.1.4 - Aggregates in Muddy Matrix Patches

It is not uncommon to find a combination of dispersed mud and mud aggregates encircling the minerals that compose the siltstones. The most abundant of these minerals are quartz, feldspar, chert, muscovite, and reworked carbonate fragments at sizes averaging 0.04-0.2 mm. Table 5.4 contains a brief petrographic description of thin sections found to contain aggregated mud mud associated with the matrix of fine siltstone (Fig. 5.3a). The degree of matrix coverage ranges from a prominent coating that is regularly distributed throughout a slide (20%), to sporadic patches of matrix scattered throughout a slide (5%). The aggregates within the mud range from 5-20 μin size, 10-15 μbeing the average, and the individual aggregates are slightly smeared into the matrix around the outer edge of the aggregate body. The amount of

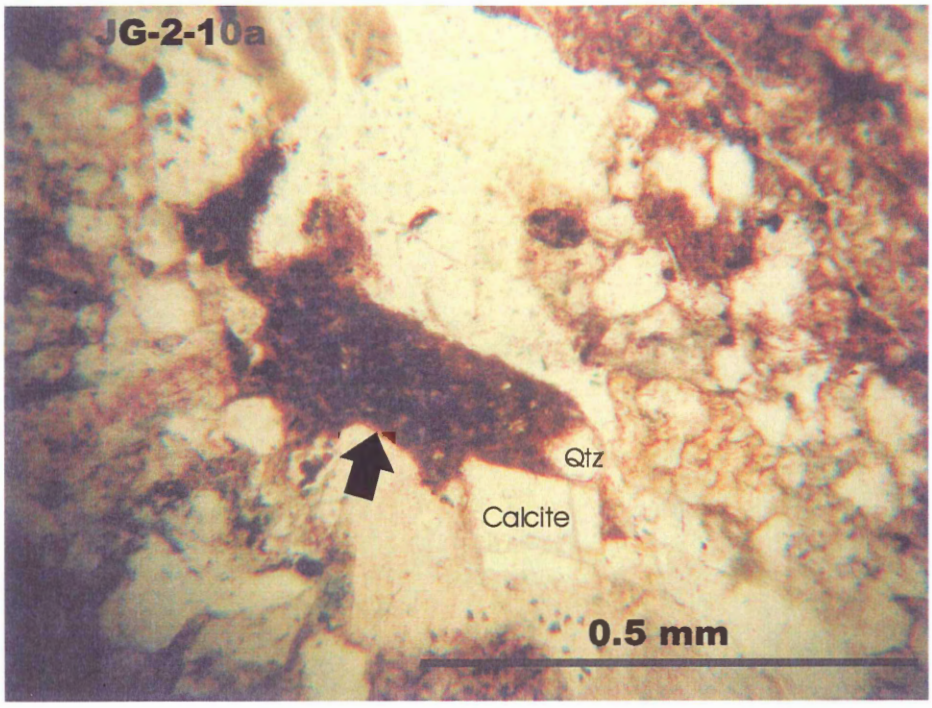

Figure 5.2a - 20x magnification of a mud fragment containing mud aggregates in a siltstone, JG-2-10a.

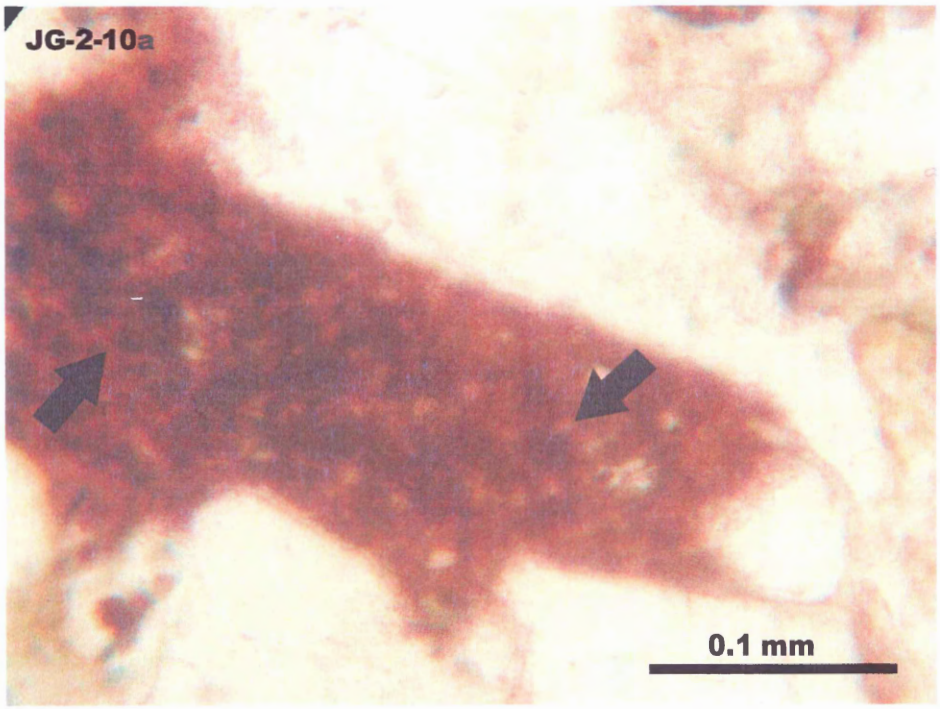

Figure 5.2b - Close up of mud fragment with aggregates in (a), 50x magnification, JG-2-10a.

Table - 5.4 Aggregates Preserved in Muddy Matrix Patches						
		Aggregate Information		Carbonate		
Thin Section	Feature	Size	Proportion	Cement/Fragments	Matrix	Aggregate Preservation
JG-3-1	Mud matrix material encircling qtz., plag., chert mineral framework.	0.005-0.015 mm	5-20 % in some areas	Approx. 5 % cement in muddy areas and 20% carbonate fragments in slide	Muddy matrix ranges from 0 in some areas up to 20% in others	Aggregate preservation in matrix is related to both mineral framework (quartz, plag., chert, carbonate fragments), and carbonate cement.
JG-2-1	Mud matrix material encircling mineral framework (qtz., plag., muscovite, etc.). Grains approx. 0.02 -0.15 mm in size.	0.008-0.015 mm	15% of slide	Well cemented, carbonate about 10-20%	Coating of mud and aggregates surrounding grains very regularly throughout slide (15-20% of slide). Aggregate texture preserved best in areas of about 10 % carbonate	Aggregate preservation in matrix is related to both mineral framework (quartz, plag, chert, carbonate fragments), and carbonate cement.
JG-2-7	Fine siltstone containing detrital quartz and mud aggregates.	0.01-0.02 mm	30% of slide	Max 5 % carbonate cement	Even ratio of detrital mud to qtz grains with a very small amount of cement. Qtz is on avg. 0.05-0.1 mm in size	Aggregate preservation in matrix is more strongly related to mineral framework, carbonate cement plays a role to some degree.
JG-2-6	Mud matrix material encircling mineral framework (qtz., plag., muscovite, etc.). Grains framework Minerals approx. 0.15-0.04 mm in size.	0.005-0.01 mm	<5% of slide	Well cemented, carbonate about 10-15%	Very thin coating of mud encircling minerals throughout slide (5-10% of slide). Aggregate texture preserved best in areas of about 10 % carbonate	Aggregate preservation in matrix is related to both mineral framework (quartz, plag., chert, carbonate fragments), and carbonate cement. Aggregates are not as abundant in this slide because not enough mud is present in the matrix.
JG-2-10b	Siltstone with areas of mud-rich matrix up to 5mm in size.					

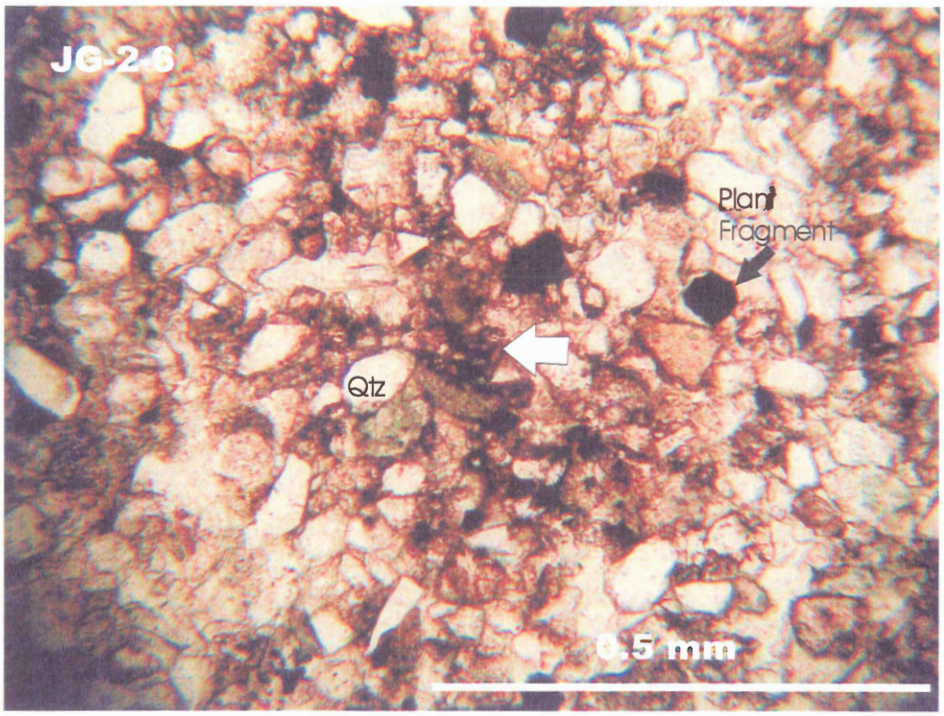

Figure 5.3a - Mud aggregates preserved in the muddy matrix material of a fine siltstone. White arrow points to aggregates, JG-2-6.

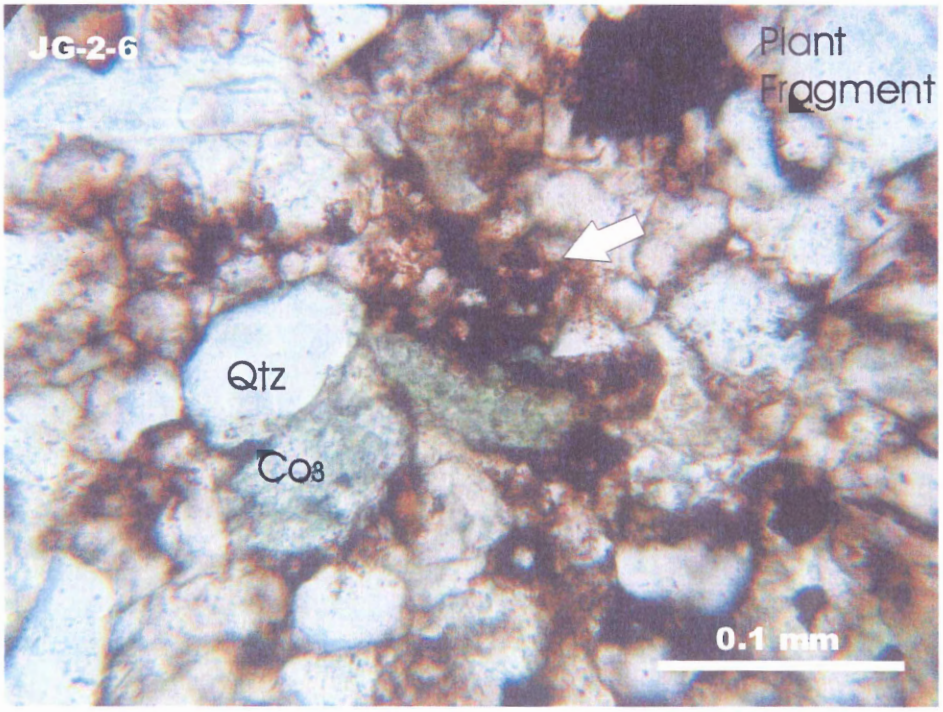

Figure 5.3b - Close up of mud matrix aggregates in (a), arrow highlights aggregate rich area. JG-2-6, 50x magnification.

carbonate cement present in the matrix ranges from about 5-20%. Matrix aggregates seem to be preserved best where carbonate is not at its highest, and about 10% carbonate appears to be an ideal proportion in these thin sections (Fig. 5.3b). The preservation of mud aggregates within matrix material is highly dependent on the strength of the mineral framework within these siltstones; carbonate is likely important as well, but the degree to which it affects preservation is uncertain.

5.1.5 - Aggregates Preserved in Reworked Mudstone

Several thin sections are composed entirely of fragmental mudstone and contain an abundance of aggregated mud. These samples came from the silty fragmental mudstone beds in field locality 2. Table-5.5 contains brief petrographic descriptions of thin sections containing aggregates preserved in mudstones. These fragments have been found to contain as much as 60% mud aggregates, 40% on average. Individual aggregates range in size from 5-20 μ with 15 μ being the average size (Fig. 5.4a, b). Some of the mud fragments contain small carbonate nodules (0.2-2.5 mm) and the mud is all generally cemented to some degree. The proportion of carbonate cement ranges from about 5-30%. Aggregate texture is preserved best where the amount of carbonate is between 5 and 15%. Essentially, moderately cemented areas contain well preserved aggregates, strongly cemented areas do not. Aggregates are also much less abundant in the more silty regions of the mud. Early cementation of the mudstone has played an important role in aggregate preservation.

Table - 5.5 Aggregates Preserved in Reworked Mudstone

Thin Section	Feature	Aggregate Information		Carbonate	Aggregate Preservation
		Size	Proportion	Cement/Fragments	
JG-2-11	Relatively large mud fragments (1-5 mm)	0.005-0.01 mm	5-60%, average 30-40%	between 5 and 10 % carbonate within the fragments	Preservation is likely due to the amount of carbonate. If there is too much carbonate in an area the texture is not preserved very well.
JG-2-12	Relatively large mud fragments (3-12 mm)	0.01-0.015 mm	40-60% but as low as 5% in quartz rich areas	between 5 and 10 % carbonate within the fragments	Preservation is likely due to the amount of carbonate. If there is too much carbonate in a fragment the texture is not preserved well.
JG-2-3	Relatively large mud fragments (2-15 mm)	0.01-0.02 mm	Approx 40% aggregates in mud less affected by carbonate	Mud contains 40% carbonate nodules. Avg 10% carbonate cement in mud, up to 25% cement in poorly preserved areas.	Preservation is likely due to the amount of carbonate present in both cement and nodule form. If there is too much carbonate cement in an area the texture is not preserved well.
JG-2-3$_{\&}$	Aggregates preserved in large mud fragments (carbonate nodules 0.2-2.5 mm within the mud)	0.01-0.015 mm	Approx 30-40% aggregates in areas of mud less altered by carbonate	Mud contains 30% carbonate nodules. Avg 5-10% carbonate cement in mud, up to 30% cement in poorly preserved areas.	Preservation is likely due to the rigid carbonate blocks and to a lesser degree quartz grains that are present, also early cementation in matrix. If there is too much carbonate cement in an area the texture is not preserved well.

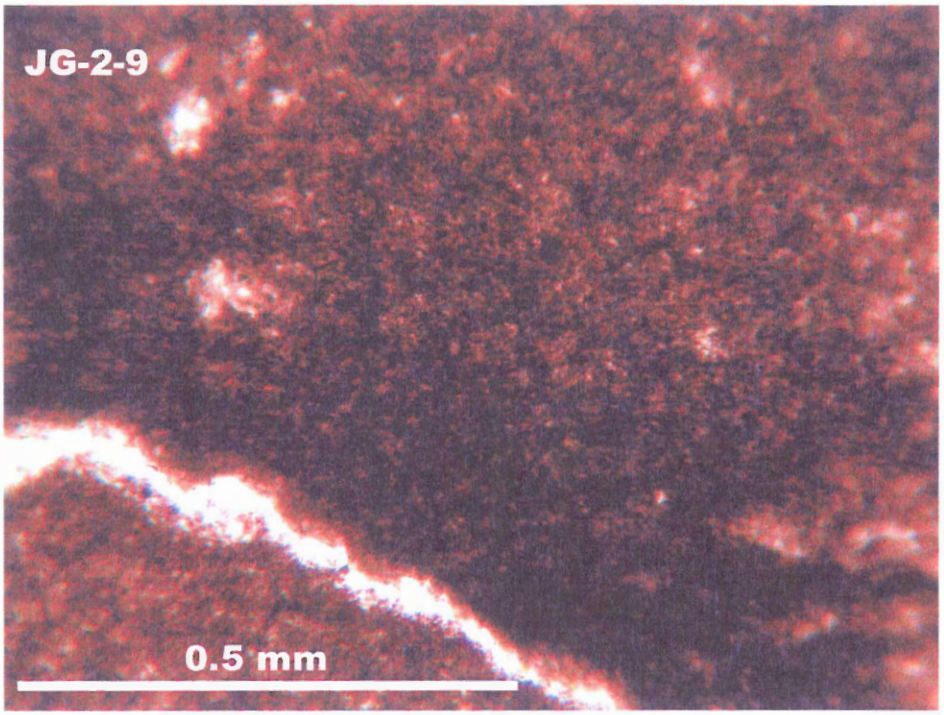

Figure 5.4a - Aggregate accumulation preserved in mudstone, JG-2-9.

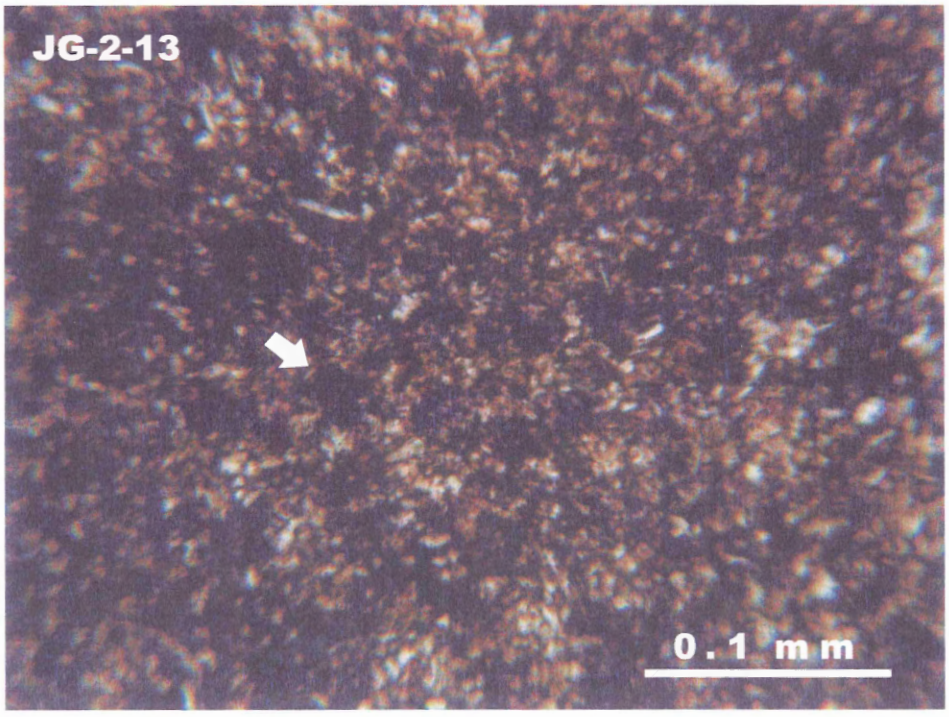

Figure 5.4b - Close up of mud aggregates preserved in mudstone, individual aggregates can be identified (arrowed), JG-2-13.

5.1.6 - Aggregates in Carbonate Rhizo Concretions and Reworked Fragments

The presence of carbonate has played an important role in many of the sedimentary structures already discussed in this chapter. Table-5.6 contains a brief description of thin sections that have aggregates preserved as a direct result of the significant degree of carbonate cementation within the rock. Carbonate nodules (0.1-2.8 mm) have been identified in both well cemented mudstone fragments and well cemented siltstone (Fig. 5.5a). Aggregates found within these carbonate nodules tend to be less abundant (10-20%) than in the carbonate-rich mud, and are on average smaller in size at 5-10 μ. One slide in particular, JG-3-1a, contains root casts with coarse sparry carbonate infilling the cast and exterior mottled carbonate, with finer crystal size surrounding the casts (Fig. 5.5b). Aggregates are concentrated near the edges of the exterior root carbonate, where they form approximately 15 to 30% of the material. The aggregate texture in carbonate blocks and around root casts is related to early carbonate concretionary growth preserving the structures originally found in the mud.

4.2 Environmental Scanning Electron Microscope (ESEM)

Under the high magnification provided by the ESEM, images of quartz, plagioclase, and K-feldspar appear to be angular and irregular in shape, whereas the aggregates are smooth and rounded (Fig. 5.6a, b). The aggregates range from approximately 5 to 20 μ in size (10 μ on average). Shape of the aggregates appears near spherical in some cases, and slightly elongated in others (Fig. 5.7). Sheet-like illite is also present in the scanned mudstone and represents an individual illite flake or a package of illite sheets (Fig. 5.8). Sheeted illite and aggregated illite have a very different appearance from each other. The aggregated illite has an obvious rounded, three-dimensional texture that is not visible in the clay sheets.

Table - 5.6 Aggregates in Carbonate Rhizo Concretions and Reworked Fragments					
		Aggregate in accumulations			
Thin Section	Feature	Size	Proportion	Matrix	Aggregate Preservation
JG-3-1a	Root cast (0.8-1.2 mm) with central carbonate and exterior mottled carbonate (2.5-3 mm). Cast and surrounding carbonate approx 20% of slide.	0.005-0.001 mm	15-30% of exterior carbonate and concentrated near carbonate edges	Very well cemented, approx 15% of slide.	Aggregate texture in the carbonate surrounding the root casts is related to early carbonate overgrowth preserving the structures in the mud.
JG-2-2	Muddy aggregate accumulations (0.1-0.25 mm) scattered through-out detrital quartz siltstone.	0.005-0.01 mm	40-50%	Very well cemented, approx 15-20% of slide. Muddy cement matrix.	Aggregate texture in the carbonate accumulations is related to early cementation preserving the structures in the mud.
JG-2-10a	Carbonate nodules (0.15-0.2 mm in size) in detrital quartz siltstone, 10% max of slide.	0.005-0.01 mm	30% of carbonate nodules	Majority of the slide has minor carbonate cement, up to 10% in places. Mud ranges from 0 to 15%.	Aggregate texture in the carbonate nodules is related to early carbonate overgrowth preserving the structures in the mud.
JG-2-3	Relatively large mudstone fragments containing approx. 40% carbonate nodules (0.1-2.8 mm in size).	0.005 mm	10-15% of carbonate fragments have aggregates and those contain approx. 10% aggregates	Mud is well cemented (10%).	Aggregate texture in the carbonate nodules is related to early carbonate overgrowth preserving the texture; aggregates in the carbonate are smaller than aggregates in the mud itself.

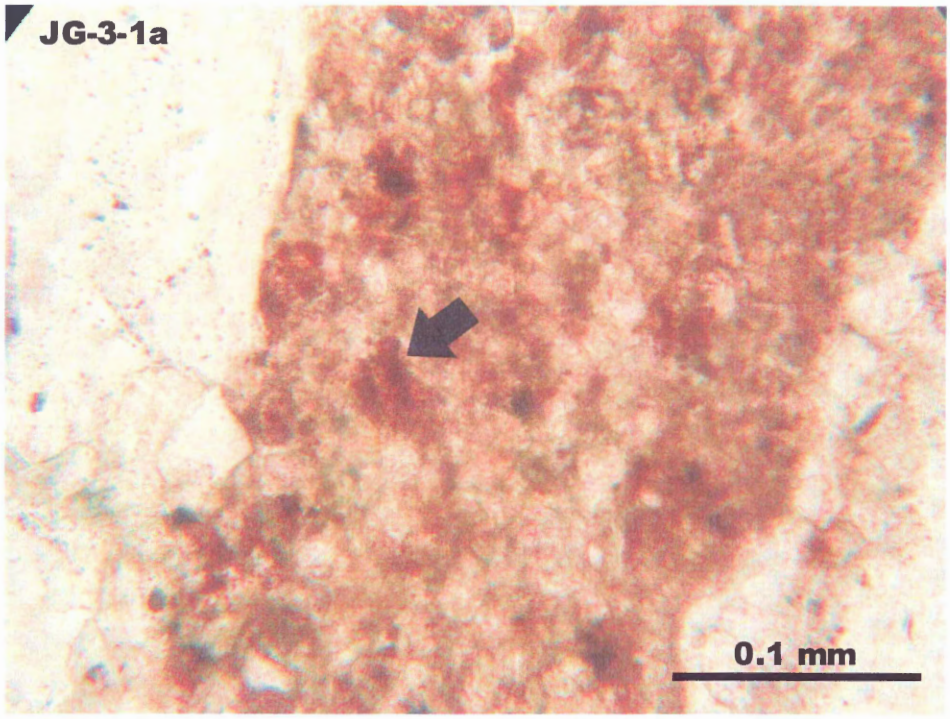

Figure 5.5a - Carbonate concretion containing 15% mud aggregate, a close up of Figure 4.5b, JG-3-1a.

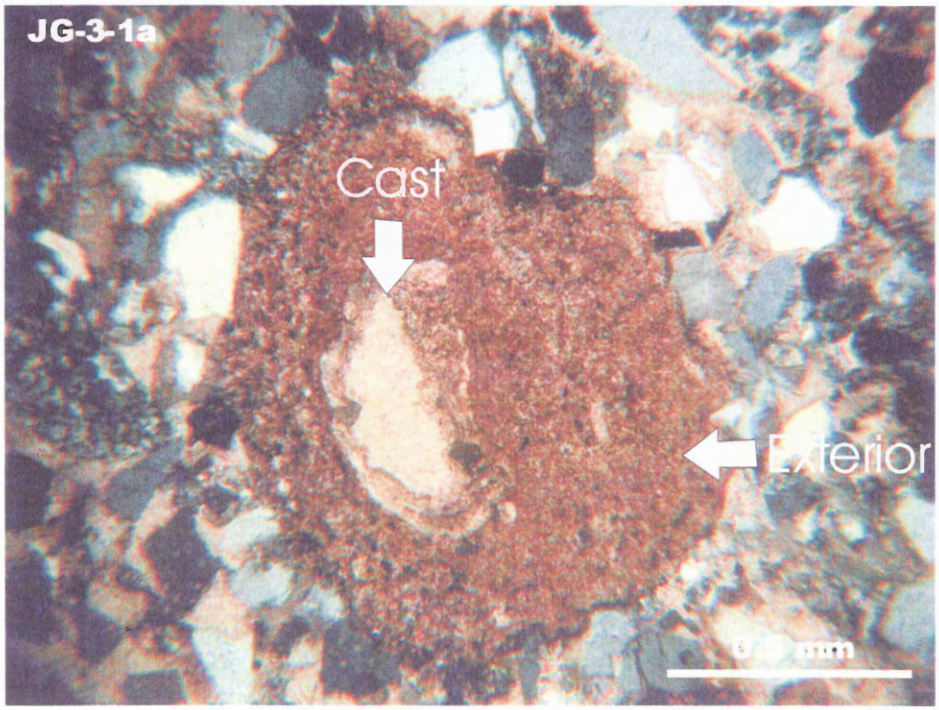

Figure 5.5b – Carbonate-filled root cast with mud aggregates preserved in the exterior mottled carbonate, photo in XN, JG-3-1a.

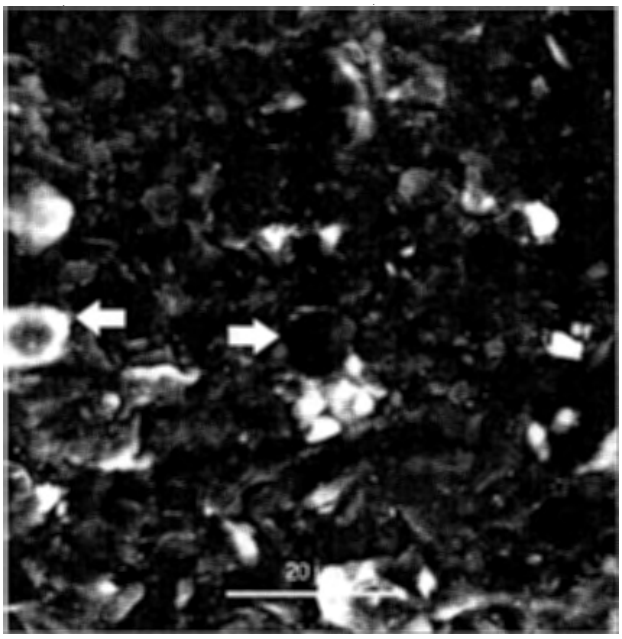

Figure 5.6a - ESEM image of two rounded illite aggregates found in sample JG-2-9, view perpendicular to lamination plane.

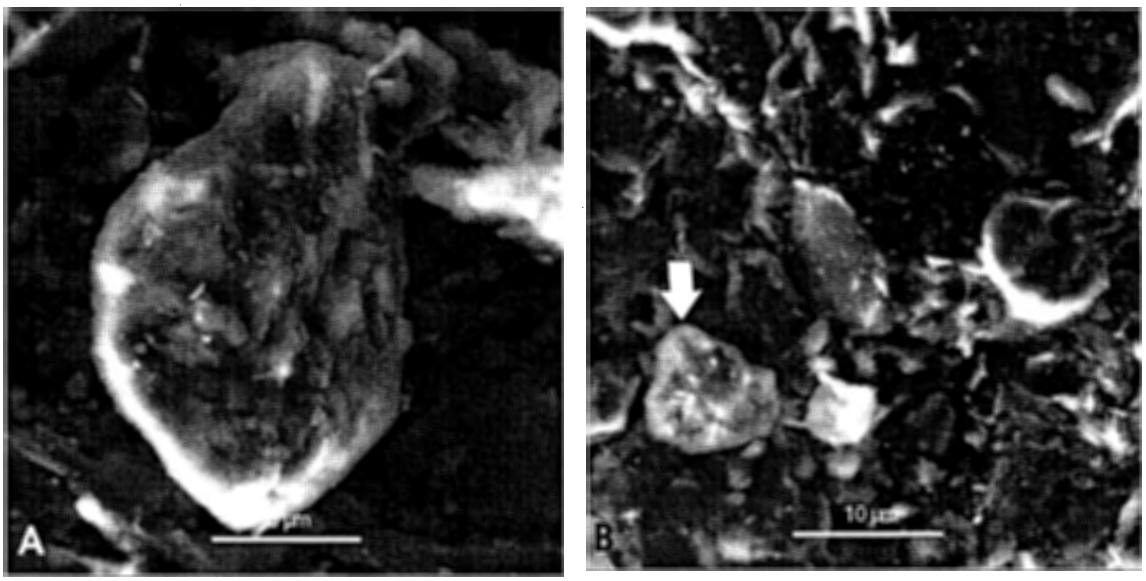

Figure 5.6b - (A) High-power magnification of a quartz grain under the ESEM, (B) ESEM image of plagioclase grain (arrowed). Both images from sample JG-2-9.

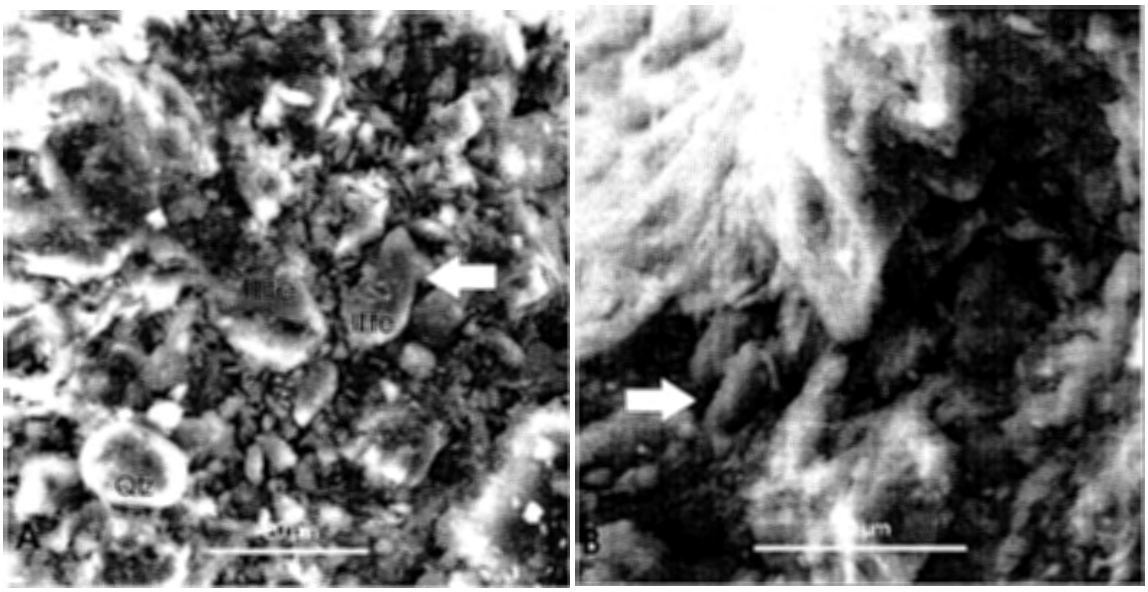

Figure 5.7 - ESEM images of illite aggregates, JG-2-9. (A) contains two analyzed aggregates and a quartz grain, the arrowed grain is a more elongate aggregate. (B) contains an elongate illite aggregate (arrowed).

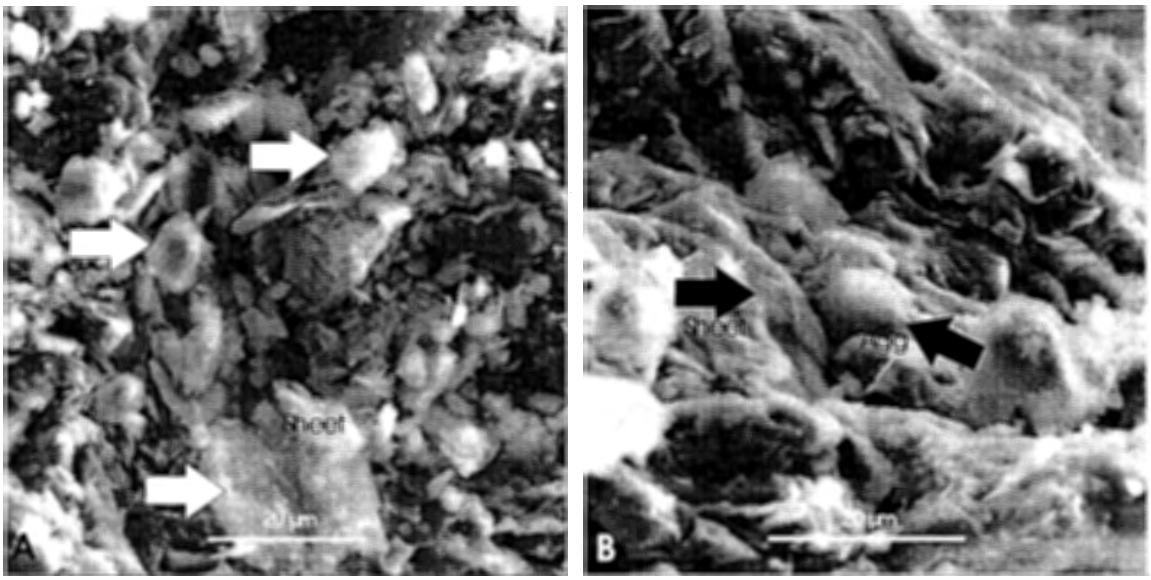

Figure 5.8 - (A) ESEM image of sheeted illite flake and aggregates composed of illite (arrowed). (B) ESEM image of an aggregate in sheeted clay sediment, view is perpendicular to lamination plane, both images from sample JG-2-9.

ESEM imaging and analysis was done from two vantage points, parallel and perpendicular to the lamination plane in the mudstone sample. Those images perpendicular to lamination reveal the presence of more aggregates than the parallel view and are instrumental in showing the relationship between the aggregates and the surrounding sediment. Figure 5.9 shows how sheets of clay appear draped around the aggregate bodies. Figure 5.10 shows the fabric within the analyzed mudstone sample, the clay minerals are visibly aligned at the scale of the ESEM. It was also apparent during this analysis, that certain laminae contain a higher abundance of aggregates than others, suggesting that for some reason aggregates have become concentrated in specific laminae. This concentration could be related to very gentle flooding events that caused reworking in the floodplain muds.

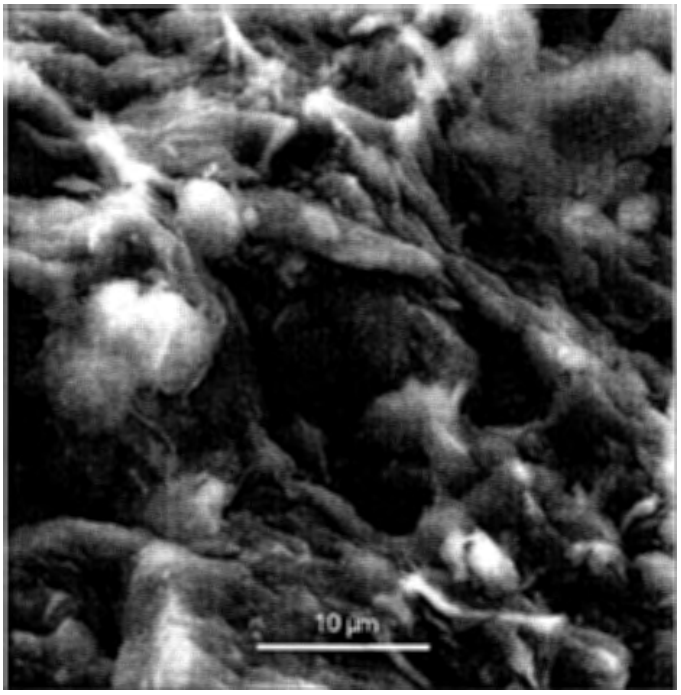

Figure 5.9 - ESEM image of clay flakes draped around an aggregate composed of illite, sample JG-2-9.

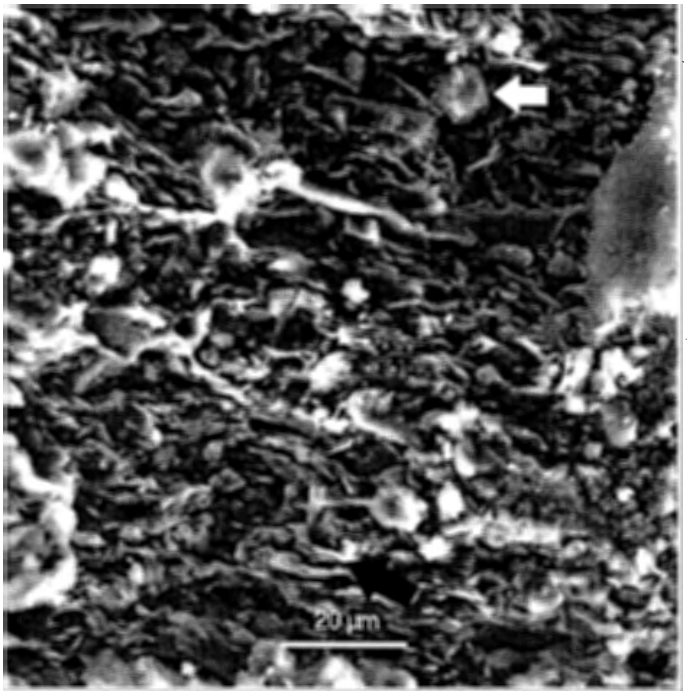

Figure 5.10 - ESEM image perpendicular to cleavage showing the fabric of the sediment, sample JG-2-9. White arrow is an illite aggregate and the black arrow shows the fabric of the rock.

6.0 Chemical Analysis

6.1 Introduction

Three types of chemical analysis have been carried out on several samples collected from the Boss Point Formation. Tools for this analysis include the X-ray diffractometer (XRD), the environmental scanning electron microscope (ESEM) with energy dispersive spectrometer (EDS), and the electron microprobe. Each piece of equipment has a unique purpose and usefulness to this study. For XRD and electron microprobe analysis, samples were chosen to show the range of sedimentary material. The five slides chosen include siltstones with high and low proportions of carbonate, mudstones with high and low proportions of carbonate, and the sample appearing to contain the most mud aggregates in thin section. Samples were chosen for ESEM based solely on the abundance of aggregates in thin section.

6.2 X-ray Diffractometer (XRD)

In this study, the X-ray diffraction technique was used to analyze the bulk composition of the sample. Through analysis, the major minerals present are identified and their approximate proportions determined (see Ch 3). Table 6.1 shows the bulk composition results of the five samples analyzed with XRD. Three of the samples analyzed are mudstones (JG-2-3, JG-2-11, and JG-2-12), and the major minerals present in the mudstone samples are, quartz, illite, chlorite, hematite, and kaolinite. Illite is the most abundant mineral found in these samples, approximately 30-34% of each sample. There is also a significant proportion of quartz (18-20%), whereas the quantity of calcite in each mudstone analyzed varies significantly, and ranges from approximately 0 to 20%.

Table 6.1 - XRD bulk composition analysis (semi-quantative)

Sample	Mineral	Diagnostic Peak (degrees 2θ)	Peak Height (cm)	Intensity Factor	Height * Intensity Factor	Mineral Percent (%)
JG-2-12	Quartz	26.45-26.95	15.3	1	15.30	19
Mudstone	Calcite	29.25-29.6	5.4	1.65	8.91	11
	Illite	8.7-9.1	4.4	6	26.40	33
	Chlorite	18.5-19.1	2	4.95	9.90	12
	Kaolinite	12.2-12.6	4	2.25	9.00	12
	Hematite	33.0-33.4	3.2	3.33	10.66	13
JG-2-11	Quartz	26.45-26.95	14.7	1	14.70	20
Mudstone	Illite	8.7-9.1	4.3	6	25.80	34
	Chlorite	18.5-19.1	2.1	4.95	10.40	14
	Kaolinite	12.2-12.6	3.9	2.25	8.78	12
	Hematite	33.0-33.4	4.6	3.33	15.32	20
JG-2-3	Quartz	26.45-26.95	14.6	1	14.60	19
Mudstone	Calcite	29.25-29.6	9	1.65	14.85	18
	Illite	8.7-9.1	4.1	6	24.60	30
	Chlorite	18.5-19.1	2.2	4.95	10.89	13
	Kaolinite	12.2-12.6	3.4	2.25	7.65	10
	Hematite	33.0-33.4	2.5	3.33	8.33	10
JG-2-10b	Quartz	26.45-26.95	16.3	1	16.30	38
Siltstone	Illite	8.7-9.1	0.8	6	4.80	11
	Chlorite	18.5-19.1	0.6	4.95	2.97	7
	Kaolinite	12.2-12.6	2	2.25	4.50	11
	Hematite	33.0-33.4	0.8	3.33	2.66	6
	Albite	27.35-27.79	4.1	2.8	11.48	27
JG-2-1	Quartz	26.45-26.95	16.9	1	16.90	37
Siltstone	Calcite	29.25-29.6	4.75	1.65	7.84	17
	Illite	8.7-9.1	1	6	6.00	13
	Kaolinite	12.2-12.6	0.95	2.25	2.14	5
	Hematite	33.0-33.4	1	3.33	3.33	7
	Albite	27.35-27.79	3.4	2.8	9.52	21

The other two samples are siltstones (JG-2-1 and JG-2-10b), and the major minerals present are quartz, illite, hematite, albite and kaolinite. Quartz is by far the most abundant mineral found in these samples with a percentage in the high 30's. Albite is also quite abundant averaging 20-26% of the sample, although this value seems high in comparison with thin section observation, and illite composes approximately 11-13% of the siltstones. Calcite presence in the siltstone ranges from 0 to 20%, as in the mudstone samples. Figure 6.1 shows the average mineral abundances of Boss Point mudstone and siltstone in graphic form. From this figure, the wide range of calcite proportion in these samples is apparent. The abundance of calcite in some samples suggests that carbonate cement is an aggregate preservation mechanism, but lack of carbonate material in other samples suggests that other preservation methods are also at work. Figure 6.2 is a sample XRD scan, and it indicates the diagnostic peaks from which mineral proportions were determined.

6.3 Environmental Scanning Electron Microscope (ESEM)

Chemical analysis of specific grains was carried out using the energy dispersive spectrometer (EDS), a device attached to the ESEM. Analysis of 44 different grains/aggregates using EDS resulted in 31 grains found to be predominantly illite, 8 to be quartz, 3 to be plagioclase, and 2 to be K-feldspar. Appendix A contains several EDS spectra from which mineral composition was determined by comparison with spectra illustrated in Welton (1984). The aggregates are found to be composed predominantly of illite with varying amounts of Fe, Mg, and Ca (Fig. 6.3a, b). The presence of these other elements, not commonly found in pure illite, suggests that other clays or impurities are

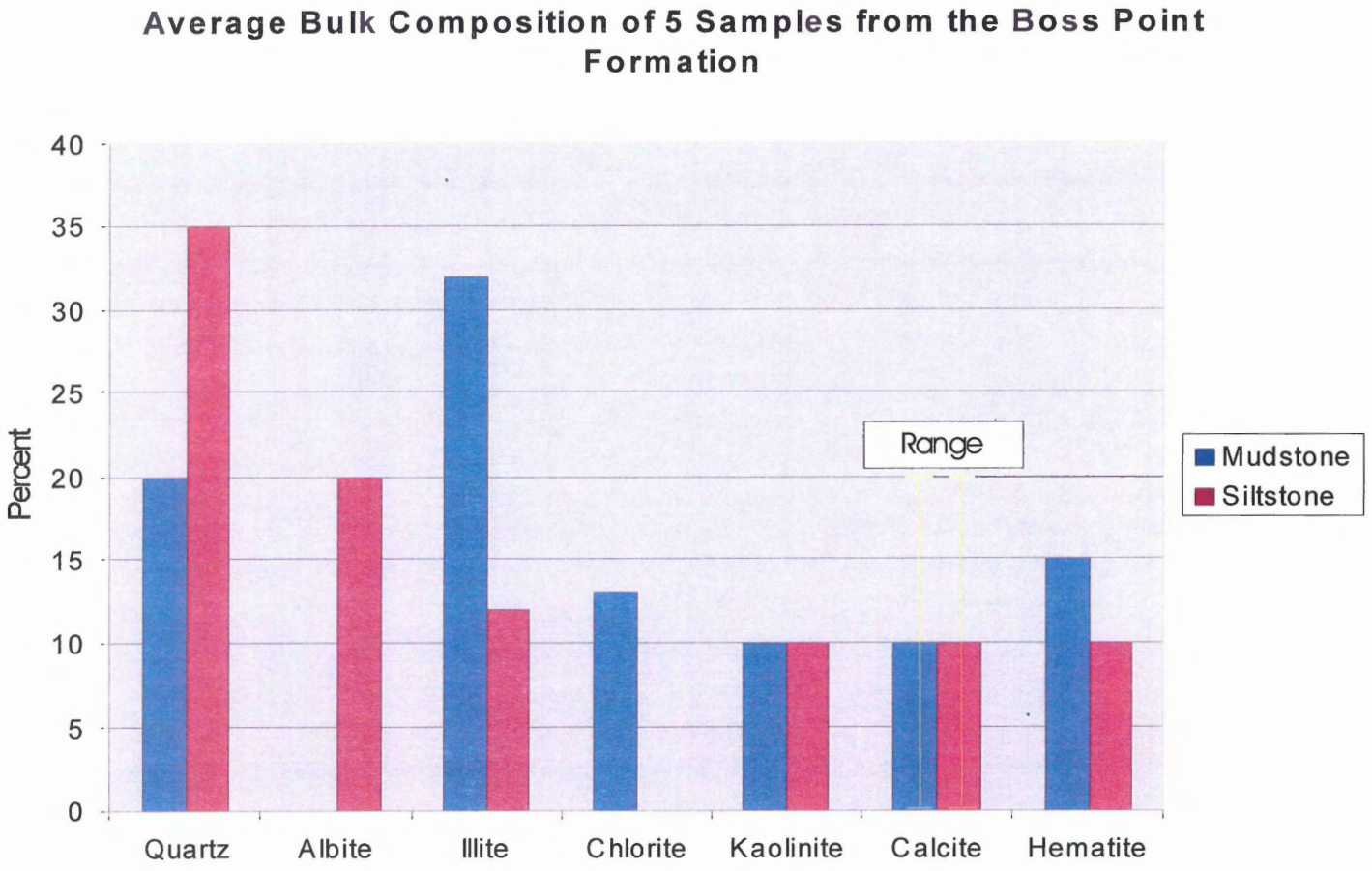

Figure 6.1 – Average mineral abundances in siltstones and mudstones of the Boss Point Formation. Note that the yellow bars in the calcite columns represent the range of calcite present within the samples.

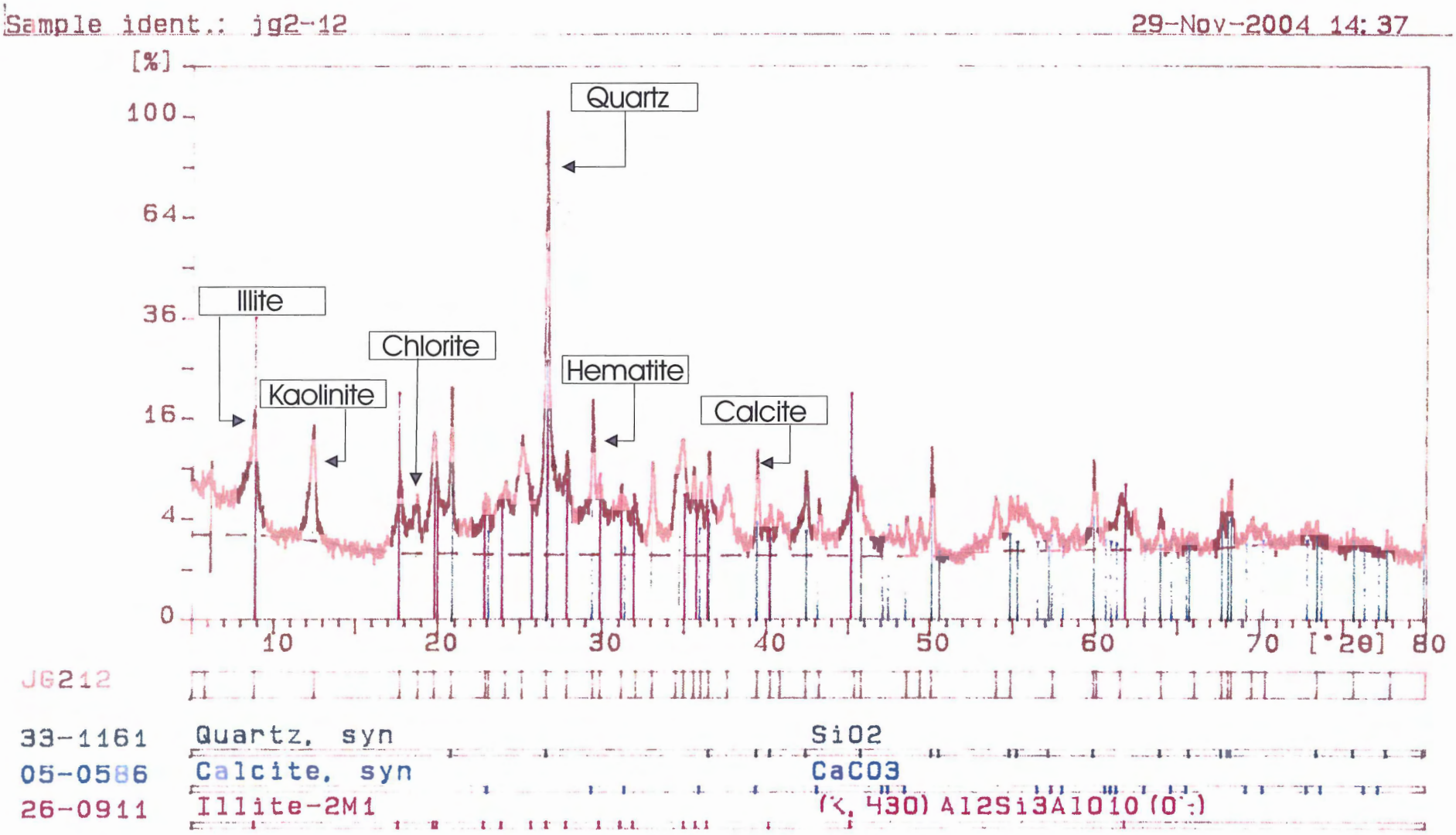

Figure 6.2 - Example XRD spectra. Diagnostic peaks used to determine semi-quantitative bulk composition of sample are identified on figure. Mudstone sample JG-2-12, from site 2.

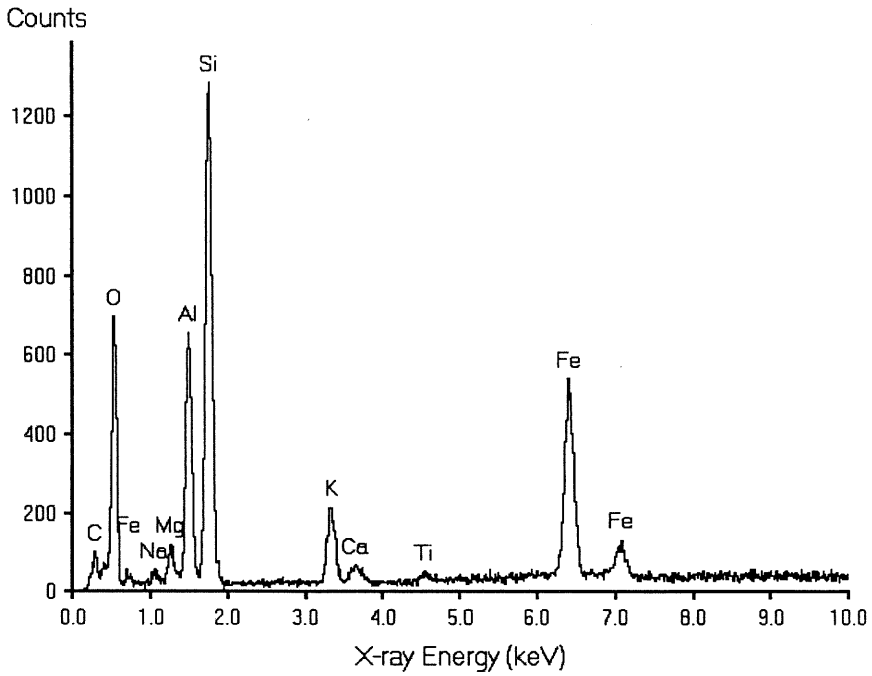

Figure 6.3a - EDS analysis of sheeted sediment clay, illite composition with Fe, Ca, Mg, Na, and Ti impurities, sample JG-2-9.

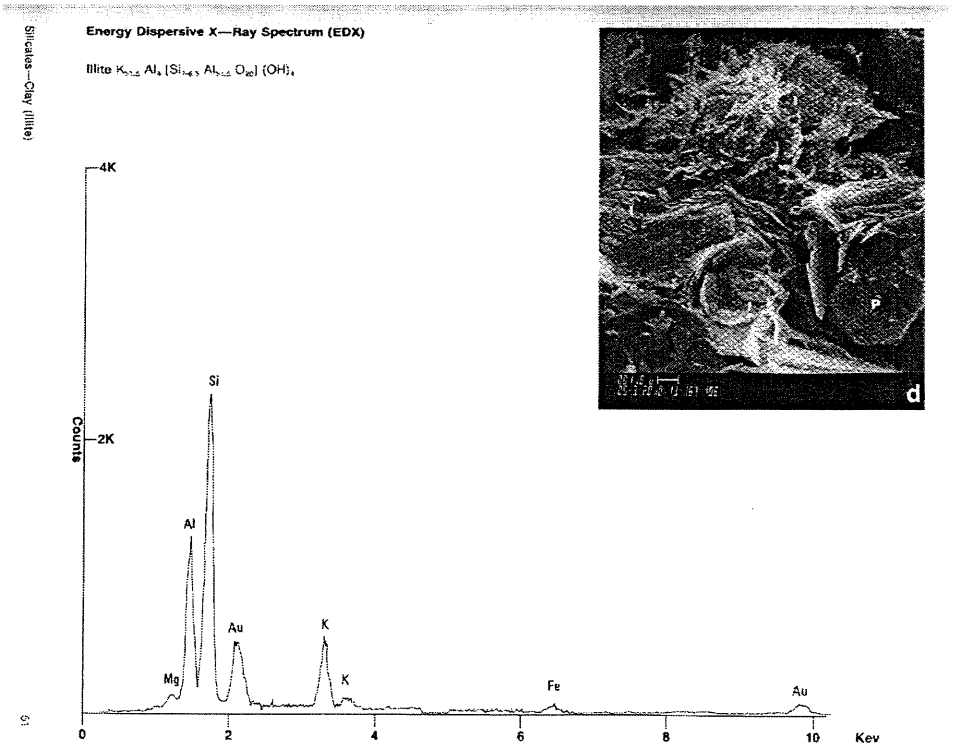

Figure 6.3b – EDS spectra from an illite grain. The diagnostic Si, Al, and K peaks found in (a) are very similar to this figure, taken from Welton, 1984.

also present within the aggregates. EDS analysis of the clay sediment surrounding the aggregates suggests that the sheeted clay is also mainly illite, but contains a very high iron content, which is possibly the result of hematite mixtures in the clay. Iron minerals are known to work as a cementing material in sedimentary rocks, and would likely provide some stability to the aggregates. The sample also contains some Ca, Mg, Ti, and Na, once again suggesting that some mixture of clays is actually present.

6.4 Electron Microprobe

Through elemental mapping, the electron microprobe was used for chemical analysis of specific areas in four thin sections obtained from the Boss Point and Little River formations. Samples were chosen for microprobe analysis based on the abundance of mud aggregates in thin section and the need to obtain a representative range of the sedimentary material present among the samples. This range includes scanning both mudstone and siltstone samples, as well as samples containing high and low proportions of cementing material. Twelve scans in total were carried out on specific areas within the slides. The data were then manipulated to create combination maps of silicon, potassium, and aluminum.

6.4.1 Elemental Mapping

Elemental maps create an image that displays where specifically chosen elements are concentrated in an analyzed area of a thin section. Aluminum, potassium, silicon, magnesium, iron, calcium, and titanium were the elements chosen for this mapping project. These elements were selected because they represent the major elements present

in the previously determined minerals, as recognized in both thin section and XRD analysis. The main focus of the elemental mapping was to interpret the distribution of potassium and aluminum, the diagnostic elements in illite, with respect to the other elements in the sample.

The colour scale for the microprobe images does not represent specific numeric elemental concentration. The images display a relative concentration for each individual scan. Figure 6.4a is a scale bar taken from an element map, showing that the colour blue represents the lowest elemental concentration, whereas, red and white indicate areas of highest concentration. Figure 6.4b is a scale bar from a combination map, showing how the elements are displayed when they occu.r alone and how elements are displayed when they occur in combination.

In figure 6.5 (JG-2-9), large quartz grains are visible in the Si window and are denoted by areas of high silicon concentration. High concentrations of aluminum show up as discrete patches in the Al window. These aluminum-rich areas often coincide with areas containing high concentrations of potassium. However, this is not always the case, as some aluminum-rich areas coincide with areas containing high concentrations of magnesium. Aluminum, magnesium and some iron occurring together imply chlorite, while aluminum and potassium occurring together imply areas rich in illite. Shape of the clay-rich areas vary from thin and elongate, suggesting an individual clay flake, to irregular and blocky patches. These 10 μirregular patches, dominantly composed of illite, indicate some aggregation of clays. Very few patches of calcite cement (Ca) are present within this scanned area. Iron is present in low abundance and evenly distributed

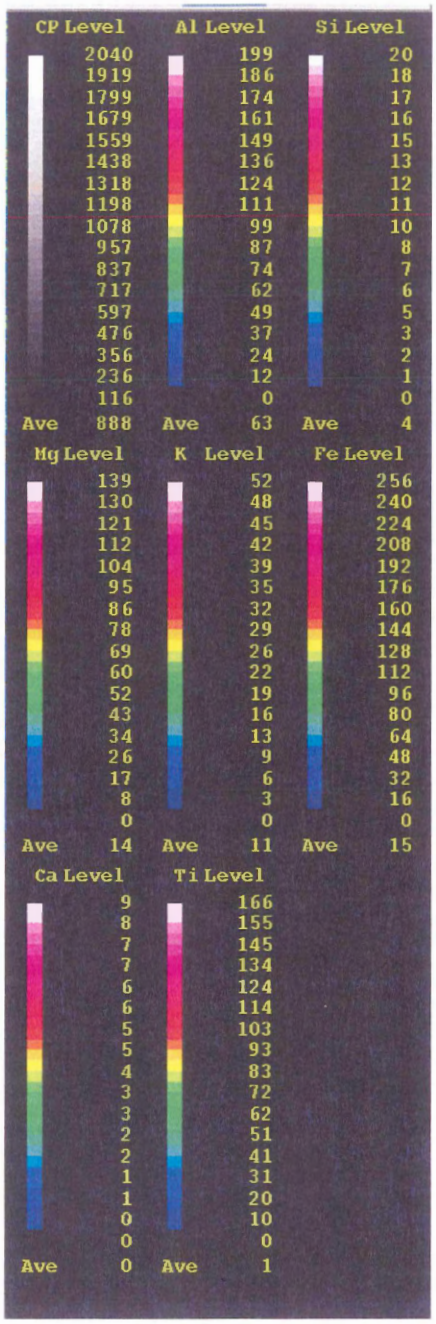

A

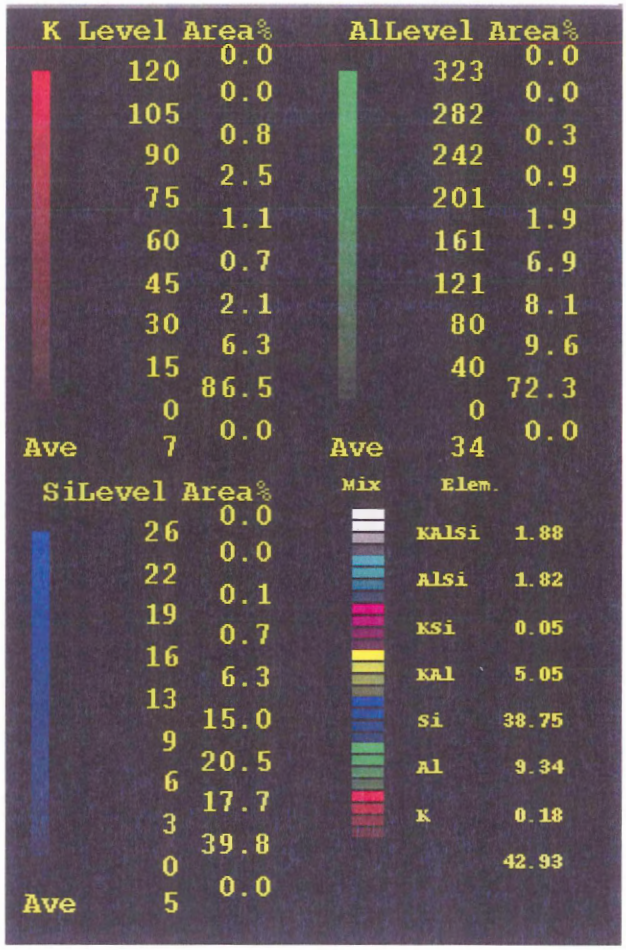

B

Figure 6.4 - (A) Legend from an elemental map. Colour scale does not represent specific numeric elemental concentration. Concentration is relative to each individual scan and numbers beside colour scale represent element counts. Blue signifies areas of lowest concentration and white signifies areas of highest elemental concentration. (B) Combination map legend. K, Al, and Si are indicated by red, green, and blue respectively. The highest concentration of each single element is indicated by the brightest shade of red, green, and blue. Combinations of elements are indicated by the following colours, yellow indicates K and Al, purple indicates K and Si, light blue indicates Al and Si, and white indicates K, Al, and Si.

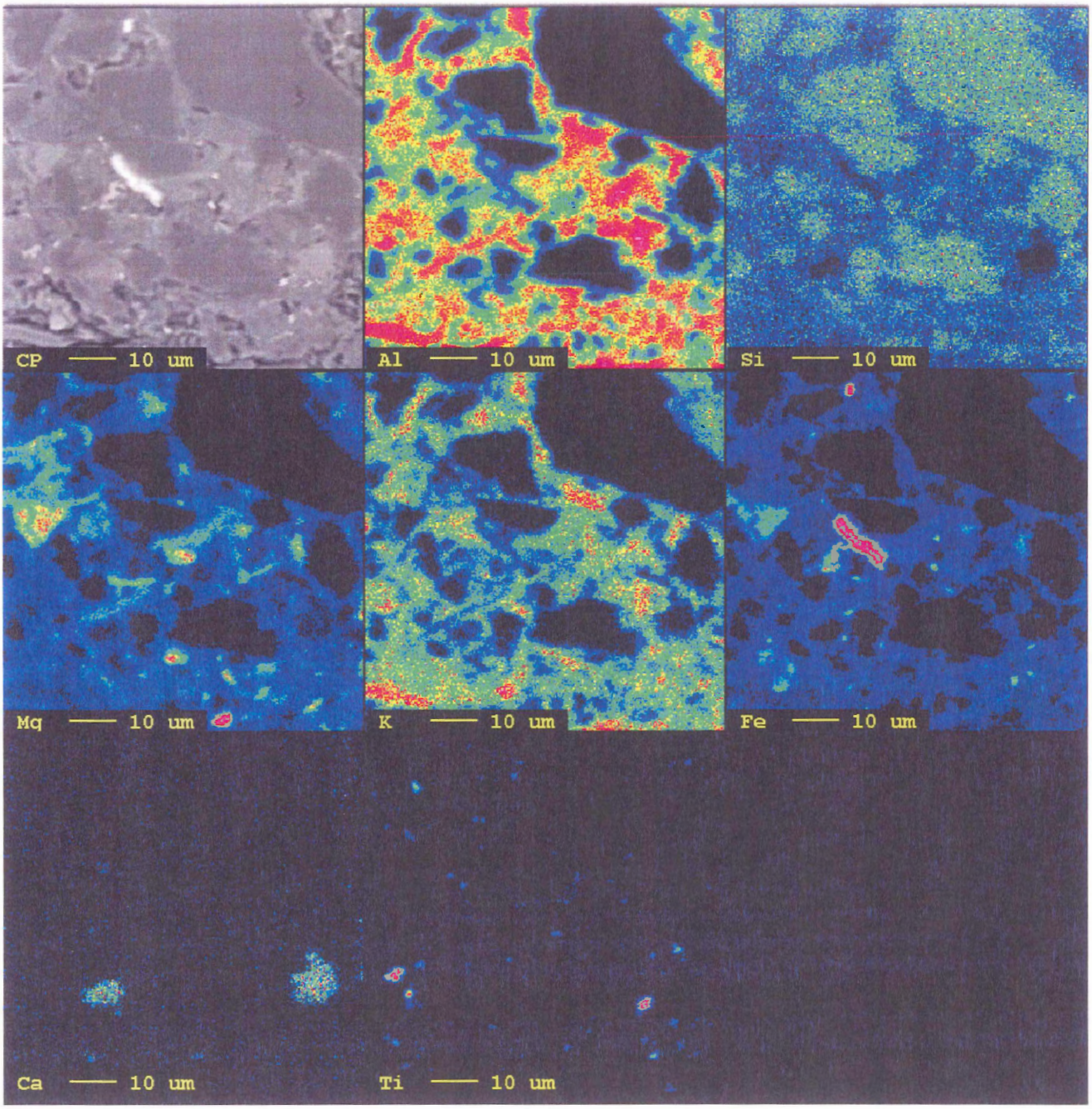

Figure 6.5 - Elemental map of sample JG-2-9, mudstone. Large quartz crystals are visible in Si window. Irregular patches of aluminum and potassium coincide and indicate aggregations of illite clay, elongate patches indicate individual mica flakes. Elongate hematite grain is present in Fe window.

throughout the slide. An elongate grain with high iron concentration is present in the Fe window, indicating a hematite grain.

Figure 6.6 is a combination map of the scan in figure 6.5. From this figure it is apparent that the clay matrix between the quartz grains is mainly a combination of aluminum and potassium, once again implying a dominantly illite composition. The illite clay (yellow) in this figure is broken up into irregular, blocky patches by areas containing higher proportions of aluminum (green), possibly indicating kaolinite.

Figure 6.7 (JG-2-2) contains a large mud fragment surrounded by quartz grains, which are visible as high concentration grains in the Si window. Very small (2-4 μ) quartz grains are also dispersed throughout the mud fragment. Irregular, blocky patches rich in aluminum, 10-15 μ in size, are present in the Al window. These high concentration patches tend to correspond with areas rich in potassium and suggest a predominance of illite. Some aluminum-rich patches correspond with areas displaying high concentrations of magnesium, indicating chlorite-rich clay. Iron is evenly distributed throughout the mud fragment in low concentration. Several small grains rich in both iron and titanium indicate that some ilmenite grains are present. Calcite cement (Ca) is not present directly within the mud fragment, however, the sediment surrounding the mud fragment appears to be cemented.

Figure 6.8 is the combination map of the scan in figure 6.7. From this image it is apparent that the mud fragment is mainly illite in composition; aluminum and potassium occur together, causing the fragment to appear yellow.

Figure 6.9 (JG-2-9) contains large quartz grains, visible as high concentration blocks in the Si window. Discrete high concentration patches of aluminum are present in

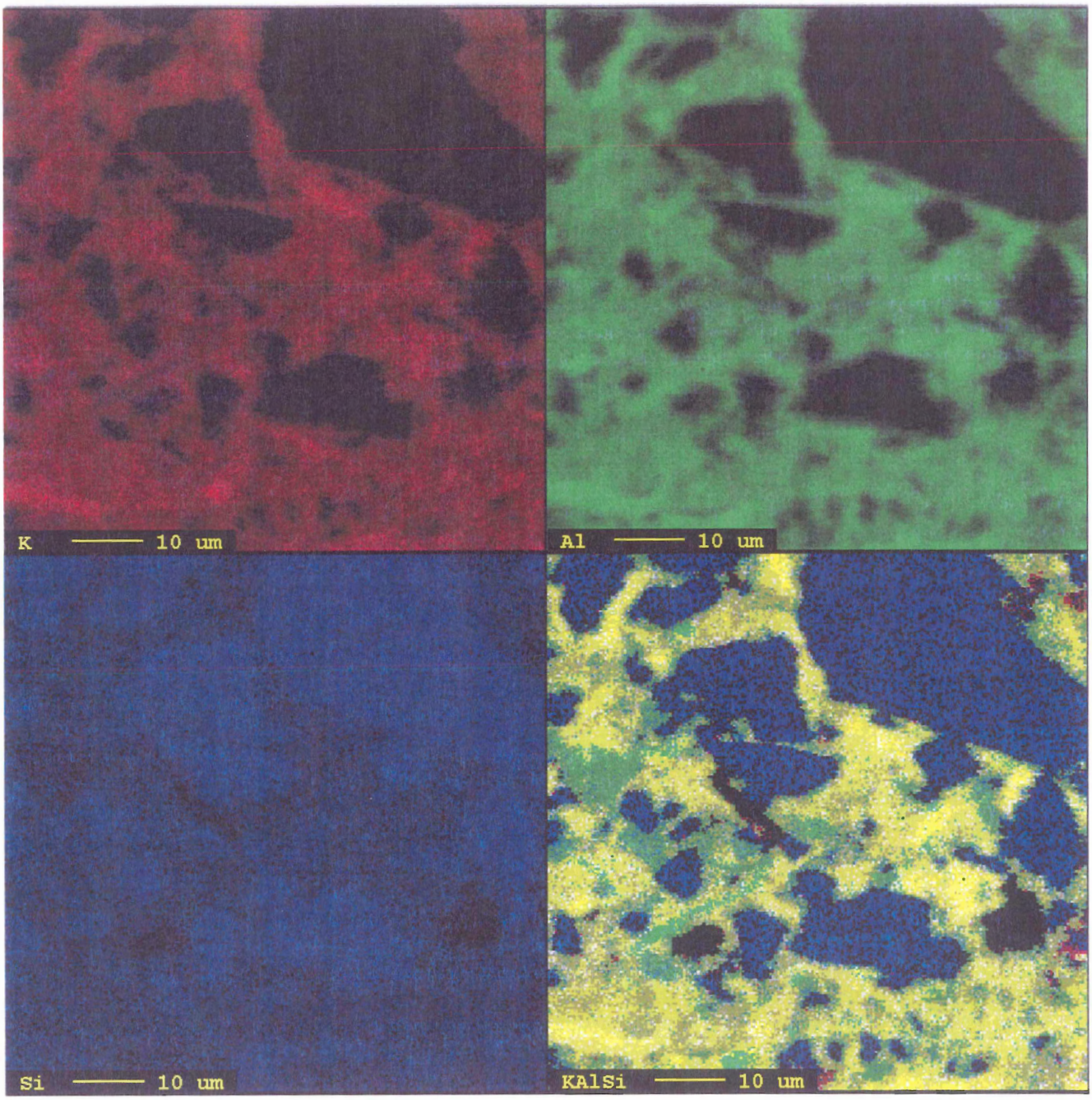

Figure 6.6 - K, Al, Si combination map of fig. 6.5. The window in the lower right is a combination of the three elements. Blue indicates the presence of quartz grains (Si), where as, the yellow and green areas represent clay material (Al and K). Sample JG-2-9, mudstone.

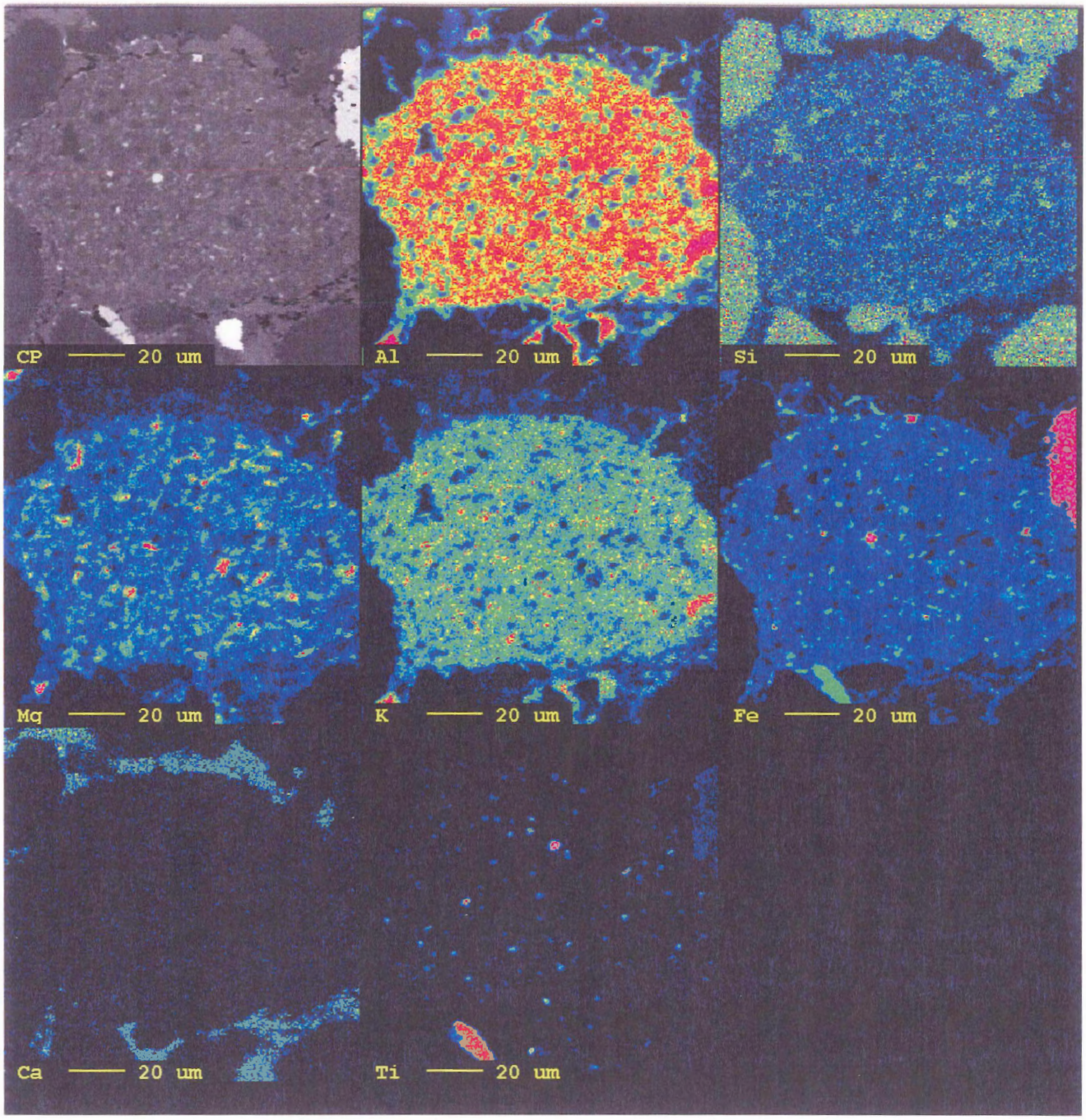

Figure 6.7 - Elemental map of sample JG-2-2, sandstone. Contains large mud fragment surrounded by quartz grains. Irregular, blocky patches rich in aluminum, 10-15 microns, correspond with areas rich in potassium suggesting illite. Some aluminum-rich patches correspond with areas displaying high concentrations of magnesium, indicating chlorite-rich clay.

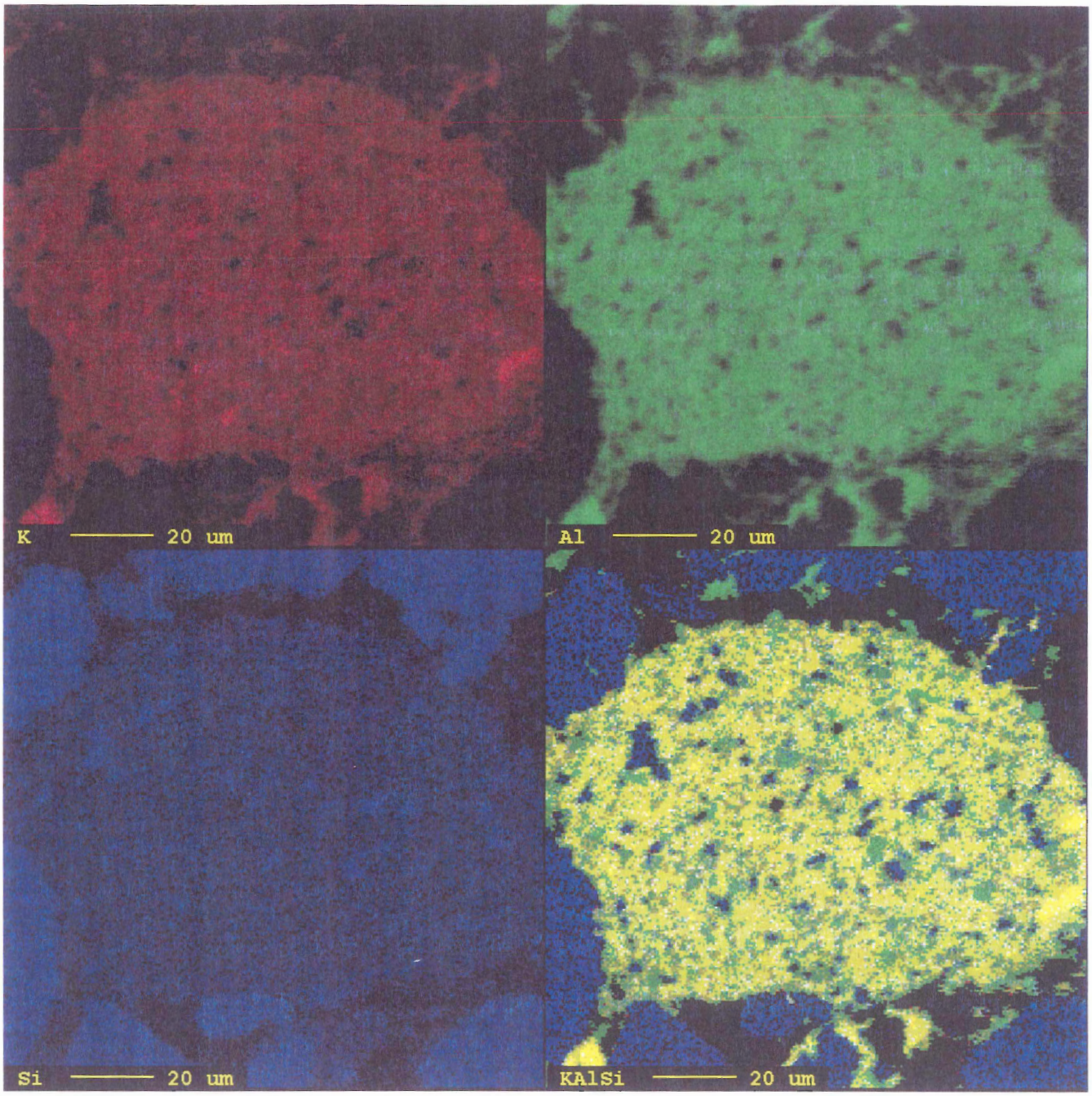

Figure 6.8 - K, Al, Si combination map of Fig. 6.7. Image displays a mudstone fragment surrounded by quartz grains. A large portion of this fragment is yellow indicating a combination of Al and K. Very small (2-4 micron) quartz grains, identified in blue, are also dispersed throughout the mud fragment. Sample JG-2-2, carbonate concretion in sandstone.

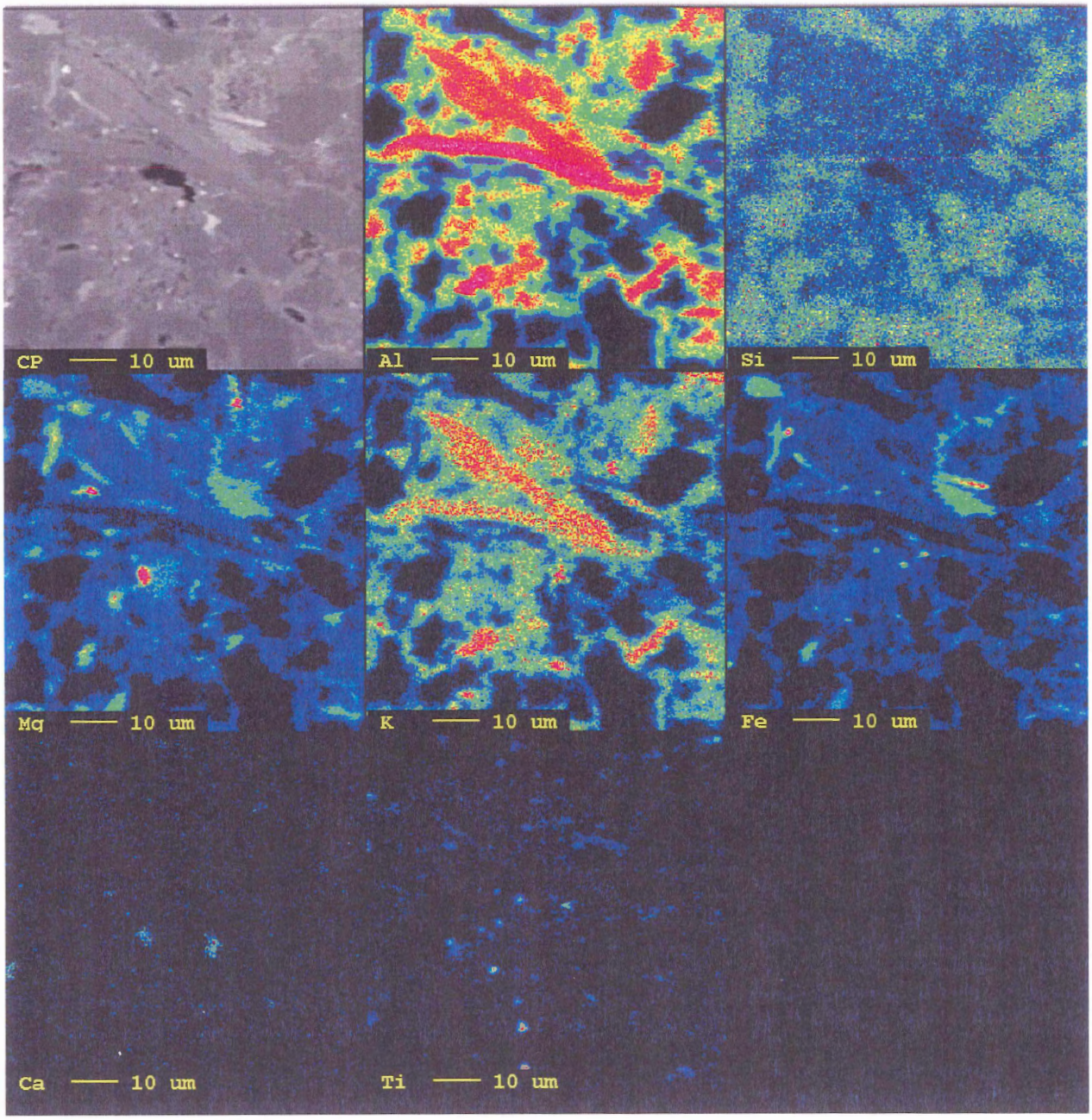

Figure 6.9 - Elemental map of sample JG-2-9, mudstone. Contains large quartz grains (Si), discrete high concentration patches of aluminum coinciding with areas of high concentration potassium. These patches vary in shape, some are distinctly thin and elongate, suggesting large mica flakes, while others occur in a blocky, irregular texture, suggesting an aggregate of illite.

the Al window. These patches often coincide with areas of high concentration in the potassium window. High-concentration aluminum and potassium patches vary in shape, some are distinctly thin and elongate, suggesting large muscovite flakes, while others occur in a blocky, irregular texture, suggesting an aggregation of illite. There are some patches dominated by aluminum and magnesium, indicating chlorite-rich areas. Iron is consistently present throughout the clay in low concentration. Few higher concentration iron patches coincide with magnesium-rich occurrences, indicating chlorite. No calcite cement (Ca) is present in this scan.

Figure 6.10 is a combination map of the scan in figure 6.9. Large muscovite flakes are visible and denoted by thin, elongate areas of aluminum and potassium occurring together (yellow). Irregular illite-dominated blocks are common in this image and are surrounded by quartz grains.

Figure 6.11 (JG-3-1a) contains quartz grains scattered throughout the scan which are visible in the Si window. Some blocky aluminum-rich patches are present in the Al window that coincide with potassium rich areas. Large, elongate patches of aluminum, magnesium, and iron occur together and indicate individual chlorite flakes. Some irregular patches of low-concentration iron occur in areas coinciding with the aluminum rich areas. This slide is well cemented with calcite, evident by the even concentration of calcium throughout the Ca window. Large hematite grains are present and visible as high iron concentration.

Figure 6.12 (JG-2-2) contains large angular quartz grains, visible in the Si window. Angular grains with very high potassium and moderate aluminum concentrations are indicative of feldspar grains. Aluminum and potassium occur together

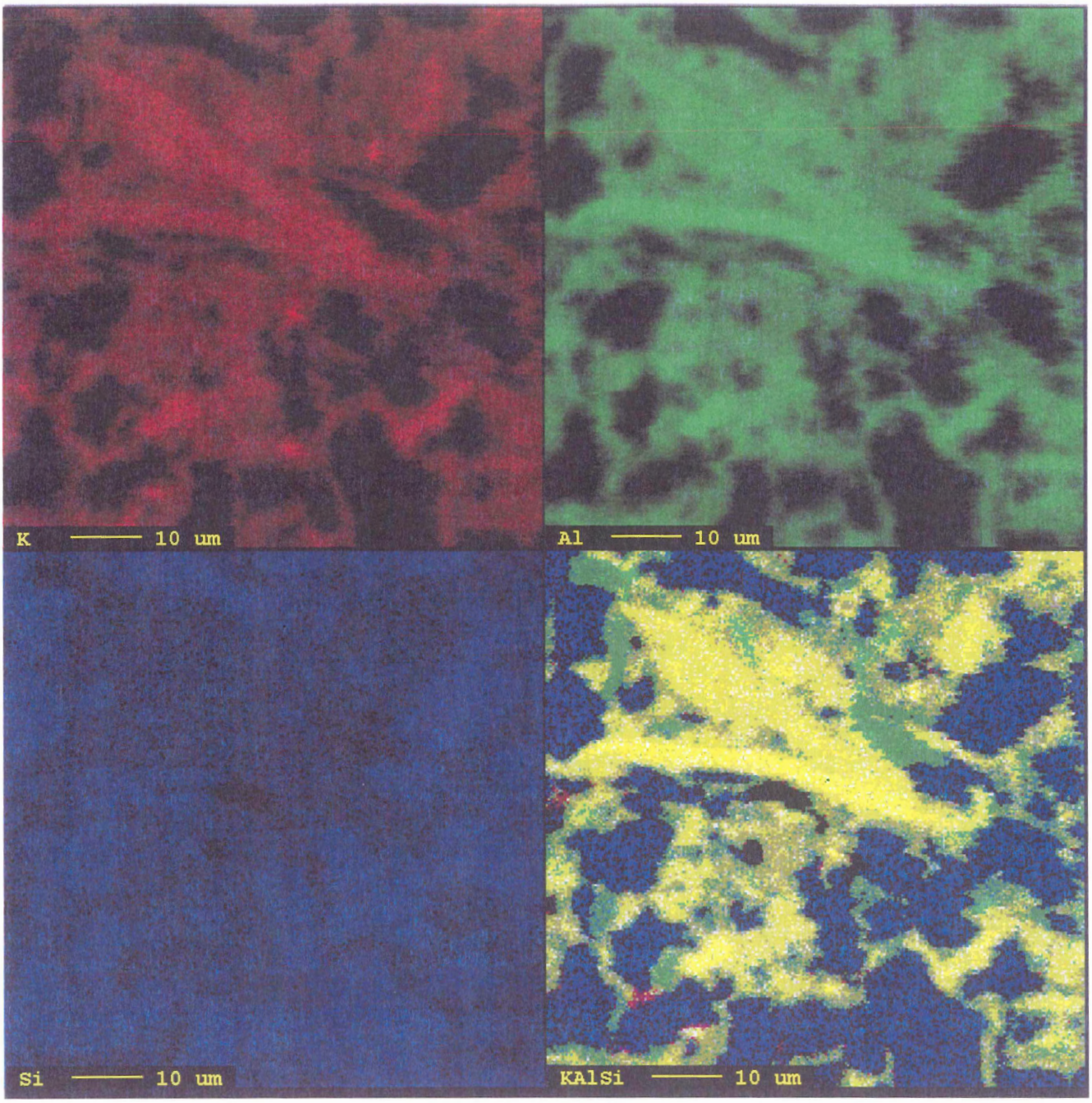

Figure 6.10 - K, Al, Si combination map of Fig. 6.9. Large muscovite flakes visible as elongate accumulations of aluminum and potassium (yellow). Irregular, blocky accumulations of aluminum and potassium indicate aggregations of illite which are surrounded by quartz grains (blue) Sample JG-2-9, mudstone.

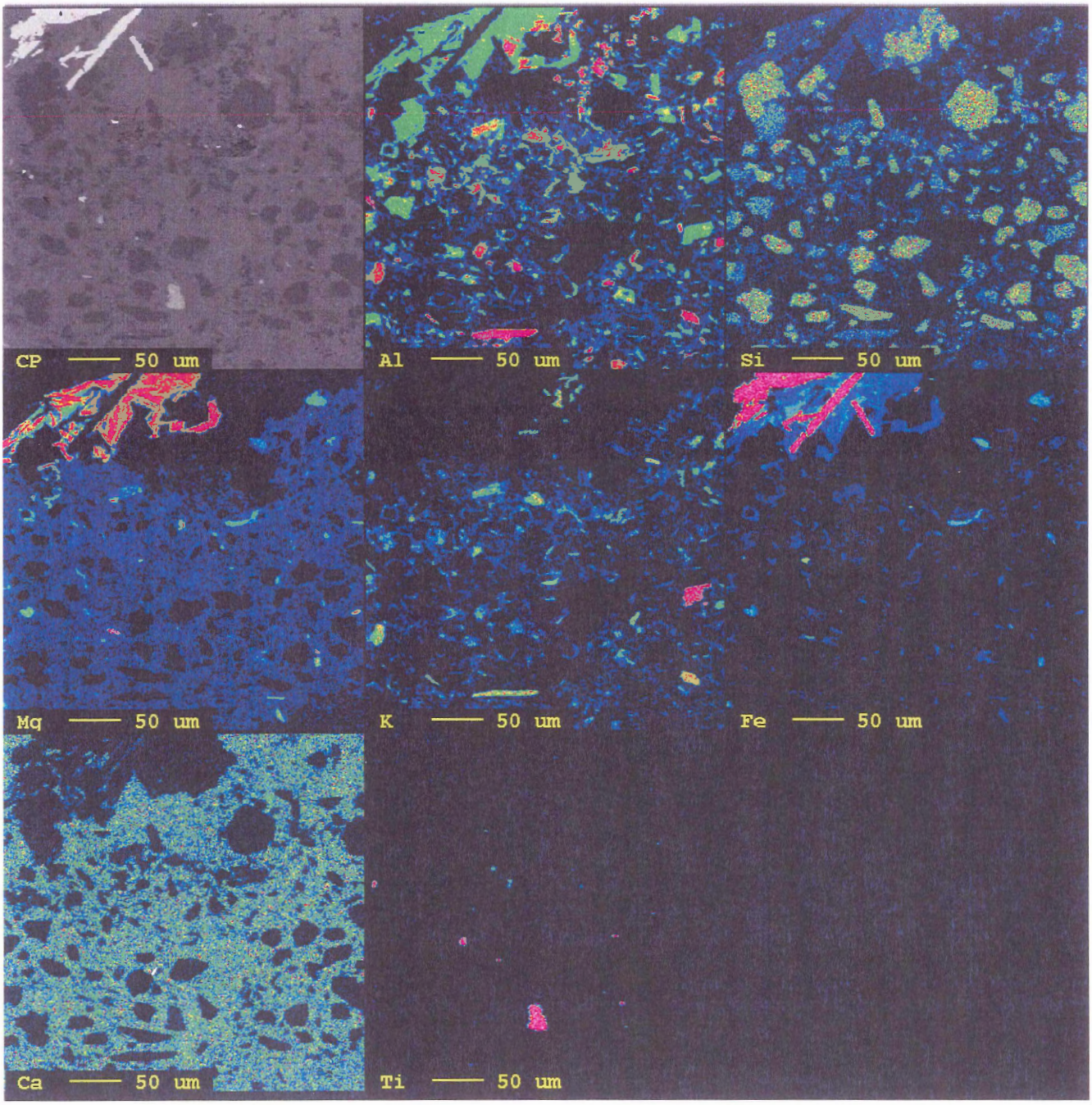

Figure 6.11 - Elemental map of sample JG-3-1a. Contains quartz grains (Si), and blocky aluminum- and potassium-rich patches indicative of illite. Large, elongate patches of aluminum, magnesium, and iron occur together indicating chlorite flakes. High concentration iron patches indicate hematite grains.

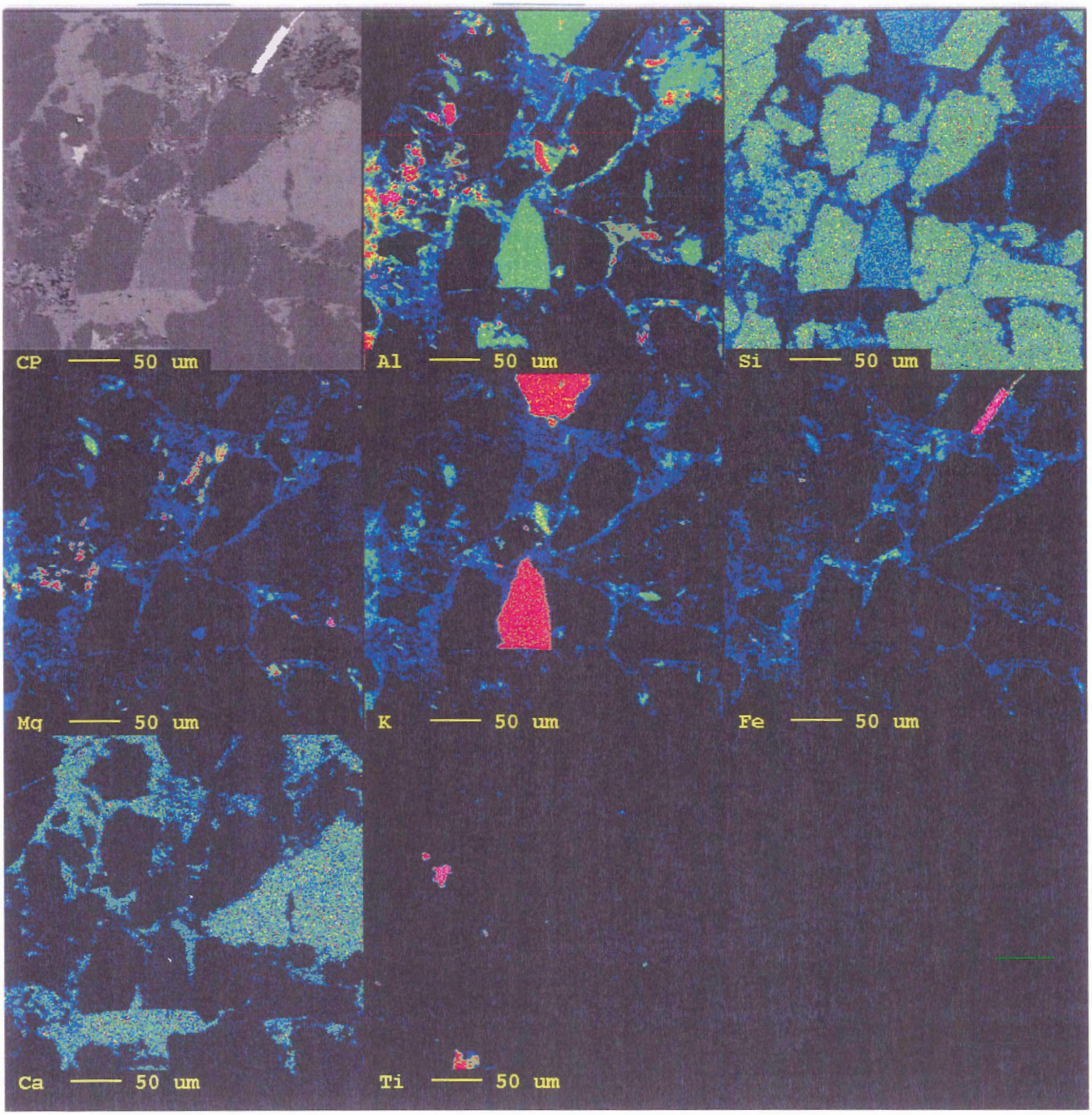

Figure 6.12 - Elemental map of sample JG-2-2, sandstone. Contains large angular quartz grains, angular feldspar grains (high potassium and moderate aluminum), and irregular10-20 micron patches of aluminum and potassium, indicating aggregates of illite.

in irregular10-20 μpatches, implying aggregates of illite. There are some patches that are mainly composed of aluminum and magnesium, indicating chlorite-dominated patches. Calcite cement is present between the quartz and feldspar grains, and iron is present throughout the clay-dominated areas of the scan. A single elongate, high concentration iron patch indicates a hematite grain.

6.4.2 Summary of Elemental Mapping Results

The difference between quartz- and clay-rich areas is apparent when looking at any of the elemental maps in this study. Clay-rich areas are dominated by aluminum, potassium, and magnesium, whereas quartz grains are dominated by a high concentration of silicon. Distinctly elongate clay-rich areas imply individual clay flakes and not aggregates of clay. Aluminum and potassium occurring together in blocky, irregular patches is indicative of aggregated illite. Aluminum-, magnesium-, and iron-rich areas are indicative of areas dominated by chlorite. The lack of circular shape in the clays is most likely the result of aggregates having diffuse boundaries when viewed at such small scale, and may also indicate that the non-aggregated matrix material is similar in composition to that of the mud aggregates. There does, however appear to be a clotted texture of clays with high aluminum and potassium concentration in many of the scans, indicating irregular aggregates of illite 10-20 μ in size. This probe data supports thin-section and ESEM observations, which have imaged aggregates directly.

It has been mentioned in earlier chapters (Ch. 2 and 5) that calcite cement plays a role in the preservation of mud aggregates during burial. Little has been said to this point on the presence of iron and how it can work as a cementing material. Hematite, goethite,

and other iron oxides are common cements in upper horizons of soils and are particularly common in acidic, sandy soils (Retallack, 2001). Extensive cementation of red beds occurs as a result of iron-bearing minerals becoming oxidized during burial. All of the microprobe scans tend to show an even distribution of iron throughout the clay rich sediment. Therefore, accumulation of ferruginous materials may actually have been an important contributing factor in mud aggregate preservation.

7.0 Discussion

7.1 Aggregate distribution and preservation in the Boss Point and Little River formations

The best preserved mud aggregates in thin section correspond with the calcrete, rubbly mudstone, and small channel body facies previously described in chapter 4. Calcrete facies are an ideal type of deposit for finding well preserved mud aggregates in the sedimentary record for several reasons: calcretes form in sedimentary deposits under the influence of pedogenic processes, processes that are also necessary for mud aggregate formation. Calcretes form in the same arid to semi-arid climatic conditions that produce shrinking and swelling soils necessary for the formation of mud aggregates. The defining characteristic of a calcrete is the amount of secondary carbonate, specifically in the form of calcite cement, in the paleosol. This secondary carbonate adds stability to the aggregates by preventing or significantly reducing compaction during burial of the sediment.

Mudstone deposits, specifically the rubbly mudstone facies, generally display the aggregate texture better than the sandstone and siltstone deposits of the Boss Point and Little River formations. The rubbly nature of the mudstone may imply that it originally formed through the accumulation of detrital mud fragments. In some of the best preserved mudstone samples, entire portions of the rock are composed almost completely of dispersed aggregated mud. Other mudstone samples contain a high proportion of aggregates, but also contain significant amounts of fine quartz and feldspar grains. Essentially, more mud aggregates are found in the mudstone deposits because this is where the aggregates originally formed. Floodplain muds were sometimes reworked

during gentle overbank floods, leading to the development of small-scale stratification of the mud aggregate-rich sediment.

Mud aggregates are also well preserved within the small channel body facies, which is composed mainly of silt and very fine sand. The proportions of mud aggregates are much lower than in the mudstone deposits and the aggregates tend to be more dispersed. Mud aggregates in sandstone and siltstone represent mud or mudstone fragments that have been reworked from floodplain mud. The lower proportion and scattered distribution of the aggregates is a product of both the reworking of loose aggregates and the erosion of consolidated mud fragments. Floods that brought sand and silt onto the floodplain and transported the aggregates into active fluvial channels were aggressive flooding events. During these floods some aggregates would have become worked into the coarser sediment and some fragments would have been eroded and transported into more distant deposits. Essentially, mud aggregates are foreign bodies to anything other than floodplain mudstone, so their presence should be limited and distribution more dispersed in sands and silts than the floodplain muds.

In all of the identified facies, preservation of mud aggregates is related to a combination of factors. Both X-ray diffraction and electron microprobe techniques (chapter 6) indicate the presence of calcite particles and calcite cements in varying amounts. In some samples, nearly 20% of the material is calcite, whereas other samples have very little. Calcite cement is known to preserve delicate sedimentary structures (e.g. burrows), but lack of calcite in some Boss Point samples implies that it is not the only force at work protecting the mud aggregates. XRD analysis shows that hematite ranges from approximately 6-20% of the samples and that mudstone samples tend to have higher

hematite concentrations than siltstone samples. Elemental maps from electron microprobe analysis show iron as being a consistently distributed element throughout all of the analyzed samples. Iron is evenly distributed throughout the clay-rich portions of the elemental maps, even more so than calcite. This consistent iron concentration suggests that hematite crystallization may play a significant role in aggregate preservation within the rock record of the Boss Point Formation. Evidence exists for extensive cementation of red beds by oxidation of iron-bearing minerals during burial, although the timing of oxidation could be either during soil formation or during burial (Retallack, 2001). Reddening of ferric hydroxides in clay-rich paleosols during shallow burial is likely. Deep burial oxidation is less likely because associated paleochannel sands have largely remained unoxidized.

Of the three sites studied in this project, the measured section of site 2 has been found to contain the most abundant and best preserved mud aggregates. Site 1 has been the least productive, with very few aggregates having been identified in thin section. The main difference between the three sites is the proportion of floodplain muds within each location. Site 2 is dominated by floodplain mudstone and small floodplain channel bodies composed of siltstone. The studied interval at site 1, on the other hand, focuses mainly on the large, sandstone channel body and siltstone crevasse splay deposits. Minor floodplain muds were present but not studied in detail. Site 3, found in the Little River Formation, is different from the previously mentioned locations in that it is entirely composed of coarse sediment, forming large channel sandstone bodies. This site experienced rapid and flashy flow conditions, and clasts composed of aggregated mud and siltstone were eroded,

transported, and deposited along with the coarse sand. Mud fragments preserved in this sandstone may have traveled a great distance before final deposition.

7.2 Aggregates in the Cumberland Basin

The Boss Point and Little River formations are not the first formations in the Cumberland Basin to yield pedogenic mud aggregates. The mid-Carboniferous Maringouin Formation, found to contain mud aggregates by Rust and Nanson (1989), is located on the Maringouin Peninsula, Chignecto Bay, New Brunswick and on the Cumberland Bay shore of Nova Scotia. Aggregates in the Maringouin Formation are larger than aggregates found in the Boss Point and Little River Formations. Aggregates are up to 10 times larger than the quartz grains with which they occur and were only preserved in sandstone deposits. Lack of aggregate texture in the mudstone of this formation was attributed to loss of structure during burial and compaction of the mud. Data on the bulk composition and cementing material present in aggregate-bearing sandstone and non-aggregate bearing mudstone is not provided in the Rust and Nanson (1989) study. Differences in composition, therefore, can not be assessed in order to explain the apparent lack of aggregate texture in the mudstone of the Maringouin Formation. However, cementing material may be present in lower quantities in the Maringouin Formation than in the Boss Point Formation, reducing the preservation potential of mud aggregates upon burial.

The Cumberland Basin was a rapidly subsiding basin during the Carboniferous Period. Müller et al. (2004) suggested that rapid burial of sediment preserves delicate sedimentary structures that are destroyed at normal or slow burial rates. Destruction of

the aggregate texture, as a result of slow burial conditions, has been established within the floodplain mud of Cooper Creek in central Australia. Rapid subsidence rate of the Cumberland Basin is likely to have played some role in maintaining the well preserved aggregates in the floodplain mudstones of the Boss Point Formation.

Plint and Browne (1994) suggested that the Cumberland Basin, specifically the Boss Point Formation, experienced catastrophic subsidence events as a result of tectonic activity. The sharp change from braidplain to lacustrine packages, and well preserved bedform structures at the top of the braidplain units, are evidence of major fault activity during the deposition of the Boss Point Formation. These catastrophic subsidence events would have resulted in rapid burial of the floodplain sediments and would have aided preservation of the aggregate structure. Rapid burial in conjunction with hematite and calcite cementation may have provided the ideal situation for aggregate preservation in the Boss Point Formation.

Mud aggregates are well preserved in the channel sandstones of the Maringouin Formation. Preservation in these units has been attributed mainly to shielding by mineral grains. A strong mineral framework, as identified in thin section, was also a contributing factor in protecting the fine aggregates in the siltstones and sandstones of the Boss Point Formation.

7.3 Paleo-environment and aggregate formation

Previous research into pedogenic mud aggregates has defined a specific set of environmental conditions where mud will naturally aggregate into small clumps. Studies by Nanson et al. (1986), Rust and Nanson (1989), Maroulis and Nanson (1996),

Gierlowski-Kordesch and Gibling (2002), and Müller et al. (2004), have all identified a similar set of paleo-environmental conditions in formations containing the mud aggregate texture. These conditions and processes of formation, outlined in detail in chapter 2, include arid to semi-arid climate conditions, shrinking and swelling clays in floodplain mud, and pedogenic processes having occurred within the mud.

Table 1.1 contains a brief summary of the formations and deposits previously found to contain pedogenic mud aggregates. From this summary table, a commonality in the sediment types can be found among the formations. All the studies contain fluvial sandstone channel bodies, crevasse splay sandstone/siltstone sheets, floodplain mudstone deposits, and evidence of pedogenic processes. All of the formations were deposited in arid to semi-arid paleo-climates. Braidplain sequences in the Boss Point Formation fit into this description. Numerous channels in Boss Point strata experienced regular to episodic flooding events as a result of the seasonally wet-dry climate, forming extensive floodplain mud deposits. These climatic conditions allowed soils to develop, churn, and self-mulch during cycles of wetting and drying. Pedogenic processes are evident from mottled appearance, root traces, plant fragments, and secondary carbonate in many of the mudstones and siltstones of this formation. Flooding events in the Boss Point Formation periodically resulted in levee collapse and caused significant amounts of sediment from the main channels to spread over the floodplain, depositing sheets of sand and silt. These floods eventually led to the activation of small floodplain channels and redistribution of floodplain sediment.

The Boss Point Formation is especially similar to the dryland river system of the Triassic Lunde Formation, not only in paleo-environment but also in preservation

mechanism (Müller et al., 2004). Preservation of aggregates in the Lunde Formation is attributed to a combination of carbonate cements and rapid burial of sediments. Like the Boss Point Formation, the Lunde Formation recorded mud aggregates preserved in floodplain mudstone, making these the only two formations on record to contain well preserved aggregates in floodplain mudstone deposits. In all other aggregate-bearing formations studied to date, mud aggregates have only been found preserved in channel sandstone and siltstone deposits. Ékes (1993) suggested that the original mud aggregate texture in the mudstone of the Ridgeway Conglomerate Formation was obliterated by compaction, but cryptic structures and evidence of vertic soil development are evidence of floodplain hydraulic processes.

Evidence for vertisol development is present within the Boss Point Formation. Conchoidal weathering, deep desiccation cracks, joint sets, drab mottles, and poor horizonation are features present at site 2 that can be attributed to paleo-vertisols. Plint and Browne's (1994) description of slickensided surfaces, pseudo-anticlines, and desiccation cracks within the Boss Point Formation, in conjunction with the structures found at site 2, provide good indication of vertisol development.

Chemical analysis techniques have shown no evidence of smectite in the paleosols, and both XRD and EDS analysis show illite as the main clay component. According to Müller et al. (2004), only a limited amount of swelling clay is necessary to form pedogenic mud aggregates. Rust and Nanson (1989) found kaolinite to be the dominant clay and smectite to be a minor clay component in the middle reaches of the Cooper Creek floodplain. If smectite was originally present in a quantity great enough to form pedogenic mud aggregates in the Boss Point Formation, burial and diagenesis may

have later resulted in smectite alteration to illite. Unfortunately, XRD does not record minerals that are present in amounts lower than about 5%.

The composition of mudstone deposits and mud aggregates in each previous study is different, with different clay combinations and clay ratios. Cooper Creek mud is typically greater than 50% clay, which varies from dominantly smectite with minor kaolinite to dominantly kaolinite with minor smectite (Nanson et al., 1986; Rust and Nanson, 1989; Maroulis and Nanson, 1996). The Lunde Formation varies from 70% smectite/illite to 60% illite and 15% smectite (Müller et al., 2004). The New Haven Arkose contains a mixture of illite, smectite, chlorite, and mixed illite/smectite (Gierlowski-Kordesch and Gibling, 2002). The Hawkesbury Sandstone contains a mixture of kaolinite/dickite, and mixed-layer species (Rust and Nanson, 1989). The commonality in most of these studies is the presence of some smectite. According to EDS analysis, the mud aggregates in the Boss Point Formation are mainly illite in composition, although, presence of Fe, Mg, Ca, and Ti suggest that other clays are present in minor quantities within the aggregates. XRD results have identified varying amounts of chlorite and kaolinite in the Boss Point Formation samples. These two clays likely form minor constituents of the mud aggregate material. No direct evidence of smectite is present in the Boss Point aggregates, as in the case of the Hawkesbury Sandstone.

In all previous studies mentioned, the mud aggregates have been in a similar size bracket, fine to medium sand sized (100-400 μ). In the Boss Point Formation, the majority of the mud aggregates are significantly smaller, around 20 μ This is an avenue that needs to be further explored.

7.4 Was smectite originally present in the Boss Point Formation?

The question remains as to whether burial depth of the Boss Point Formation was great enough to cause alteration of smectite to illite. This question can be addressed by determining the vitrinite reflectance levels of coal seams in the formation. Vitrinite reflectance (Ro) is a measure of the reflectivity of a polished surface of vitrinite (Ryan and Boehner, 1994). This is a precise method for quantifying organic maturation related to burial depth and thermal parameters. Vitrinite reflectance in the area of Boss Point has been recorded in the range of 0.55-0.89 according to Ryan and Boehner (1994). These vitrinite reflectance values can be correlated to the thermal maturation index of smectite. According to Héroux et al. (1982), vitrinite reflectance levels of approximately 0.7 suggest a level of thermal maturation high enough to cause alteration of smectite in mudstone. Plint and Browne (1994) noted the presence of smectite in siderite concretions found in the Boss Point Formation, where it appears to have been protected during burial and diagenesis. A combination of the vitrinite reflectance values and smectite in siderite concretions provides strong evidence that smectite was once present in the Boss Point Formation and altered to illite during burial and diagenesis.

7.5 Can other mechanisms for aggregate formation be ruled out?

Aeolian mechanisms are an unlikely source for aggregate formation in the Boss Point and Little River formations because there is no evidence in either formation to suggest aeolian processes; no structures such as wind-blown dunes and no evidence of saline influence in these formations. Dare-Edwards (1982) believed that aeolian pellets

lose structure and collapse during pedogenic processes. Boss Point mudstones retain strong evidence of pedogenesis in aggregate-bearing mudstone.

The abundance of aggregates in the floodplain mudstone facies would seem to rule against fecal pellet origin. Independent evidence of strong biogenic activity would have to be present in the study intervals for this option to be considered, whereas megascopic burrows appear to be uncommon in the Boss Point Formation.

Although eroded mud fragments are common in the studied sections, it is also unlikely that the fine aggregates originated as mud-rich lithoclasts. The uniform size and shape of the aggregates imply a pedogenic origin rather than an erosional origin.

7.6 Advantages and disadvantages of imaging and composition analysis techniques

The transmitted light microscope and the environmental scanning electron microscope (ESEM) were the main imaging devices used to identify pedogenic mud aggregates in this study. Viewing thin sections through a transmitted light microscope is an effective method to identify the presence of the mud aggregate texture in a sample. This technique is useful in identifying the size and distribution of the aggregates, as well as showing how they occur in thin section in relation to other minerals and cementing materials.

The ESEM operates on a very small scale, and therefore requires more time and patience to find individual aggregates. In terms of this study, viewing a sample perpendicular to its lamination plane is a much more effective vantage point for finding and imaging mud aggregates. ESEM images are an excellent method of displaying the three dimensional shape of mud aggregates because natural broken surfaces are imaged,

as opposed to the cut surfaces seen in thin sections. A real contrast is visible between sheeted clay and aggregated clay using this imaging device.

X-ray diffraction (XRD), energy dispersive spectrometer (EDS), and electron microprobe are the tools used for chemical analysis of samples in this study. The XRD is an effective tool for determining the bulk composition and mineral ratios of a sample. With respect to this study, interest lay in the proportions and types of clay present in the samples, making XRD analysis quite useful. Determining the composition of individual aggregates, however, is not feasible with this analysis technique. XRD equipment is not capable of identifying minerals present in abundances of 5% or less. If small amounts of smectite are present in the samples, the XRD will not detect the mineral's presence.

The EDS (attached to the ESEM) has been another useful tool for chemical analysis in this project. The benefit of this analysis technique is the ability to accurately target and analyze specific grains and aggregates, and receive immediate compositional feedback. The predominant mineral present in the aggregate grain is easily identifiable. There is some speculation that analyses may pick up interference from other grains, leading to an impure result; analysis is only able to identify the main mineral present for each point.

Initial electron microprobe work focused on point analysis. This method proved incredibly difficult because the clay-rich areas appear as a mass of material and not as rounded grains. A second approach focused on elemental mapping, essentially using chemical analysis as an imaging tool. This technique proved useful for showing the distribution of clays with respect to other minerals. This imaging system, however, does

not easily identify individual mud aggregates, making it difficult to obtain a precise chemical composition of a single aggregate.

8.0 Conclusion

The main objectives of this thesis were to determine the presence of pedogenic mud aggregates in the Boss Point and Little River formations through imaging and chemical analysis, to study the texture and occurrence of the aggregates in key stratal intervals, and to link aggregate preservation to processes that occurred within these formations. Dryland, semi-arid channel and floodplain successions of the two formations resemble modern, as well as other ancient deposits that have yielded aggregates. The selection of these formations has led to a successful search for mud aggregates using thin-section and ESEM. Aggregates are typically 10-15 μin diameter and range in proportion from about 10 to 50% of the samples. Some of the best occurrences are found in strata containing evidence of pedogenic modification, specifically in the calcrete, rubbly mudstone, and small channel body facies. The aggregates are present both in-situ and reworked over short distances in calcretes, floodplain mudstone, and soil fragments in channel deposits. Reworked individual aggregates are found in silt/sandstone deposits of large trunk channels and small floodplain channels.

XRD analysis indicates a predominance of illite clay with lesser amounts of chlorite and kaolinite in the samples. ESEM-EDS indicates that the aggregates are dominantly composed of illite with minor other clays, and electron microprobe analysis supports these findings. Chemical analysis did not identify smectite in any of the samples. However, evidence of vertisol development and vitrinite reflectance values of coal seams in the Boss Point Formation indicate that smectite was likely present and altered to illite during burial/diagenesis.

The mud aggregate texture is unusually well preserved in the Boss Point and Little River formations. This preservation is attributed to a combination of mineral cements, calcite and iron oxides/hydroxides (hematite), the strong mineral framework in siltstones, and the rapid burial of the Cumberland Basin during the Carboniferous.

Thin-section work is a reliable way to identify the presence of fine mud aggregates in a sample. Determining size, proportion, and distribution, as well as aggregate occurrence with respect to other minerals and cements is relatively straightforward by means of this method. ESEM provides an excellent high magnification image of aggregate grains. This imaging technique presents a three dimensional view of the aggregates that shows a distinct difference in shape from that of sheeted clay.

8.1 Future Work

It could be very useful to see data from the electron microprobe elemental maps manipulated into triangular diagrams of Al, K, and Mg. The distribution of plotted points on the diagram may make it possible to identify minor amounts of smectite clay among the predominant illite, chlorite, and kaolinite.

Imaging the aggregates via blue-light microscope may be a beneficial approach to identifying mud aggregates (Gierlowski-Kordesch and Gibling, 2002). This technique emphasizes the contrast between clays and other clastic minerals, possibly making the aggregates stand out more in thin section.

The presence of mud aggregates should be considered in other formations containing floodplain mudstones deposited in semi-arid to sub-humid paleoclimates. It

would be interesting to extrapolate this study into the Joggins Formation, which directly overlies the Little River Formation and represents a more humid climatic setting.

References

Bates, R.L. and Jackson, J.A. 1987. Glossary of Geology, third edition. American Geological Institute. Alexandria, Virginia., pp. 723.

Browne, G.H., and Plint, A.G., 1994, Alternating braidplain and lacustrine deposition in a strike-slip setting: the Pennsylvanian Boss Point Formation of the Cumberland Basin, Maritime Canada: Journal of Sedimentary Research, **B64**: 40-59.

Calder, J.H., Rygel, M.C., Ryan, R.J., Falcon-Lang, H.J., and Hebert, B.L. Stratigraphy and sedimentology of Early Pennsylvanian red beds near Lower Cove, Nova Scotia, Canada: The Little River Formation with redefinition of the Joggins Formation. Submitted to Atlantic Geology.

Cook, H.E., Johnson, P.D., Matti, J.C., and Zemmels, I. 1975. Methods of sample preparation and X-ray diffraction data analysis, X-ray mineralogy laboratory, Deep Sea Drilling Project, University of California, Riverside. Contribution No. 74-5, in DSDP Summary Reports.

Dare-Edwards, A.J. 1982. Clay pellets of clay dunes: Types, mineralogy, origin and effect of pedogenesis. Quaternary Dust Mantles of China, New Zealand and Australia. Edited by Wasson, R.J. Australian National University, Canberra City, Australia, pp. 179-189.

Davies, S.J., and Gibling, M.R. 2003. Architecture of coastal and alluvial deposits in an extensional basin: The Carboniferous Joggins Formation of eastern Canada. Sedimentology, **50**: 415-439.

Ékes, C. 1993. Bedload-transported pedogenic mud aggregates in the Lower Old Red Sandstone in southwest Wales. Journal of the Geological Society, London, **150**: 469-471.

Falcon-Lang, H.J. 2003. Late Carboniferous tropical dryland vegetation in an alluvial-plain setting, Joggins, Nova Scotia, Canada. Palaios, **18**: 197-211.

Gibling, M.R. 1987. A classic Carboniferous section; Joggins, Nova Scotia. Geological Society of America Centennial Field Guide, Northeastern Section, 409-414.

Gibling, M.R., Nanson, G.C., and Maroulis, J.C. 1998. Anastomosing river sedimentation in the Chanel Country of Central Australia. Sedimentology, **45**: 595-619.

Gierlowski-Kordesch, E., and Gibling, M.R.. 2002. Pedogenic mud aggregates in rift sedimentation. SEPM Special publication. Sedimentation in Continental Rifts. **73**: 195-206.

Héroux, Y., Chagnon, A., and Bertrand, R. 1982. Compilation and Correlation of Major Thermal Maturation Indicators.Hydrocarbon Generation and Source Rock Evaluation (Origin of Petroleum III). Edited by Cluff R.M. and Barrows M.H., pp. 128-144.

Machette, M.N. 1985. Calcic soils of the southwestern United States. Geological Society of America, Special Paper 203., pp. 1-21.

Mack, G.H., James, W.C., and Monger, H.C., 1993, Classification of paleosols. Geological Society of America Bulletin, **105**: 129-136.

Maroulis, J.C., and Nanson, G.C. 1996. Bedload transport of aggregated muddy alluvium from Cooper Creek, central Australia: a flume study. Sedimentology, **43**: 771-790.

Marriott, S.B. and Wright, P.V. 2004. Mudrock deposition in an ancient dryland system: Moor Cliffs Formation, Lower Old Red Sandstone, southwest Wales, UK. Geological Journal, **39**: 1-22.

Müller, R., Nystuen, J.P., and Wright, P.V. 2004. Pedogenic mud aggregate and paleosol development in ancient dryland river systems: criteria for interpreting alluvial mudrock origin and floodplain dynamics. Journal for Sedimentary Research, **74**: 537-551.

Nanson, G.C., Rust, B.R., and Taylor, G., 1986, Coexistent mud braids and anastomosing channels in an arid-zone river: Cooper Creek, central Australia: Geology, **14**: 175-178.

Plint, A.G., and Browne, G.H., 1994, Tectonic event stratigraphy in a fluvio-lacustrine, strike-slip setting: the Boss Point Formation (Westphalian A), Cumberland Basin, Maritime Canada: Journal of Sedimentary Research, **B64**: 341-364.

Prothero, D.R., and Schwab, F. 1996. Sedimentary Geology: an introduction to sedimentary rocks and stratigraphy. W.H. Freeman Company, New York, pp. 107.

Retallack, G.J. 2001. Soils of the Past, An Introduction to Paleopedology. Second Edition. Blackwell Science Ltd. Great Britain, Alden Press Ltd., pp. 93.

Rust, B.R., and Nanson, G.C. 1989. Bedload transport of mud as pedogenic aggregates in modern and ancient rivers. Sedimentology, **36**: 291-306.

Rust, B.R., Gibling, M.R., and Legun, A.S. 1984. Coal deposition in an anastomosing-fluvial system: the Pennsylvanian Cumberland Group south of Joggins, Nova Scotia, Canada. Special Publication International Association of Sedimentologists, **7**:105-120.

Ryan, R.J. and Boehner, R.C. 1994. Geology of the Cumberland Basin, Cumberland, Colchester and Pictou Counties, Nova Scotia. Mines and Energy Branches. Memoir 10. Nova Scotia Department of Natural Resources, pp. 129-130.

Welton, J.E. 1984. SEM Petrology Atlas. The American Association of Petroleum Geologists, Tulsa, Oklahoma. pp. 15, 23-37, 29.

Appendix A

ESEM spectra of analyzed mineral grains and the diagnostic mineral scan from Welton, 1984.

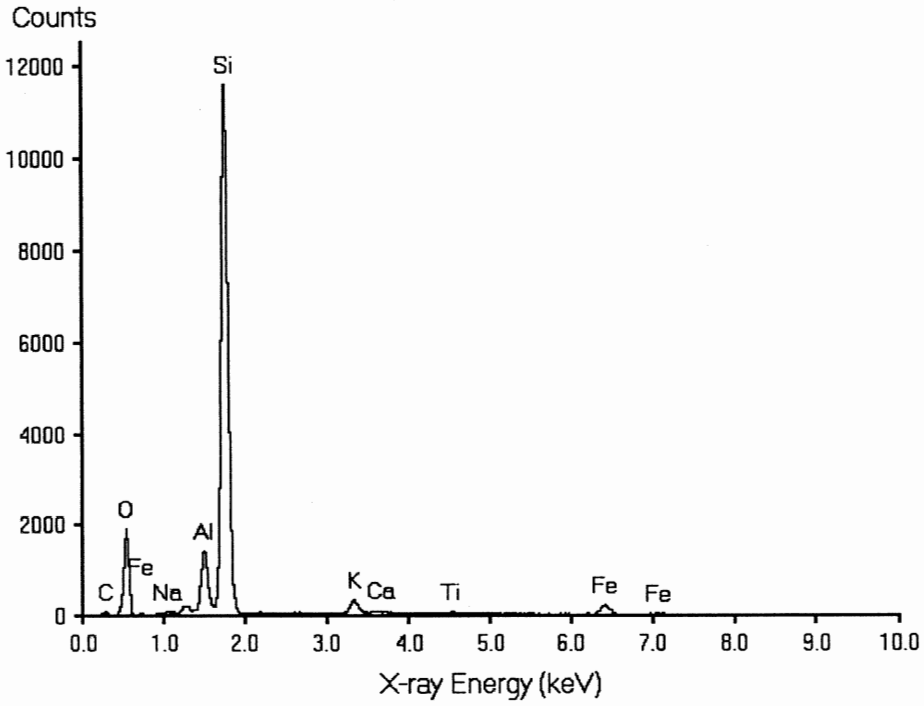

Quartz

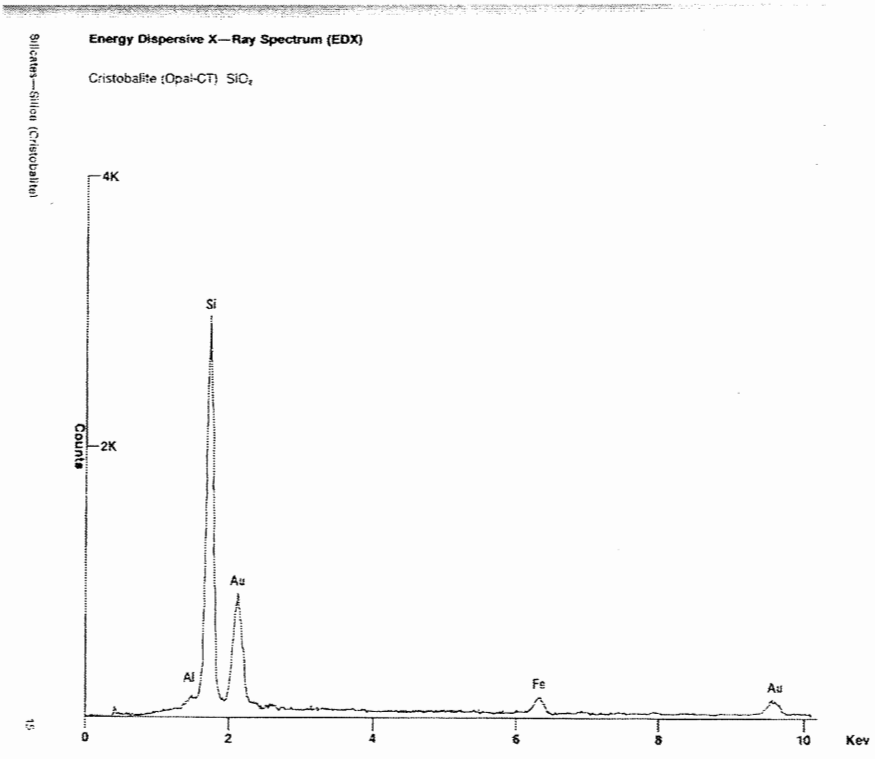

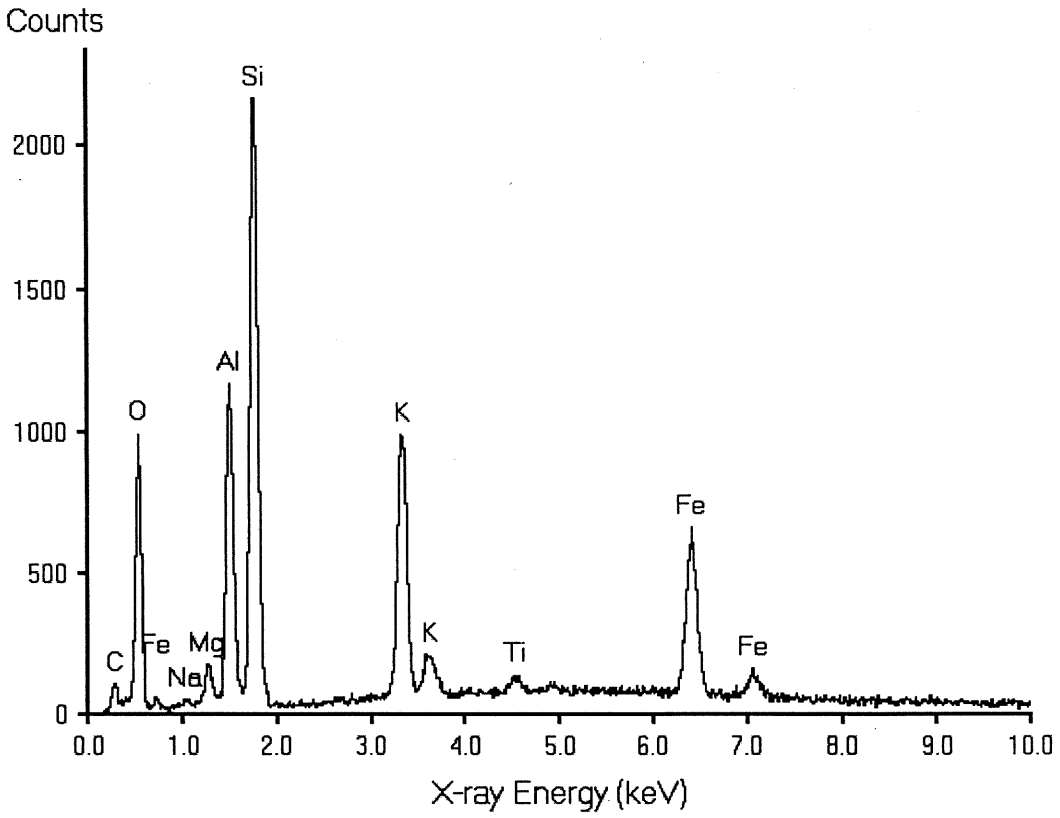
Counts
2000
1500
1000
500
0
Si
Al
O
K
Fe
C
Fe
Mg
Na
K
Ti
Fe
0.0
1.0
2.0
3.0
4.0
5.0
6.0
7.0
8.0
9.0
10.0
X-ray Energy (keV)

K feldspar

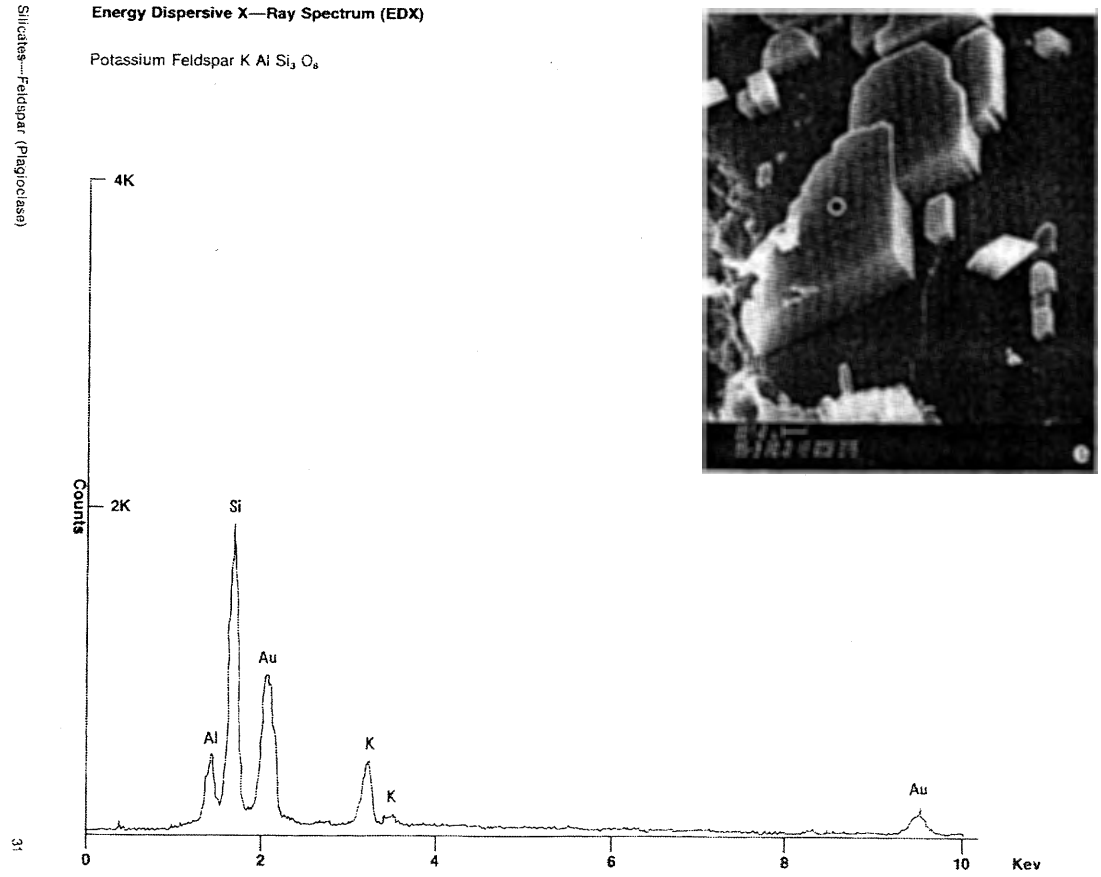
Energy Dispersive X—Ray Spectrum (EDX)
Potassium Feldspar K Al Si3 O8
Silicates—Feldspar (Plagioclase)
4K
2K
Counts
Si
Au
Al
K
K
Au
0
2
4
6
8
10
Kev
31

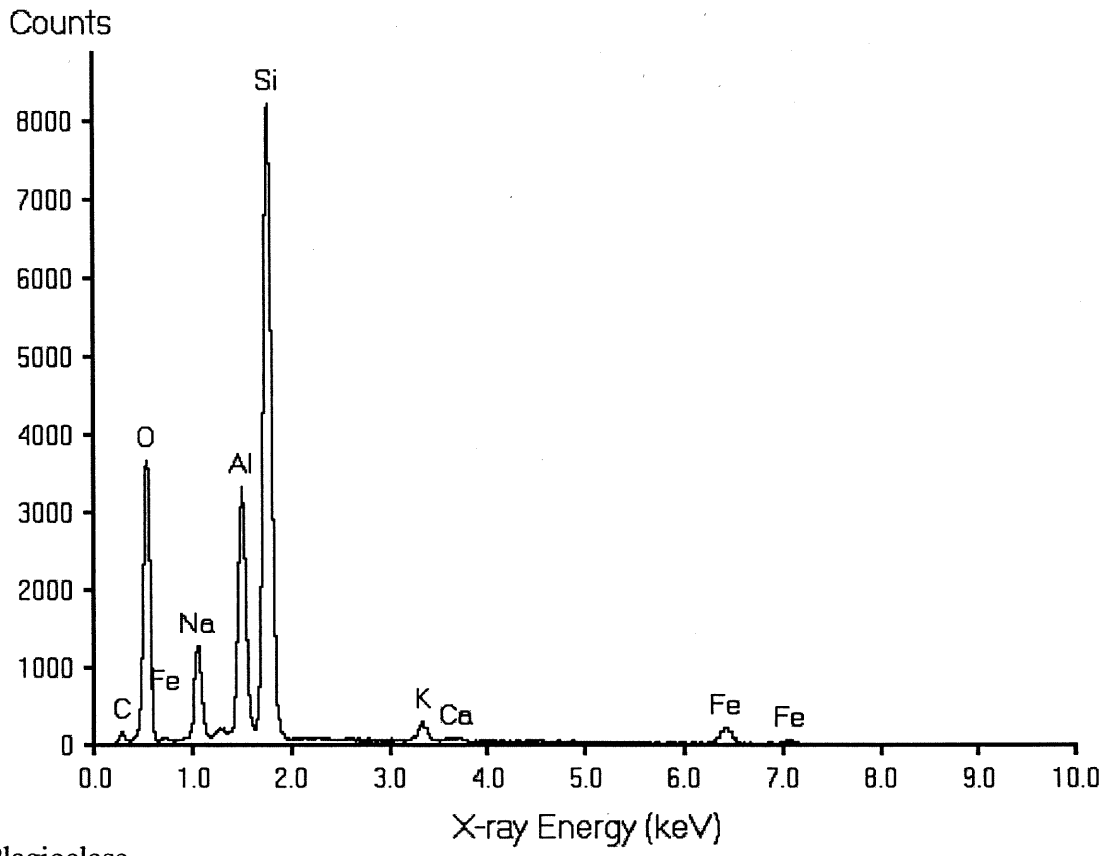

Plagioclase

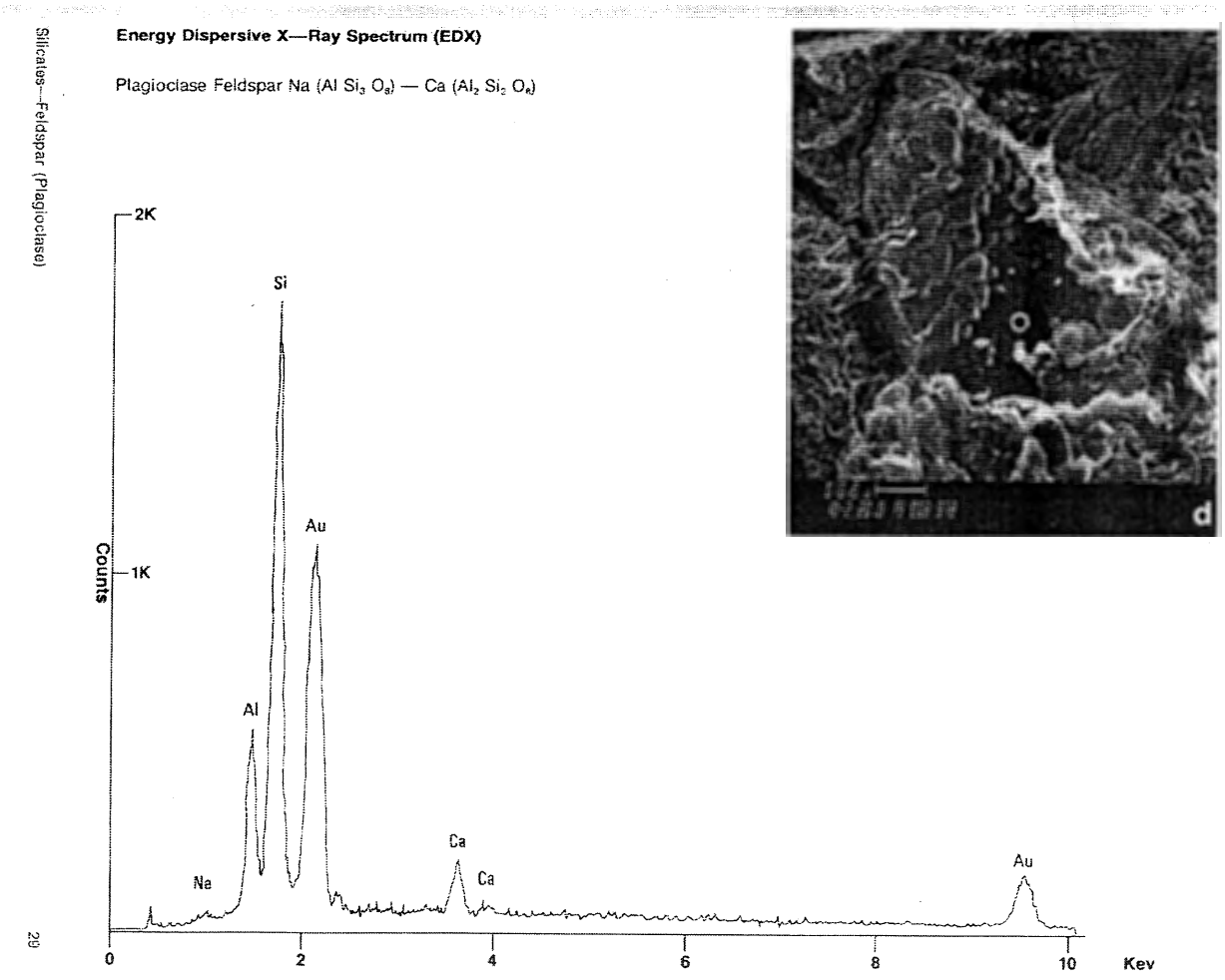

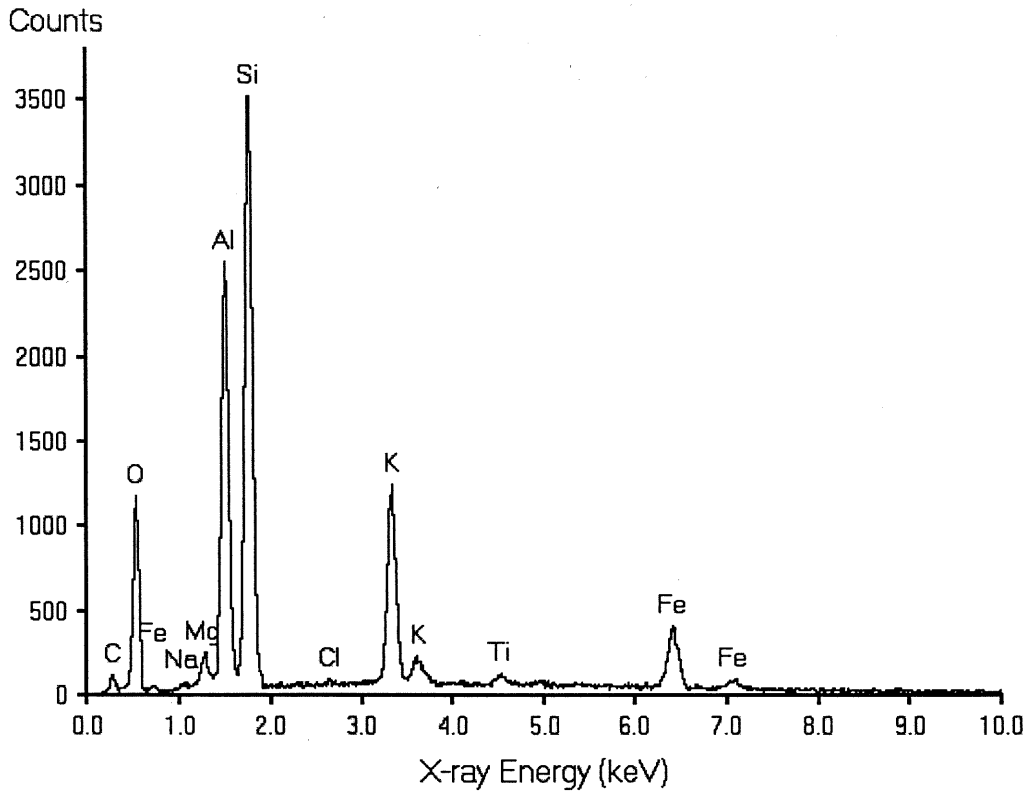
Counts
3500
3000
2500
2000
1500
1000
500
0
Si
Al
O
K
Fe
Mg
Na
C
Cl
K
Ti
Fe
Fe
0.0
1.0
2.0
3.0
4.0
5.0
6.0
7.0
8.0
9.0
10.0
X-ray Energy (keV)

Illite

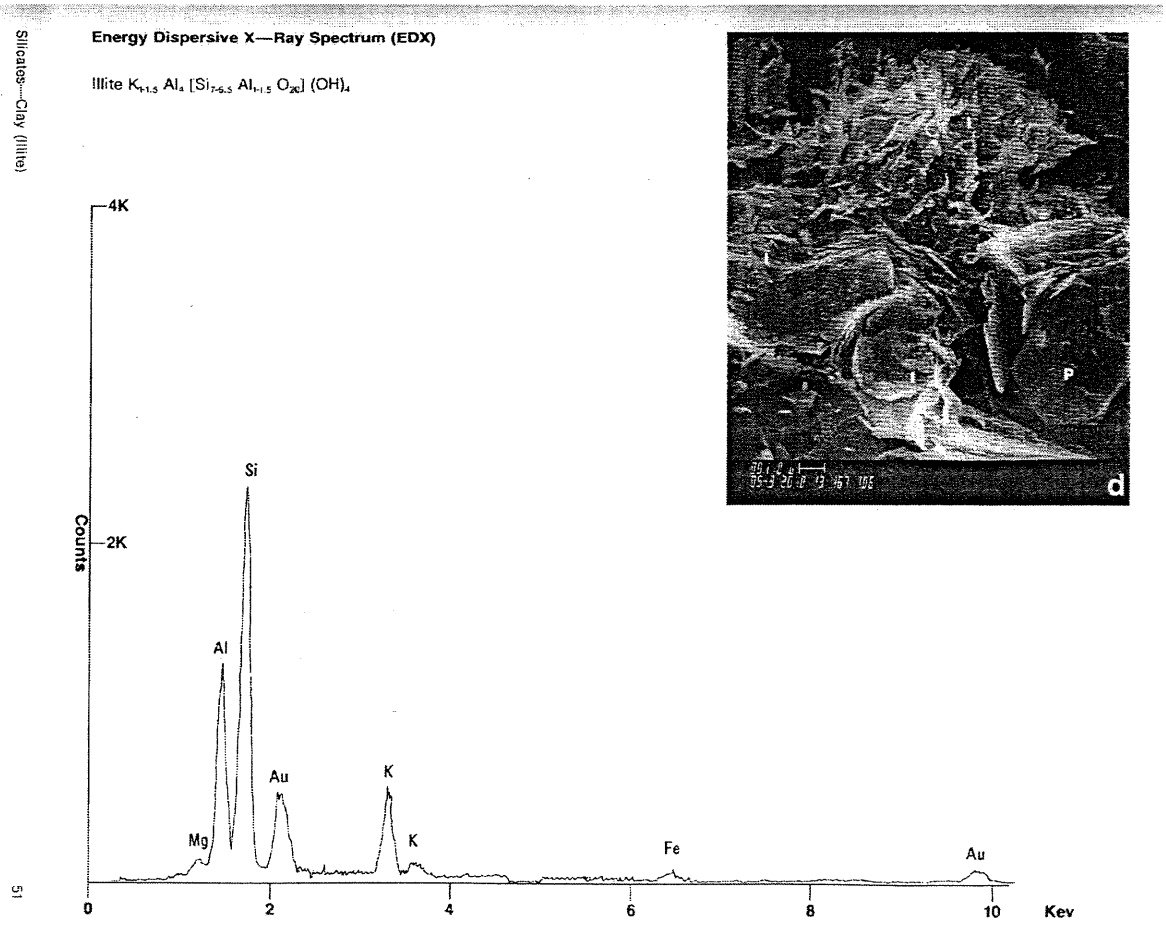
Energy Dispersive X—Ray Spectrum (EDX)
Illite $K_{+1.5}$ Al_4 $[Si_{7-6.5}$ $Al_{+1.5}$ $O_{20}]$ $(OH)_4$
Silicates—Clay (Illite)
4K
2K
Counts
Si
Al
Au
K
K
Mg
Fe
Au
0
2
4
6
8
10
Kev
P
d
51

Appendix B

Contains a list of all samples, the lithology of each sample, and the analyses caried out on each sample.

Sample	Lithology	Analyses
JG-1-1	sandstone	petrography
JG-1-2	sandstone	petrography
JG-1-3	sandstone	petrography
JG-1-4	siltstone	petrography
JG-1-5	sandstone	petrography
JG-2-1	siltstone	petrography, XRD
JG-2-2	carbonate concretion in sandstone	petrography, microprobe
JG-2-3	mudstone	petrography, XRD
JG-2-4	siltstone	petrography
JG-2-5	siltstone	petrography
JG-2-6	sandstone	petrography
JG-2-7	mudstone	petrography, ESEM/EDS
JG-2-8	siltstone	petrography
JG-2-9	mudstone	petrography, ESEM/EDS, microprobe
JG-2-10a	siltstone	petrography, microprobe
JG-2-10b	siltstone	petrography, XRD
JG-2-11	mudstone	petrography, XRD
JG-2-12	mudstone	petrography, XRD
JG-2-13a	mudstone	petrography
JG-2-13b	mudstone	petrography
JG-2-14	siltstone	petrography
JG-3-1a	sandstone	petrography, microprobe
JG-3-1b	sandstone	petrography